Reliability Metrics for Renewable Resources and Self-Reserve

Final Project Report

M-33

Power Systems Engineering Research Center

Empowering Minds to Engineer
the Future Electric Energy System

Reliability Metrics for Renewable Resources and Self-Reserve

Final Project Report

Project Team
Kory W. Hedman, Project Leader
Junshan Zhang
Arizona State University

Shmuel Oren
University of California Berkeley

Alberto Lamadrid
Lehigh University

Graduate Students
Mojgan Hedayati
Pranavamoorthy Balasubramanian
Arizona State University

Georgios Patsakis
University of California, Berkeley

Kwami Senam A. Sedzro
Lehigh University

PSERC Publication 17-06

November 2017

For information about this project, contact:

Kory W. Hedman
Arizona State University
School of Electrical, Computer, and Energy Engineering
P.O. BOX 875706
Tempe, AZ 85287-5706
Phone: 480 965-1276
Fax: 480 727-2052
Email: kory.hedman@asu.edu

Power Systems Engineering Research Center

The Power Systems Engineering Research Center (PSERC) is a multi-university Center conducting research on challenges facing the electric power industry and educating the next generation of power engineers. More information about PSERC can be found at the Center's website: http://www.pserc.org.

For additional information, contact:

Power Systems Engineering Research Center
Arizona State University
527 Engineering Research Center
Tempe, Arizona 85287-5706
Phone: 480-965-1643
Fax: 480-727-2052

Notice Concerning Copyright Material

Acknowledgements

The work described in this report was sponsored by the Power Systems Engineering Research Center (PSERC).

The authors thank industry collaborators including: Khaled Bahei-eldin (GE); Hong Chen (PJM); Yonghong Chen (MISO); Erik Ela (EPRI); Bob Entriken (EPRI); Evangelos Farantatos (EPRI); Nikhil Kumar (GE); Eamonn Lannoye (EPRI); Nivad Navid (PG&E); Milorad Papic (Idaho Power); Jim Price (CAISO); Dejan Sobajic (NYISO); Aidan Tuohy (EPRI); Tongxin Zheng (ISONE); and Dr. Deepak Rajan from the Lawrence Livermore National Laboratory for allowing the use of computational resources to make the execution of some of the simulations possible.

Executive Summary

With the significant growth in the integrated capacity of wind power generation, the variability of wind energy production poses new challenges to power system operations. The need for flexible resources is higher than ever. More rapid reserve is required, which results in the scarcity of balancing services. While existing practices rely predominantly on conventional generators to provide the flexibility to sustain reliable operations, with the push to integrate more renewables, there is a need for a paradigm shift. In particular, it is expected that, at some point, these renewable sources will have to take part in the electricity system balancing tasks. In this report, the focus is on the ability for renewables to provide reserve and ramping capabilities in order to address this challenge of integrating high levels of semi-dispatchable resources into the grid. The primary goal is to develop models to determine the optimal amount of reserve margins that such renewable resources can provide. Due to its significance as one of the most common forms of renewable generation, the work is focused on wind farm generation.

Part I: Flexible Dispatch Margin Optimization

Part I of the report investigates new methods to improve the energy and reserve scheduling in presence of renewable resources and develops an approach to enhance the reliability of service from renewable resources in real-time operation.

While the share of renewable generation is increasing, existing market structure does not adequately account for uncertainty that such renewables impose. Uncertainty encourages the use of stochastic approaches. However, stochastic programming is complicated, time consuming, and poses new challenges for market integration including market pricing issues. Operators prefer to use approximate models to schedule energy and operating reserves and the operating reserve is usually determined based on an ad-hoc deterministic rule.

In this report, stochastic models are used offline to derive deterministic operation policies for scheduling energy and reserve from renewables. This concept is an extension and enhancement of the existing deterministic procedures. Such an offline approach eliminates real-time computational burden and market pricing issues, while accounting for uncertainty in the operating conditions of the system.

The proposed approach is based on creating policy functions for real-time operation of the system. A policy function is an operation rule which is a function of the operating state of the system. In the report, the reserve margin policy is derived through stochastic analysis based on the forecast of the wind generation.

Given an operating state, the policy function structure can return a scheduling decision for the renewable generator, which takes into account both the current and look-ahead operating conditions. By shifting computational complexity to offline analysis, the prediction-based policy approach has minimal added computational complexity to the existing energy management systems in real-time. The results presented for the case study indicate that the policy function based approach has performance close to that based on stochastic programming. By using the proposed

approach, the risk is reduced with minimal added computational complexity to the existing market management structure.

In summary, the key takeaway points of this project are as follows:

- A flexible reserve margin based algorithm is applied to generate offline policies for discounting wind generation and scheduling energy and reserve in the presence of wind generation. A two-phase framework is described to obtain appropriate policies for scheduling wind generation. In the first phase, a generation dispatch is performed to obtain the energy and reserve schedule for generation units. This phase leverages a scenario-based stochastic programming approach to capture the effect of the representative wind generation scenarios based on short-term forecast. This initial phase minimizes the aggregate operating costs and risk costs relative to the modeled scenarios. In the second phase, the decision from the first phase is tested against a larger set of scenarios to ensure the adequacy of the scheduled energy and reserve.
- A testing method is derived based on the real-time scheduling procedure to assess the performance of the policies obtained through the proposed training procedure for scheduling wind reserve margin. The performance of the proposed policy training algorithm is compared with its counterparts without applying the trained policies.
- A SCED (security constrained economic dispatch) model is derived for both the prediction-based method and the no-policy method to enable comparison of the behaviors of the two models. A notion of quality of service is derived for assessing the performance of the reserve from renewables.
- The market implications of deploying the proposed prediction-based policy are analyzed and compared with its counterparts without applying the trained policies. The results confirm that the prediction-based policy along with a proper market structure can improve the quality of service for scheduling energy and reserves from renewables.
- While a stochastic approach is used to generate the reserve margin policy functions in this report, the policy functions can also be derived using other techniques or be designed using various forms of data mining approaches. The policy function based approach has tractable computational complexity for a large-scale power system and can also effectively enhance the operation of renewable generators. The policy function based approach is a scalable approach that can be applied to power systems and energy market.

Part II: The Value of Flexible Wind Dispatch in Stochastic Unit Commitment

Renewable power generation, such as wind power, is commonly considered a must-take resource in power systems and only curtailed in cases where technical feasibility is compromised. This prioritization is currently in force in the European Union (Directive 2009/28/EC), even though the discussion to amend it is currently ongoing. We attempt to show that, given the technical capabilities of current wind turbines, this approach could lead to major economic inefficiency as wind integration levels in power systems increase. More specifically, our methodology consists of the following basic steps:

- We explore the expected benefit from dispatching wind resources at a lower level than their available output in a Stochastic Unit Commitment (SUC) setting. We provide a complete framework to understand and evaluate the expected benefit from flexible wind dispatch in the SUC setting.
- We present small motivating examples to offer intuition regarding the most common setups where such benefit may occur.
- We utilize existing wind speed modeling techniques, which we enhance with a non-parametric modeling methodology for the aggregate power curve.
- We extend a decomposition technique from recent literature that utilizes global cuts and Lagrangian penalties to reach an optimal solution and adapt it to solve the problem.
- We propose a combined scenario reduction and decomposition algorithm to provide a quicker answer by eliminating similar scenarios throughout the iterations of the decomposition algorithm. The main idea behind this elimination is evaluating the similarity of two scenarios based on them having comparable impacts when applied to the specific problem as the decomposition algorithm iterations progress.
- We test our framework on a reduced model of the Western Electricity Coordinating Council (WECC) system.

Part III: Risk-aware Optimal Bidding for Renewable Farms

To help renewable farms be marketable while keeping the grid reliable, the focus of a significant amount of research in the literature is on devising better methods of integrating renewable energy sources (RES) to the existing power grid.

We derive a criterion for renewable farms' participation in the grid reliability efforts. The renewable energy farms' bidding strategy is formulated as a portfolio optimization problem assuming a storage system. The portfolio is made of the day-ahead, real-time and reserve offers.

- We formulate the renewable farm's day-ahead bidding decision as a newsvendor problem.
- We evaluate renewable farm's reliability performance assuming the derived news' vendor based optimal policy.
- We provide further market opportunity to the renewable farm by assuming it can participate in the reserve market as well. We assume the farm dispose of energy storage.

The approach developed in this work has two original defining concepts. First, its principal aim is not to arbitrage the day-ahead versus the real-time markets. Rather, it purposes to provide a reliable and yet economically sound day-ahead energy offer. Second, it provides risk-sensitive real-time and reserve offers that account for all possible imbalance penalties and real-time prices along with reasonable storage size and cost function.

Project Publications:

[1] M. Hedayati, J. Zhang, and K. Hedman, "Wind Power Dispatch Margin for Flexible Energy and Reserve Scheduling with Increased Wind Generation," *IEEE Transactions on Sustainable Energy,* vol. 6, no. 4, pp. 1543-1552, Aug. 2015.

[2] M. Hedayati, K. Hedman, and J. Zhang, "Reserve Policy Optimization for Scheduling Wind Energy and Reserve," *IEEE Transactions on Power Systems,* accepted for publication.

[3] M. Hedayati, P. Balasubramanian, K. Hedman, and J. Zhang, "Market Implications of Wind Reserve Margin," *IEEE Transactions on Power Systems,* under review.

[4] G. Patsakis and S. Oren, "Value of Flexible Wind Dispatch in Stochastic Unit Commitment," *IEEE Transactions on Power Systems,* to be submitted.

[5] K. S. Sedzro and A. J. Lamadrid, "Renewable Self-Reserve and Storage Management Under Market and Generation Uncertainties: Application to Ocean Wave Energy Farms," *USAEE Annual Conference,* October 2016.

Student Theses:

[1] Mojgan Hedayati. *Flexible Reserve Margin Optimization for Increased Wind Generation Penetration,* Ph.D. Dissertation, Arizona State University, Tempe AZ, December 2016.

[2] Kwami Senam A. Sedzro. *Reliability and Resiliency Driven Solutions for Power Systems Operation and Planning*, Ph.D. Proposal, Lehigh University, Bethlehem, PA, January 2016.

Part I

Flexible Dispatch Margin Optimization

Mojgan Hedayati
Pranavamoorthy Balasubramanian
Kory W. Hedman
Junshan Zhang

Arizona State University

For information about this project, contact:

Kory W. Hedman
Arizona State University
School of Electrical, Computer, and Energy Engineering
P.O. BOX 875706
Tempe, AZ 85287-5706
Phone: 480 965-1276
Fax: 480 727-2052
Email: kory.hedman@asu.edu

Power Systems Engineering Research Center

The Power Systems Engineering Research Center (PSERC) is a multi-university Center conducting research on challenges facing the electric power industry and educating the next generation of power engineers. More information about PSERC can be found at the Center's website: http://www.pserc.org.

For additional information, contact:

Power Systems Engineering Research Center
Arizona State University
527 Engineering Research Center
Tempe, Arizona 85287-5706
Phone: 480-965-1643
Fax: 480-727-2052

Notice Concerning Copyright Material

Table of Contents

List of Figures

List of Tables

Nomenclature

- Acronyms

ANN	Artificial neural network
AR	Autoregressive
ARIMA	Autoregressive integrated moving average
ARMA	Autoregressive moving average
FERC	Federal energy regulatory commission
FOR	Forced outage rate
LMP	Locational marginal price
PDF	Probability distribution function
RPS	Renewable portfolio standard
RTS	Reliability test system
SCED	Security constrained economic dispatch
SCUC	Security constrained unit commitment
EENS	Expected energy not served
QOS	Quality of service
SVM	Support vector machine

- Indices and Sets

g	Index of generators, $g \in G$.
$g(n)$	Set of generators connected to node *n*.
k	Index of transmission lines, $k \in K$.
n	Index of buses $n \in N$,.
s	Index of scenarios, $s \in S$.
t	Index for time periods, $t \in T$.
w	Index of wind generators, $w \in W$.
$\delta^+(n)$	Set of lines specified as to node *n*.
$\delta^-(n)$	Set of lines specified as from node *n*.
Ω_g	Set of generators.
Ω_n	Set of buses.

- Parameters

B_k	Electrical susceptance of branch *k*.
C_c^n	Load curtailment cost at bus *n* (\$/MWh).
C_g^e	Operational cost of conventional unit *g*.
C_g^{rc}	Capacity cost of conventional unit *g* for providing spinning reserve.
C_g^{re}	Energy cost of conventional unit *g* for providing spinning reserve.
C_p	Penalty cost for wind farm if not able to abide by its scheduled output.
C_w^e	Operational cost of wind unit *w*.
C_w^{rc}	Capacity cost of wind unit *w* for providing spinning reserve.
C_w^{re}	Energy cost of wind unit *w* for providing spinning reserve.
N_w	Number of states in *S*.
P_g^{max}, P_g^{min}	Maximum output and minimum output of unit *g*.

P_w^{max} Maximum output of wind unit *w*.
P_k^{max} Maximum active power capacity of transmission line *k*.
P_{wt}^f Point forecast of the output of wind unit *w* for period *t*.
Per_{wt}^f Distribution forecast 90th percentile of wind unit w for period t.
R_g^{10} 10-miniute ramp rate of unit *g*.
S State space of Markov chain.
Γ_k Wind farm generation at level *k*.
$\overline{U}_{gt}$ Scheduled unit commitment status of unit *g* in period *t*.
W_{wst} Predicted power output level of wind unit *w* in scenario *s* for period t.
π_s Probability of scenario *s*.
τ_k Average duration of state k.

- Variables

d_{nt} Demand at bus *n* in period *t*.
ls_{nst}^+, ls_{nst}^- Violations in node power balance equation (load shedding) at bus *n* in scenario *s* for period *t*.
p_{gt} Scheduled real power output of conventional unit *g* in period *t*.
p_{kt} Real power flow of line *k* in period *t*.
p_{kst} Real power flow of line *k* in scenario *s* in period *t*.
p_{wt} Scheduled real power output of wind unit *w* in period *t*.
$p_{wst}^{penalty}$ Violation from the scheduled wind generation in scenario *s* for period *t*.
LP Load payment.
RAP_{gt} Reserve activation payment of unit g in period t.
r_{gt} Scheduled spinning reserve from conventional unit *g* in period *t*.
r_{gst} Actual exercised reserve from conventional unit *g* in scenario *s* for period *t*.
r_{wt} Scheduled spinning reserve from wind unit *w* in period *t*.
r_{wst} Actual exercised reserve from wind unit *w* in scenario *s* for period *t*.
rr_{gst} Residual reserve from conventional unit *g* in scenario *s* for period *t*.
rr_{wst} Residual reserve from wind unit *w* in scenario *s* for period *t*.
α Flexible wind reserve margin policy factor.
β Reserve adjustment factor.
Δ_{wst} Uncompensated potential reserve from wind unit *w* in scenario *s* for period *t*.
δ_{nt}, γ_{gt} Dual variables of power balance constraint and reserve capacity constraint.
θ_{nt} Voltage angle at bus *n* in period *t*.
θ_{nst} Voltage angle at bus *n* in scenario *s* in period *t*.
$\lambda_{n,t}^c$ Dual variables of power balance constraint at bus *n* in contingency *c* in period *t*.
ξ_{wt} Additional reserve required for period *t* due to the integration of wind unit *w*.
σ_{wt} Variance of the output of wind generator *w* for period *t*.

1. Introduction

1.1 Background

Due to the increasing environmental concerns and the need for a more sustainable power grid, power systems have seen a fast expansion of renewable resources in recent years. In the U.S, thirty states have enforced Renewable Portfolio Standards (RPS) or other mandated renewable capacities policies [1]. Due to the recent technology and efficiency improvements as well as government financial support, the proportion of renewable resources in the generation mix is increasing. By the end of 2012, the worldwide installed wind capacity has reached 282.5 GW [2] and the installed capacity for solar has reached 100 GW [3]. As the penetration level of renewable generation increases, the electric industry looks for efficient solutions to enable large-scale integration of renewable resources. To accommodate the increasing generation from such resources, important changes are needed both in the planning and the operation aspects of power systems. Emerging developments in computational capabilities within the realm of smart grid appear to provide promising solutions for planning and operation of the system in the presence of intermittent resources such as wind and solar energy.

This report discusses the algorithms the operators of power systems can use to deal with the uncertainty of generation from renewable resources. The focus of the report is on the system operations, namely energy and reserve scheduling, in presence of wind generation.

With the significant penetration of wind generation, the variability and uncertainty of wind energy requires the system to have additional flexibility. Flexibility requirements in a power system are a function of grid infrastructure, the existing generation mix, and operating procedures. When studying the operational aspects, flexibility is usually described within the context of operating reserves, entailing the system to be able to balance out the deviations of the realized generation and load from their forecasted values.

Due to the uncertainty and variability of renewable generation, additional operating reserves may be needed to maintain the reliability of the system. Wind fluctuations in-crease requirements for rapid reserve, which may result in the scarcity of balancing services. While existing practices rely predominantly on conventional generators to provide the flexibility to sustain reliable operations, with the push to integrate more renewables, there is a need for a paradigm shift. Such a paradigm shift will be based on having the renewable resources behave similar to the conventional generators. With the increasing share of renewable generation, it is expected that, at some point, these renewable resources will take part in providing ancillary services, too. There is also a regulatory push for such a paradigm shift. As an example, FERC (Federal Energy Regulatory Commission) has proposed an order to eliminate the exemption for wind generators from the requirement to provide reactive power [4]. Recent research works

have investigated the possibility of having ancillary services from renewable resources. For example, reference [5] discusses the capability of wind and solar plants to provide voltage regulation.

It is envisaged that renewable resources may be required to contribute towards the system balancing tasks. One approach is to provide operational flexibility by allowing for a discounted energy scheduling from wind generation. This will allow wind generators to provide a flexible dispatch margin by withholding their own potential production in forward markets so as to hold some expected output to balance out their own intermittency. Excess wind can then be used as spinning reserve to mitigate forecast errors and other system uncertainties. Dispatching the wind generator below the forecasted level allows for a higher degree of flexibility in the system operation.

This study focuses on the ability of wind generators to provide reserve (in the form of dispatch margins) in order to address the challenge of integrating high levels of semi-dispatchable resources into the grid.

One primary objective of this study is to determine the optimal amount of dispatch that such renewable resources can provide. The aim has been to use stochastic models of wind generation to develop an affine policy function for scheduling energy and reserve from wind generators, which strikes a balance between the operating costs and the risk associated with the mismanagement of wind generation that leads to an imbalance between demand and supply.

Subsequently, the focus of the work has been on developing scheduling and reserve policies when multiple dimensions of uncertainty are involved in the operating conditions of the system. Uncertainty complicates the process of economic dispatch and reserve scheduling for the system and renders the deterministic optimization approach less effective. The existing optimization approaches for handling uncertainty, such as scenario-based stochastic programming and robust programming are also computationally expensive and are thus, less practical for making real-time operation decisions. The present study investigates the possibility of exploiting offline stochastic calculations for training deterministic operation policies. Such deterministic policies are then applied to real-time system models to find the dispatch and reserve schedule. The offline policy generation technique is proposed based on stochastic dispatch margin scheduling to hedge against the real-time uncertainty of wind farm generation.

Such offline analysis allows for modeling a broader range of uncertainty, making it applicable when there are multiple sources of uncertainty.

1.2 Summary of Chapters

This report is structured as follows. Chapter 2 provides a review of wind power forecasting approaches. The existing short-term wind power forecasting techniques and their general methodologies are discussed. Subsequently, the detailed procedure of the

Markov chain model-based wind generation forecast, which is the method used for generating wind scenarios in this report, is described.

In chapter 3, a combined dispatch and reserve scheduling model is proposed by determining a flexible wind dispatch margin. A framework is presented to find the optimal policy to incorporate the flexible wind dispatch margin into the hour-ahead market. A finite-state Markov chain wind power forecast model, based on spatio-temporal analysis, is utilized to find the appropriate level of wind dispatch margin.

In chapter 4, an offline policy generation technique is proposed based on stochastic dispatch margin scheduling to hedge against the real-time uncertainty of wind farm generation. The proposed policy generation structure is developed in a forecast-based framework by taking into account both the wind generation status and the loading conditions of the system. The proposed approach is tested and the costs are compared to those obtained by using ad-hoc rules to analyze the effectiveness of the presented model in handling uncertainty.

Chapter 5 investigates the market implications of deploying the deterministic reserve policy based on the offline stochastic analysis. The generators' bids for energy and ancillary services are modeled. In addition, a market settlement scheme is proposed that can be used for the proposed policy. In the proposed structure the generators are compensated for the energy and reserve that they provide. The reserve providers are compensated both for the reserve capacity and the reserve activation. The reserve activation payments are dependent upon the performance of the reserve resource for various realization scenarios. The proposed approach is compared with a typical deterministic approach that uses no policy.

In chapter 6, the conclusions to this report are presented.

2. Wind Farm Generation Forecasting

2.1 Introduction

With an expected high penetration level, wind generation integration is expected to change the existing power systems operating procedures including unit commitment, economic dispatch and ancillary services procurement, which are critical to ensuring the adequacy of bulk power systems. Compared to conventional generation (e.g., thermal, hydro, nuclear), wind generation has two distinct characteristics: variability and uncertainty. This is because wind power is dependent on the volatility of the wind. As a result, wind generation is considered to be semi-dispatchable meaning that the power output of a wind farm cannot be simply dispatched at the request of power system operators. To be specific, semi-dispatchable resources refer to intermittent resources that have a limited degree of controllability, unlike conventional generators that have full controlability. Due to the aforementioned characteristics, wind generation forecasting is critical to ensure that adequate resources for dispatch, ancillary services and ramping requirements are available all the time.

It is worth mentioning that wind power forecasting methods can be classified according to forecast time-scale [6][6]. Seasonal or long-term forecast is used for resource planning and contingency analysis. Day-ahead forecast is used for market trading and day-ahead unit commitment and scheduling. Short-term forecast is used for hour-ahead unit commitment, real-time dispatch, regulation and load following [6].

Due to the semi-dispatchability and uncertainty of wind, accurate forecasting models are needed to enable efficient integration of wind energy. The existing forecasting techniques for wind power can be categorized into a few broad categories [7][7]; physical methods, statistical methods, and artificial intelligence methods. Physical methods are based on numerical weather prediction and use comprehensive weather data and advanced meteorological techniques for wind speed forecasting [8][8]-[9]. Statistical methods try to find the inherent relationship within the interdependent measured power data. These models include time-series approaches such as auto regressive (AR) models [10], auto regressive moving average (ARMA)[11], and auto regressive integrated moving average (ARIMA)[12]. The artificial intelligence based approaches have also been applied in forecasting wind speed and power. These methods include artificial neural network (ANN) [13]-[14], support vector machine (SVM) [15]-[16], and evolutionary optimization algorithms [17].

There are also other hybrid approaches that take advantage of multiple forecasting methods by combining various individual models and their information [18]-[19].

A vast amount of work in the existing literature focuses on wind speed forecast, assuming that wind generation from the farm can be directly calculated as a function of wind speed at one specific location in the farm. In reality, however, the power outputs of wind

turbines within the same wind farm can be quite different, even if the wind turbines are of the same class as well as being physically located close to each other. Therefore, forecast errors for existing approaches can be large [20].

In this study, a spatio-temporal approach for wind power generation forecast is used, which takes into account the diurnal non-stationarity and the seasonality of wind [20]. Due to the inherent variability and uncertainty of wind farm generation, distributional forecast methods can manage the uncertainty better than point forecast methods. In this report, a Markov chain model-based wind generation forecast is used base on the analysis provided by authors of [20]. Their model is used in chapter 3 and chapter 4 of this report to generate distributional forecasts for wind generation. The critical observations and the principles of their forecast model is described in the following sections.

2.2 Spatio-temporal Dynamics of Wind Farms

A critical reported observation from the measurement data is the spatial dynamics [21]. The power outputs of wind turbines within a wind farm can be quite different, even if the wind turbines are of the same class and physically located close to each other [22]. Although the variable power outputs of wind turbines are not identical, it is assumed that they follow the same probability distribution if the wind turbines are of the same class.

The other key observation is the temporal characteristic, i.e. the diurnal non-stationarity and the seasonality of wind farm generation. The diurnal non-stationarity can be tackeled by identifying a time epoch such that the wind generation exhibits stationary behavior within each epoch. The forecast model can then be developed for each of these epochs separately. According to [20], a three-hour epoch seems to be reasonable, i.e. the probability distributions of wind farm generation over three consecutive 1-hour intervals are consistent.

2.3 Markov Chain-based Short-term Forecasting

The procedure for developing the Markov chain short-term forecast is described in this section based on [20]-[22]. The objective is to address the statistical distribution and temporal dynamics of aggregate wind farm generation using a Markov chain.

In this approach, in order to capture the spatial correlation between the power outputs from the wind turbines, a minimum spanning tree is constructed based on graph theory. The spatial correlation between the individual wind turbines is determined by using a linear regression model. The probability distribution of the aggregate wind generation can then be characterized using the wind speed measured at the reference meteorological tower in the farm. The temporal correlation is analyzed by using a finite state Markov chain model. The seasonality is tackled by designing the forecast model for each month individually.

Assume the Markov chain is discrete time, of order 1, and has N_w states. Let S denote the state space of the Markov chain. Each state $S_k = [\Gamma_k, \Gamma_{k+1})$, k ∈ {1, . . . , N_w} is defined as an interval of generation level, with extreme values given by $\Gamma_k = 0$ and $\Gamma_{N_{w+1}} = P_w^{max}$, where P_w^{max} is the maximum generation of wind farm w. The finite state Markov chain model is developed as follows:

Define the quantity τ_k as the average duration that P_w, wind generation, stays in state S_k.

$$\tau_k = \frac{F_w(\Gamma_{k+1}) - F_w(\Gamma_k)}{L_w(\Gamma_{k+1}) - L_w(\Gamma_k)} \tag{2.1}$$

where $F_w(\cdot)$ denotes the cumulative distribution function (CDF) of the farm aggregate wind generation and $L_w(.)$ denotes the level crossing rate. Level crossing rate is defined as the number of times per unit time that the farm aggregate power P_w crosses Γ_k in positive/negative direction only. The cumulative probability distribution F_w of farm aggregate wind generation is characterized based on the historical data of wind farm generation.

The level crossing rate is given by

$$L_w(\gamma) = \int_{-\infty}^{\gamma} Pr(P_w(t) > \gamma | P_w(t-1) = p_w)\, dF_w(P_w). \tag{2.2}$$

It is worth noting that, τ_k plays a critical role in the Markov chain model and determines how well the stochastic random process P_w is captured. A small value of τ_k suggests that P_w is more likely to switch out of the state S_k within a time slot, i.e., nonadjacent transitions are more likely to occur, and hence the transitional behaviors of P_w are not captured efficiently by the discrete-time Markov chain. Large values of τ_k indicate that the quantization by the Markov chain is not fine grained, and the corresponding forecast would be less accurate. One objective of state space design is, thus, to make each τ_k fall into a reasonable range [23]. In order to do that, one way is to introduce a constant τ and find the $N_w$variables $\{\Gamma_2, \ldots, \Gamma_w\}$by solving (2.1) numerically with$\tau_k = \tau$, ∀k ∈ $\{1, \ldots, N_{w-1}\}$.

Once the state space S is designed, the transition probabilities can be estimated as proposed in [24]. The probability of a transition from S_i to S_j is given by

$$Q_{i,j} = \frac{n_{ij}}{\sum_{k=1}^{N_w} n_{ik}}, i, j \in \{1, \ldots, N_w\} \tag{2.3}$$

where n_{ij} is the number of transitions from S_i to S_j occurred in historical data. The representative generation level for each state S_k can be determined using the minimum mean square error principle, given by

$$P_{w,k} = arg\ min\ E\left\{\left(P_k - P_w(t)\right)^2 \middle| P_w(t) \epsilon [\Gamma_k, \Gamma_{k+1}]\right\}$$

$$= \frac{\int_{\Gamma_k}^{\Gamma_{k+1}} p_w dF_w(P_w)}{F_w(\Gamma_{k+1}) - F_w(\Gamma_k)} \quad (2.4)$$

Therefore, given the current wind generation state of the wind farm output, the distributional forecast of the wind farm generation in next interval is given by

$$Pr\left(P_w^{t+1} = P_{w,j} \middle| S_w^t\right) = Q_{S_w^t.j}, \forall j \in \{1, \dots, Nw\} \quad (2.5)$$

Using this framework, the probability distribution of the immediate future state of the wind farm output can be predicted based on the most recent state of the system. This probability distribution expresses the transition probability from the current state to the future one.

The scheduling framework modeled in this study is for the short-term, since it deals with hour-ahead decisions for acquiring energy and reserve. To determine the short-term schedule, the short-term wind power forecast model based on the finite state Markov chain model has been used. This model predicts the wind farm generation level in the next time epoch (10-min) to be among a few defined states with certain probabilities, thereby improving the tractability for stochastic programming.

3. Wind Power Reserve Margin for Flexible Energy and Reserve Scheduling

In this chapter, a method is developed for scheduling energy and reserve from wind generators. The method is designed to strike a balance between the operating costs and the risk associated with the mismanagement of wind generation, which can lead to an imbalance between demand and supply.

3.1 Introduction

Due to the uncertainty and variability of renewable generation, additional operating reserves may be needed to maintain the reliability of the system. In order to operate the system in a secure and stable manner, sufficient reserve capacity must be in place to overcome load and renewable forecast errors or unexpected failures of generators. When renewable resources drop below their anticipated production level, fast acting up reserves should be called upon. When the actual wind generation is above the forecasted value, however, a different complication arises in terms of ramping down conventional generators. In some power systems, the operators are required to incorporate all the available wind power. Even in deregulated systems, the actual dispatched wind exceeds the cleared amount due to the low real-time price of the wind and lack of over-provision penalty. A significant amount of down reserve is needed, as a result, to balance these intermittent resources.

These operational aspects give rise to an interest in developing better approaches to determine the right amount and the location of reserve for systems with wind resources [25] -[29]. In [30], a review of the different assumptions and methods used to calculate the amount of different types of reserves with high penetrations of wind power is presented. The authors of [31] used a stochastic optimal power flow to supplement traditional energy scheduling and reserve procurement while considering the uncertainty of equipment outages, errors in demand forecasts, and intermittent generation. Another work, [32], balances the costs and benefits of spinning reserve while solving unit commitment. Wind power forecast errors are modeled by a Gaussian distribution and the benefit is expressed as a function of the reduction in the expected energy not served (EENS). Recent work [33] uses probability functions for conventional generator outages as well as discretized probability functions for wind power and load to create a distribution function of the system generation margin. The authors use a loss of load expectation threshold to calculate the required reserve to shift the generation margin curve to the right (positive direction). An overview of the current practices of operating reserves and methodologies used to estimate the increase in reserve allocation due to wind power is presented in [34].

As the wind penetration level increases, wind power producers are expected to behave similar to other market participants, e.g., renewable resources may be required to contribute towards the system balancing tasks. Recent studies [35]-[38] have considered

the participation of wind generators in the balancing markets. The results suggest that the wind farm is able to play a proactive role in providing downward regulation and increase its profits. The above studies have presented specific structures to determine the required reserve from conventional generators to cope with the uncertainty of wind generation. While this approach is feasible, it will impose a high cost on system operations since sufficient flexible capacity must be on-line to manage the uncertainty of the wind production. An alternative method is to allow wind generators to provide a flexible reserve margin by under-scheduling in forward markets. The concept of flexible wind reserve margin is a way to hedge against the uncertainty at an earlier stage. In order to provide a flexible reserve margin as proposed by [39], wind generators under-schedule in the hour-ahead energy market so as to hold some expected output as reserves. Excess wind can then be used as spinning reserve to mitigate forecast errors and other system uncertainties.

Dispatching the wind generator below the forecasted level allows for a higher degree of flexibility. The concept of wind reserve margin enables the wind farm generators to behave similar to other generators and partake in the system balancing tasks. Fig. 3.1 illustrates the concept of wind reserve margin. By withholding the potential output in the hour-ahead, the wind farm can mitigate the uncertainty related to the various possible realizations.

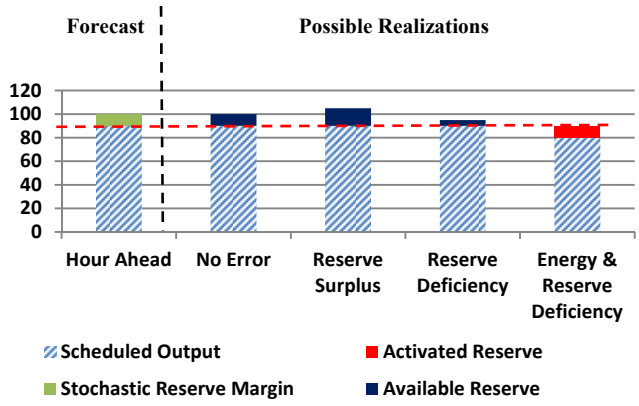

Fig. 3.1. Possible realizations with wind reserve margin.

The importance of operational flexibility has been recognized in the literature. Recent works have studied flexibility from both technical and economic perspectives [40]-[41] and proposed systematic definition for flexibility [42]-[43].

The dispatch framework introduced in this report is seeking to provide operational flexibility by allowing for a discounted energy scheduling from wind generation.

It is critical to analyze both the features of the wind power production and the reserve procurement approaches, as well as the associated tradeoffs, in order to ensure an

efficient energy schedule and flexible wind dispatch margin reserve margin. As the operator relies on more wind energy production, the system faces more uncertainty, thereby requiring additional reserve. System reliability may be jeopardized if the wind energy production is less than what the operator anticipated. Thus, costly ancillary services and fast acting reserves have to be called upon to maintain the secure operation of the system. Dispatching a low level of wind, on the other hand, will result in inefficient utilization of wind power. The operational costs are, thus, expected to be higher since more energy will be scheduled from conventional units. To address these tradeoffs, one must account for the scheduling costs and the risk imposed to the system due to the intermittency of renewable resources.

In this chapter, a two-phase framework is developed to obtain appropriate policies for scheduling wind generation. In the first phase, a generation dispatch is performed to obtain the dispatch and reserve schedule for generation units. A scenario-based stochastic programming approach is leveraged to capture the effect of various possible wind scenarios. This initial phase minimizes the aggregate operating costs and risk costs relative to the modeled scenarios. In the second phase, the decision from the first phase is tested against a larger set of scenarios to ensure the adequacy of the scheduled energy and reserve.

3.2 Wind Farm Generation Model

In this subsection, wind generation models used for this study are described.

3.2.1 Short-term Wind Forecast Model

In this study, the Markov chain-based wind forecast model is used. This model takes into account the diurnal non-stationarity and the seasonality of wind [20] Using this framework, the probability distribution of the immediate future state of the wind farm output can be predicted based on the most recent state of the system. This probability distribution expresses the transition probability from the current state to the future one.

The scheduling framework modeled in this study is for the short-term, since it deals with hour-ahead decisions for acquiring energy and reserve. To determine the short-term schedule, the finite state Markov chain model is used. This model predicts the wind farm generation level in the next time epoch (10 minutes) to be among a few defined states with certain probabilities, thereby improving the tractability for stochastic programming.

3.2.2 Wind Scenario Generation

In the current study, the short-term 10-minute wind generation forecast based on the finite state Markov chain model is used to develop a scenario tree for the wind generation in the next hour, i.e., for the next 6 time intervals of 10 minutes. A scenario tree is generally represented by a finite set of nodes. It starts from a root node (state) at the first

period and branches into nodes (states) at each next period. Every scenario represents a sequence of wind farm states, in the next 6 time intervals. The transition probabilities are derived using the finite state Markov chain model developed based on the wind farm data. Fig. 3.2 shows the structure of the scenario tree for 6 time intervals.

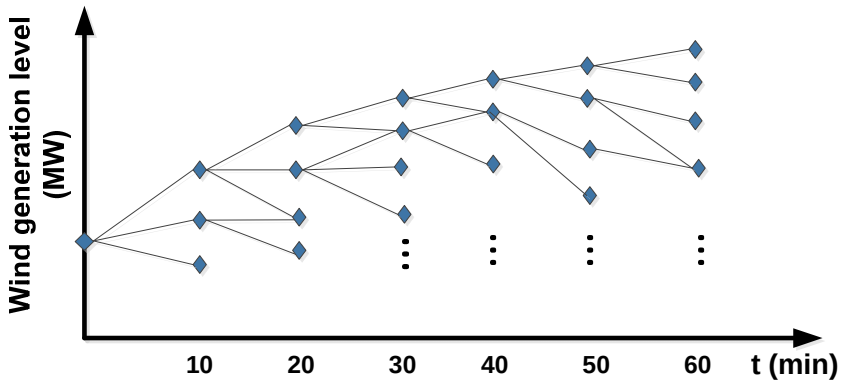

Fig. 3.2. Scenario tree generated for the next hour.

3.2.3 Scenario Selection

The computational effort for solving a scenario-based stochastic program depends on the number of modeled scenarios. In this study, in order to reduce the computational burden, a scenario reduction procedure is executed on the original set of scenarios. A clustering technique is used to come up with a few scenarios that properly represent the whole set of scenarios. In this study, the technique introduced by [44][44] is used, which reduces the scenarios to their best approximation based on the Kantorovich distance of probability distributions.

For two discrete probability distributions P and Q, with scenarios $\xi^j, \tilde{\xi}^j$ and probabilities p_i, q_j respectively, the Kantorovich distance is defined as:

$$D_k(P,Q) = inf\left\{ \begin{matrix} \sum_{i=1}^{S}\sum_{j=1}^{\tilde{S}} \eta_{ij} C_T\left(\xi^j, \tilde{\xi}^j\right): \eta_{ij} \geq 0, \\ \sum_{i=1}^{S} \eta_{ij} = q_j\,, \sum_{j=1}^{\tilde{S}} \eta_{ij} = p_i\,, \forall i,j \end{matrix} \right\} \quad (3.1)$$

where $C_T\left(\xi^j, \tilde{\xi}^j\right) \coloneqq \sum_{\tau=1}^{t} \left|\xi_T^j - \xi_T^j\right|, t = 1, \ldots, \mathrm{T}$ measures the distance between scenarios over the time horizon. If Q is the reduced probability distribution of ξ, the support of Q consists of scenarios ξ^j for $j \in \{1, \ldots, s\} \backslash J$ where J represents the index set of deleted scenarios. For a fixed J, the scenario set Q that has minimal distance to P can be computed. The minimal distance is

$$D_k(P,Q) = \sum_{i \in J} p_i \; min_{j \notin J}\, C_T\left(\xi^j, \tilde{\xi}^j\right). \quad (3.2)$$

The new probability of a remained scenario equals the sum of its previous probability and the probabilities of deleted scenarios that were closest to it with respect to C_T. The optimal choice of an index set for scenario reduction with fixed cardinality is an optimal reduction problem that can be solved using the iterative algorithm in [44]. The algorithm omits one scenario at a time till the desired number of scenarios is achieved.

3.3 Joint Energy and Reserve Scheduling with Flexible Wind Reserve Margin

In this section, a scenario-based stochastic dispatch and reserve scheduling problem based on the short-term wind farm generation forecast is formulated. In the proposed structure, it is assumed that the market operator clears the energy and ancillary services simultaneously, rather than clearing them sequentially [45]. The goal is to find the appropriate energy and reserve that can be scheduled from the wind farm to minimize the total cost. This total cost consists of the operational cost associated with procuring energy and reserve as well as the expected costs associated with inadequate appropriation of ancillary services.

The proposed procedure has a two-phase structure and aims to find the expected level of wind farm generation, relative to the predicted value, that the operator can utilize. It is assumed that the operator intends to perform the scheduling procedure for the next hour. This look-ahead dispatch allows for better planning of the resources, considering the 10-minute ramp up and ramp down constraints of the conventional generators.

In this study, the expected amount of the wind generation that the operator can utilize is expressed as a fraction of the predicted wind generation for that hour. This fraction is referred to as the flexible wind reserve margin policy factor throughout this report.

To find the best policy, the proposed two-phase procedure is performed for various factors. Initially, a certain fraction of the predicted wind generation is assumed to be utilizable. In the first phase, a stochastic program is solved. In the second phase, a risk analysis model is run to test the robustness of the first phase decisions. Section 3.3.1 and Section 3.3.2 describe these two phases. The process is repeated for various policy factors in order to find the optimal policy. The complete hour-ahead scheduling procedure can be viewed in Fig. 3.3.

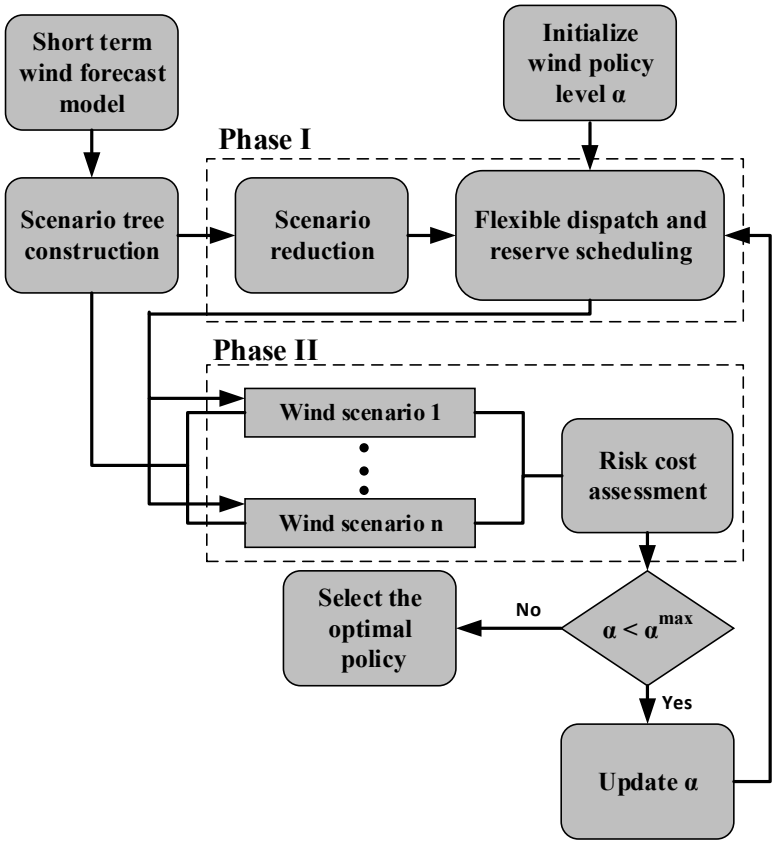

Fig. 3.3. Procedure to determine flexible wind reserve margin policy.

3.3.1 Mathematical Formulation of the Hour-ahead Risk-aware Energy and Reserve Scheduling

The stochastic energy and reserve scheduling problem can be shown by (3.3)-(3.28):

$$\textbf{Min} \quad \sum_{g,t}\left(C_g^e p_{gt} + C_g^{rc} r_{gt}\right) + \sum_{w,t}(C_w^e p_{wt} + C_w^{rc} r_{wt}) + \sum_{s,t}\pi_s\{\sum_n C_c^n(ls_{nst}^{+} + ls_{nst}^{-}) + \sum_w(C_p + C_w^{re})p_{wst}^{penalty} + \sum_g\left(C_g^{re} r_{gst}\right) + \sum_w(C_w^{re} r_{wst}) + \sum_w(C_w^{rc}\Delta_{wst})\} \quad (3.3)$$

Subject to:

Base case constraints:

$$P_g^{min}\overline{U}_{gt} \le p_{gt}, \forall g, t \quad (3.4)$$

$$p_{gt} + r_{gt} \leq P_g^{max} \overline{U}_{gt}, \forall g, t \quad (3.5)$$

$$0 \leq r_{gt} \leq R_g^{10} \overline{U}_{gt}, \forall g, t \quad (3.6)$$

$$\sum_{g \in G} r_{qt} \geq p_{gt} + r_{gt} + \sum_w \xi_{wt}, \forall g, t \quad (3.7)$$

$$\xi_{wt} \geq p_{wt} - \left(P_{wt}^f - \beta \sigma_{wt}\right), \forall w, t \quad (3.8)$$

$$p_{gt} - p_{g,t-1} \leq R_g^{10}, \forall g, t, \overline{U}_{gt} = 1, \overline{U}_{g,t-1} = 1 \quad (3.9)$$

$$p_{g,t-1} - p_{gt} \leq R_g^{10}, \forall g, t, \overline{U}_{g,t-1} = 1, \overline{U}_{gt} = 1 \quad (3.10)$$

$$p_{wt} + r_{wt} \leq \alpha P_{wt}^f, \forall w, t \quad (3.11)$$

$$p_{kt} - B_k(\theta_{nt} - \theta_{mt}) = 0, \forall k, t \quad (3.12)$$

$$-P_k^{max} \leq p_{kt} \leq P_k^{max}, \forall k, t \quad (3.13)$$

$$\sum_{g \in g(n)} p_{gt} + \sum_{k \in \delta^+(n)} p_{kt} - \sum_{k \in \delta^-(n)} p_{kt} + \sum_{w \in w(n)} p_{wt} = d_{nt}, \forall n, t \quad (3.14)$$

$$p_{wt}, r_{wt} \geq 0, \forall w, t \quad (3.15)$$

Second-stage constraints:

$$p_{kst} - B_k(\theta_{nst} - \theta_{mst}) = 0, \forall k, t \quad (3.16)$$

$$-P_k^{max} \leq p_{kst} \leq P_k^{max}, \forall k, t \quad (3.17)$$

$$\sum_{g \in g(n)} \left(p_{gt} + r_{gst}\right) + \sum_{k \in \delta^+(n)} p_{kst} - \sum_{k \in \delta^-(n)} p_{kst} + \sum_{w \in w(n)} (p_{wt} + r_{wst}) + ls_{nst}^+ - ls_{nst}^- = d_{nt}, \forall n, s, t \quad (3.18)$$

$$r_{gst} \leq r_{gt}, \forall g, s, t \quad (3.19)$$

$$-r_{gst} \leq r_{gt}, \forall g, s, t \quad (3.20)$$

$$P_g^{min} \leq p_{gt} + r_{gst} \leq P_g^{max}, \forall g, s, t \quad (3.21)$$

$$rr_{gst} = r_{gt} - r_{gst}, \forall g, s, t \quad (3.22)$$

$$-r_{wst} \leq r_{wt} + p_{wst}^{penalty}, \forall g, s, t \quad (3.23)$$

$$0 \leq p_{wt} + r_{wst}, \forall w, s, t \quad (3.24)$$

$$p_{wt} + r_{wst} + rr_{wst} \leq W_{wst}\ , \forall w, s, t \tag{3.25}$$

$$\Delta_{wst} \geq r_{wst} + rr_{wst} - r_{wt}, \forall w, s, t \tag{3.26}$$

$$\sum_{g \in g(n)} rr_{gst} + \sum_{w \in w(n)} rr_{wst} \geq p_{gt} + r_{gt}, \forall g, w, s, t \tag{3.27}$$

$$rr_{wst}, \Delta_{wst}, ls^{+}_{nst}, ls^{-}_{nst}, p^{penalty}_{wts} \geq 0, \forall w, n, s, t. \tag{3.28}$$

In the objective function (3.3), the first two summation terms represent the cost for scheduling energy and reserve capacity from generation units, including both conventional and wind generators. The remaining terms express the expected cost incurred over the set of considered scenarios. This part includes the load shedding cost, the penalty cost associated with the wind farm not being able to abide by its scheduled output, the cost of exercised reserve in each scenario, and the cost of the residual reserve from the wind. This last term will be further explained in the description of the constraints. Please note that c_c^n would be set to a relatively high value to prevent load shedding/generation surplus as much as possible. For situations where additional wind production is not beneficial, it is assumed that there will be wind spillage, preventing the generation surplus to occur.

Equation (3.4) provides the lower bound on generation dispatch. Equation (3.5) provides the upper limit on the energy and reserve scheduled from a conventional unit. Equation (3.6) enforces the reserve scheduled from each unit for each time interval to be within the 10-min ramping capability of the unit. Equation (3.7) presents the reserve requirement of the system; it indicates that the total reserve scheduled from conventional generation units should account for the outage of any single generator (N-1 reliability criterion) as well as a security margin added to account for the uncertainty of the scheduled wind energy.

Equation (3.8) presents the security margin considered for acquiring reserve in the presence of wind generations. Here, it is assumed that the operator should obtain additional reserve if the amount of scheduled wind is higher than a certain threshold. The threshold is set to be equal to the mean of the wind probability distribution function (predicted value) minus a factor β of the standard deviation. It is worth noting that this factor can also be used to set up a policy to determine reserve. A methodology similar to the one described for obtaining wind reserve margin can be applied for coming up with this reserve policy by addressing the trade-off between the scheduling and the risk costs. In the present study, however, this factor is assumed to be previously known and fixed, to avoid replicating the procedure.

Equations (3.9)-(3.10) show the ramp up and ramp down constraints for generators. Equation (3.11) sets the limit on the total energy and reserve that is scheduled from the

wind generator. This limit is expressed as a factor α of the predicted value. This factor is referred to as the flexible wind reserve margin policy factor. P_{wt}^{f} is the point forecast of the output of wind unit *w* for period *t* and is determined by calculating the expected value of wind generation for each time period, based on the generated scenarios.

Equation (3.12) describes the linearized line flow for each transmission asset. Equation (3.13) represents the transmission line operational limits. Equation (3.14) enforces the power balance at each node.

The second-stage constraints are intended to check the security of the first-stage decisions and must be satisfied for each of the modeled scenarios. Equation (3.18) enforces power balance in each node for each scenario. The second-stage generator outputs are based on the fixed first-stage generation dispatch plus the available reserve that is procured from the first-stage. The load violation terms have been added to ensure the feasibility of the problem for all scenarios.

Equations (3.19)-(3.20) enforce the actual implemented reserve to be less than the amount scheduled in the first-stage. Note that r_{gt} is the amount of reserve procured for both the upward and downward directions and, hence, has a positive value. Variable r_{gst} is the actual exercised reserve and can be both positive and negative. Equation (3.22) shows the residual reserve from conventional units, which is the amount of acquired reserve in the first-stage that has not been exercised in the recourse stage. This residual reserve can count toward the *N*-1 reliability criterion.

Equation (3.23) states that if the implemented downward reserve happens to be greater than the amount scheduled in the first-stage (due to wind intermittency), it should be penalized (a penalty term is added to the objective). Note that it is also possible to have a violation of the upward reserve; for situations where additional wind production is not beneficial, it is assumed that there will be wind spillage. Equation (3.24) ensures that the implemented downward-reserve will not exceed the scheduled energy from wind. Equation (3.25) indicates that if the realization of wind is more than the amount used as energy and reserve in the second-stage, it can be considered as residual reserve and count towards the N-1 reserve criterion. Equation (3.26) shows the amount of potential reserve provided by wind unit in scenario s that has not been compensated for in the first-stage. Equation (3.27) conveys that the residual reserve after dealing with wind power uncertainty should suffice for satisfying the *N*-1 contingency reserve requirement.

The solution of this first phase determines the dispatch and reserve decisions, i.e., p_{gt}, r_{gt}, p_{wt}, r_{wt}. The optimal values of these variables are then fed as inputs to the risk analysis phase.

3.3.2 Mathematical Formulation for the Risk Analysis Phase

The risk analysis phase is a verification of the first-stage decisions. In this phase, a deterministic model is used to test the first phase decision against every possible scenario in the scenario tree. Given the first phase decisions for energy and reserve schedule, the second phase tries to minimize the realized costs associated with each possible scenario, including the cost of exercised reserve, the penalty cost associated with the wind farm not being able to abide by its scheduled output, the cost of the residual reserve from the wind, and the load shedding cost. The model is formulated as follows:

$$\text{Min} \quad \sum_t\Big(\sum_g\big(C_g^{re} r_{gst}\big) + \sum_w\big(C_w^{re} r_{wst}\big) + \sum_w\big(C_w^{rc}\Delta_{wst}\big) + \sum_w\big(C_p + C_w^{re}\big)p_{wst}^{penalty} + \sum_n C_c^n\big(ls_{nst}^{+} + ls_{nst}^{-}\big)\Big) \tag{3.29}$$

Subject to:

constraints (3.18)-(3.28).

In this phase p_{gt}, r_{gt}, p_{wt}, r_{wt} are fixed parameters determined in the previous phase. The risk analysis model is run for a larger number of scenarios to test the performance of the model from the first phase. The cost in this second phase is a measure of the risk imposed to the system operation by the decisions made in the first phase. If the decisions of the first phase are robust against the deterministic runs in the second phase, less cost would be incurred in this second phase.

3.3.3 Wind Scheduling Policy Determination

As mentioned in the previous section, parameter α is introduced into the dispatch structure to allow for determining the appropriate policy for scheduling energy and reserve from wind. Beginning with a small value for α, the optimization problem described in Section 3.3.1 is solved. The obtained solution gives the optimum schedule as well as the operational cost for that specific value of α. The resulting energy and reserve schedule is then used as the input for the risk analysis problem described in Section 3.3.2 to come up with the risk cost associated with that scheduling policy.

This procedure is repeated for various α values and the optimum operational and risk cost associated to each policy is recorded. The policy that has the minimum sum of the scheduling cost and the risk cost is expected to be the least-cost policy for scheduling energy and reserve from wind.

3.4 Numerical Results

3.4.1 Test System and Simulation Setup

The proposed structure has been applied to the IEEE Reliability Test System (RTS)-96 [46]. It is assumed that each generator's reserve bid is 15% of its energy bid. The test system is modified by integrating a 500 MW wind farm, at bus 4. The wind generation data of a wind farm for the year 2010 [20] is used after proper scaling to suit the chosen wind farm capacity. The average wind penetration (energy produced by wind generation / load capacity) is 7%.

Before running the hour-ahead dispatch, a deterministic day-ahead unit commitment (UC) is performed using the day ahead persistent point forecast to determine the commitment schedule for the 24-hour horizon. The restrictions, such as the minimum up and down time limits, are enforced in this stage. While it is assumed that wind is not allowed to provide reserve within the day-ahead UC model, the proposed model is amenable to such a day-ahead UC solution. The resulting on/off status of the generators is fed into the modeled hour-ahead energy and reserve scheduling program.

The optimality gap for the unit commitment problem has been set to 0.01. The original problem has 7128 binary and 9360 continuous variables, with 42278 constraints. This is decreased to 7008 binary and 9184 continuous variables with 26086 constraints in the reduced MIP problem. The resulting on/off status of the generators is fed into the modeled hour-ahead energy and reserve scheduling program.

The hour-ahead model includes 10-minute intervals across a 1-hour horizon. For the current simulation, the finite state Markov model of the spatio-temporal analysis for the 9 AM-12 AM epoch is used since the output of the wind farm exhibits a high variability in this epoch [20]. In this report, the hour-ahead scheduling has been performed for four typical days in different seasons. The wind scenarios are generated in a scenario tree format for the next 6 time intervals, i.e., a 6-stage scenario tree is constructed. As explained in Section 3.2.2, in each stage a set of branches are added to the tree to represent the possible transitions to the next interval based on the 1-step Markov chain transition matrix. Due to the strong time-correlation that the wind data exhibit, the number of probable paths of this tree stays within a reasonable range (about 3000 scenarios for a 100-state Markov model, instead of 100^6). For the first phase, i.e., the stochastic programming phase, the number of scenarios is further reduced using the clustering algorithm described in Section 3.2.3 and a total of 50 scenarios are considered. The standard deviation factor for (8) is set to 1 (β=1). The problem is a linear program; existing commercial grade linear programming solvers can efficiently handle this SCED problem today for large-scale systems.

In the second phase, the risk analysis model is run for all the possible scenarios. The optimal policy is determined based on the results obtained from these two phases.

All simulations are performed using the Gurobi solver in AMPL environment on an Intel (R) Core (TM) i7-3770 CPU @3.4 GHz computer with 16 GB of memory. The solution time is of the order of a few seconds for each scheduling run in the first phase and less than 0.1 second for each risk analysis run in the second phase.

3.4.2 Results and Discussions

Starting from an initial wind policy, the first and second phase optimizations are solved for various values of α as described in Section 2.3. These simulations started from a no wind policy ($\alpha = 0$), but the initial policy can be set to a higher value, e.g., the minimum predicted level in the scenario tree to speed up the process. The simulation results for the 9 AM-10 AM epoch of April 1st are plotted in Fig. 3.4. As Fig. 3.4 shows, the scheduling cost decreases monotonically as the expected utilizable generation from wind is increased. The reason is that more energy is scheduled from the cheap wind generators. The risk cost, however, increases with α since, by scheduling more wind, there will be a higher probability of not being able to supply the load. In other words, there are more instances that the actual wind is less than what is counted on in the first-stage. The figure suggests that, for the simulated hour, the total cost of the two stages reaches its minimum around $\alpha = 1.1$, i.e., when the total scheduled energy and reserve is 1.1 times the predicted value. Figures 3.5, 3.6 and 3.7 show the scheduling cost versus the risk cost for the same time interval on 3 other days in other seasons. The optimal policy factor α is different for different months, ranging from 0.7 to 1.1, but the trends are similar in all of the figures.

Note that in this procedure the simulations are performed for a discrete set of values for α and thus, the lowest total cost found in this way is not the exact minimum cost for the continuous range of α.

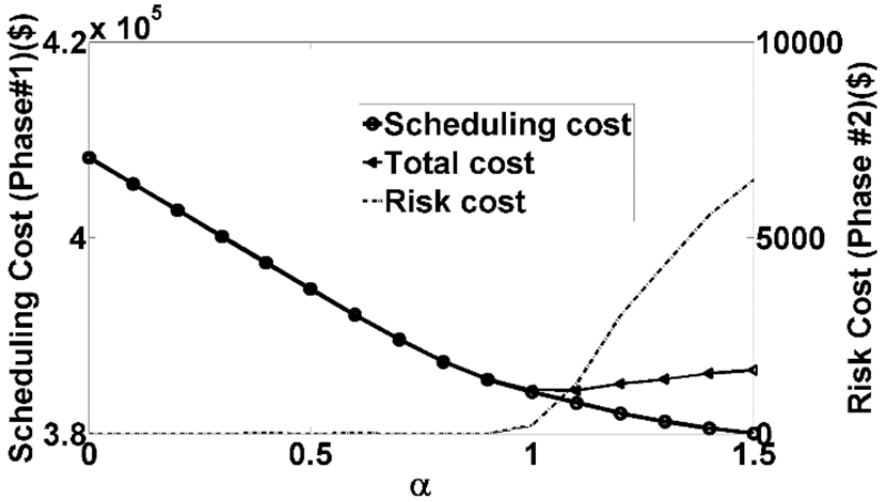

Fig. 3.4. Scheduling cost and risk cost as a function of the flexible wind reserve margin policy factor (April).

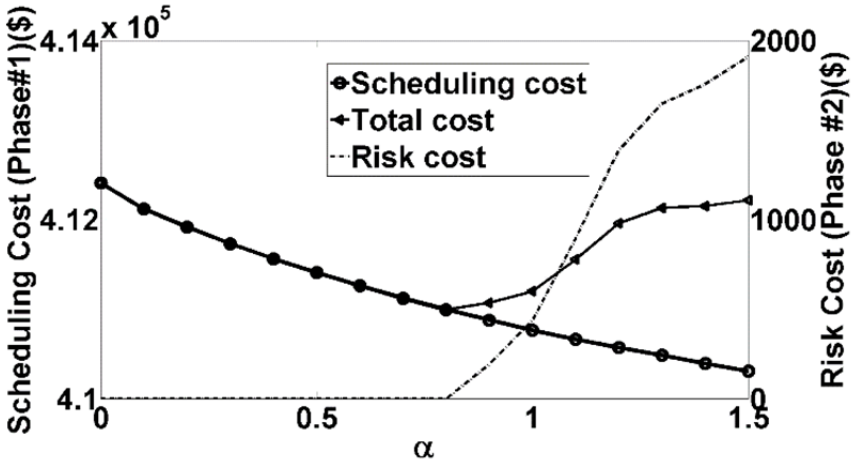

Fig. 3.5. Scheduling cost and risk cost as a function of the flexible wind reserve margin policy factor (August).

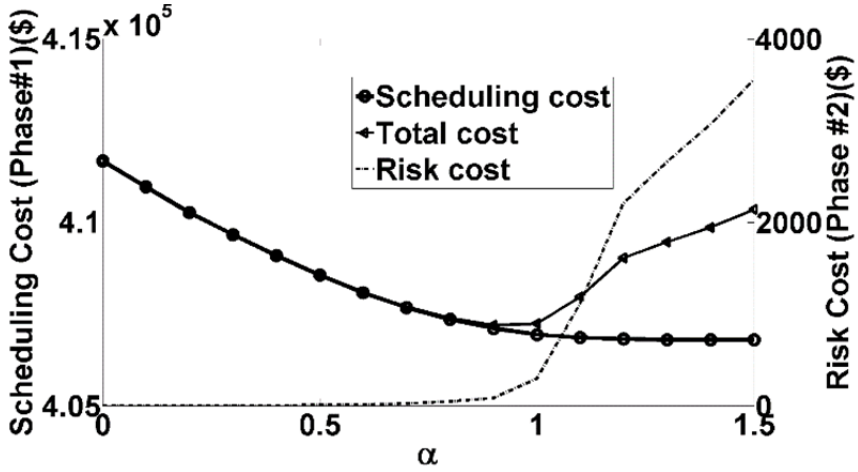

Fig. 3.6. Scheduling cost and risk cost as a function of the flexible wind reserve margin policy factor (October).

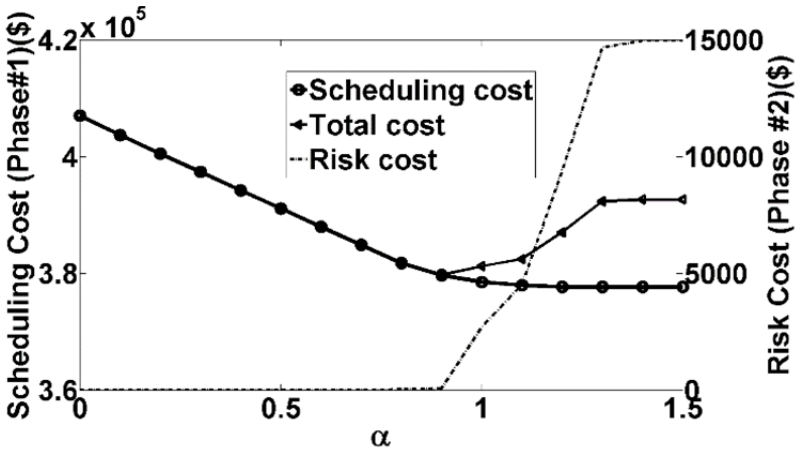

Fig. 3.7. Scheduling cost and risk cost as a function of the flexible wind reserve margin policy factor (February).

Fig. 3.8 presents the scheduled energy and reserve from wind unit for the 6 future 10-min intervals, with respect to the predicted value. Note that the energy scheduled from the wind is below the forecasted mean but the total energy and reserve scheduled from the wind can go above the forecasted mean to provide an opportunity of using extra wind for balancing tasks. Also note that, as explained earlier, a scenario tree structure has been used for deriving the future possible scenarios. The number of possible outcomes increases as we move forward in the scenario tree. Hence, the standard deviation of the forecast error increases with the prediction horizon. As a result, the operator is less confident about the outcome of the wind farm and commits less energy and instead more reserve from wind generation in later time intervals as suggested by Fig. 3.8.

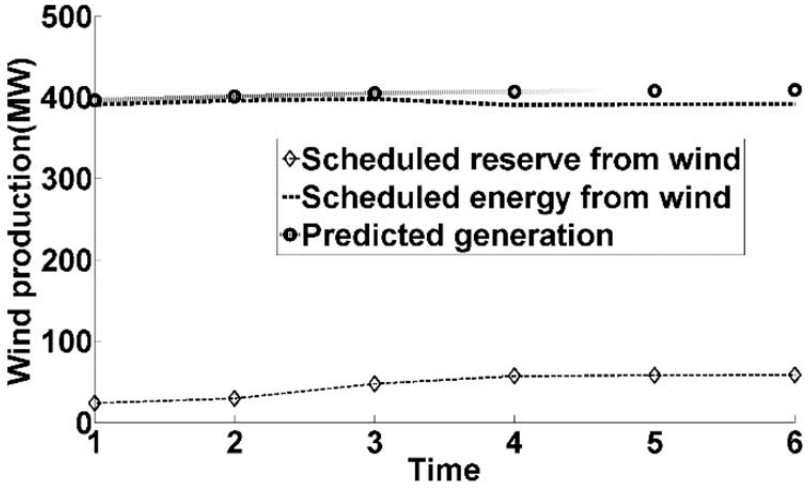

Fig. 3.8. Scheduled energy and reserve from wind vs. the forecasted level.

As described in Section 3.3.3, the stochastic procedure to determine the wind policy is performed offline. To evaluate the actual performance of the selected policy, the obtained policy needs to be tested against real-time data. In this study, the data for a specific hour of one day have been used to come up with the optimum policy factor. For this particular example, it is assumed that the determined policy based on this offline analysis is then used for the same hour in the following day. Fig. 3.9 shows the simulation results for the first week in October. The results are compared to a benchmark policy for the assumed set of scenarios; this benchmark policy would be obtained if the operator had the ability to run this offline approach in real-time. As Fig. 3.9 suggests, using the proposed forecast based policy can decrease the operational costs compared to the case where no flexible wind reserve margin policy factor is applied. The forecast based policy also performs well relative to the benchmark, without imposing the same real-time computational burden to the system.

Fig. 3.10 illustrates the amount of energy and reserve under different wind penetration schemes. Compared with the case of 10% penetration level, more energy and reserve is scheduled from wind farms for higher penetration levels. Also, the amount of energy scheduled from conventional units is less when wind penetration is increased. The results suggest that the proposed model is beneficial for dealing with the large integration of wind, which is assumed to introduce more uncertainty to the operation of the system.

It is worth noting that the optimal choice for the flexible wind reserve margin policy factor depends on the wind generation forecast, as well as the operating conditions of the power system. Therefore, the policy factor is going to be different for different wind generation levels, load levels, and the system operation conditions. Future work should investigate various load parameters (e.g., hourly data, weekday and weekend data) as well as other system operational parameters (e.g., transmission congestion patterns) to assort the policy factors based on wind generation levels and system operational conditions. These issues are further discussed in the next chapter.

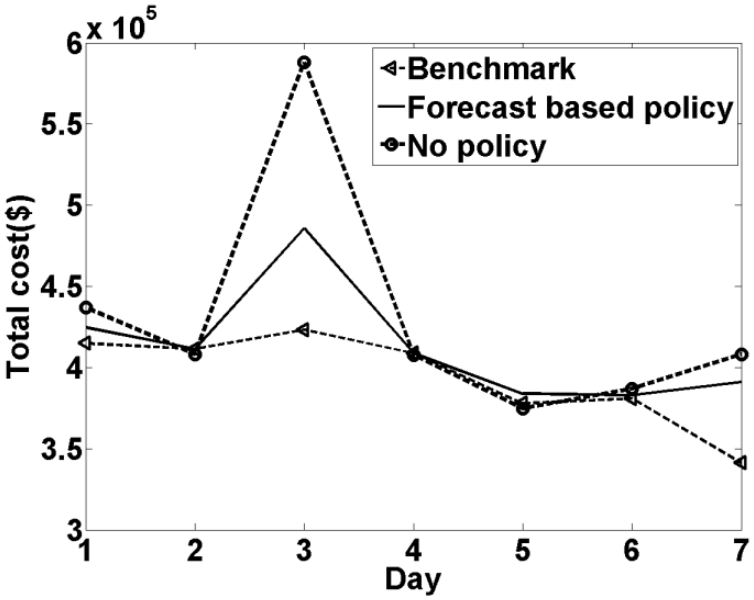

Fig. 3.9. Performance of the proposed policy determination vs. no policy and benchmark policy for a sample week in October.

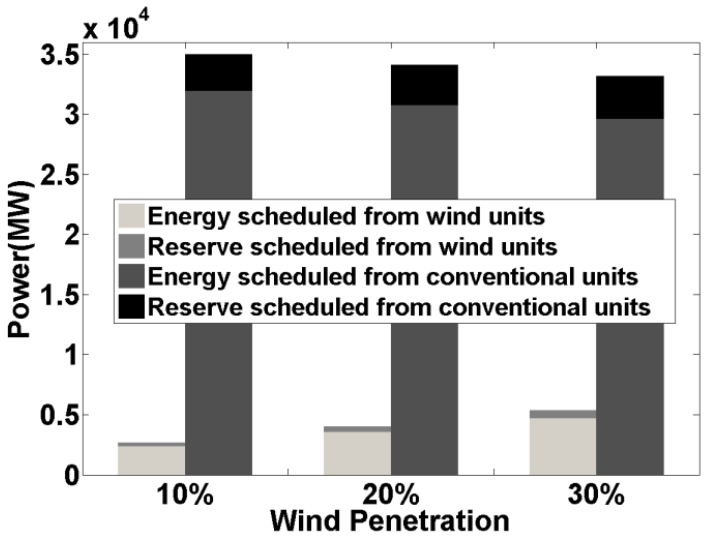

Fig. 3.10. Scheduled energy and reserve vs. penetration level.

The proposed flexible dispatch model seeks a balance between the operational costs and risk by allowing for flexible scheduling from wind power producers. Underestimating wind power allows the wind producer to ramp up when extra wind power production is

available. Control mechanisms such as controlling the blade pitch would allow for adjusting the rotation speed and the generated power. Another simple way is to allow the wind production from the previously locked turbines. To elaborate, out of the entire wind farm turbines, a subset are producing power whereas the rest are locked and not producing even though they could. They can be unlocked and allowed to produce. In the proposed model, if the wind is underestimated and there is the ability to generate more and the system needs it, other turbines can be turned on as required by the system to provide reserve. If the system does not need the extra wind generation, wind curtailment is allowed, which would be performed by shutting down the extra wind turbines.

It is apparent that the optimal choice for the wind policy depends on the cost of curtailing load. In this study, the demand is considered to be perfectly inelastic and a fixed value of lost load (VOLL) has been applied to penalize the load shedding. However, if the demand is considered to be elastic, i.e., if demand response is taken into account, the risk costs can be reduced. Considering demand response can allow for larger wind reserve margin policy factors by introducing another degree of freedom in the proposed flexible dispatch.

3.5 Conclusions

Integration of large-scale wind generation in the power system increases the uncertainty that the operator has to deal with due to the variability of the wind energy. The predicted wind generation using forecasting methods may not be the amount that is reliable for the operation of the system. Utilizing the concept of flexible wind reserve margin allows the operator to allocate a discounted amount of wind for energy, leaving a reliability margin to hedge against uncertainty. The extra production of the wind farm can then be used for balancing purposes. In this report, a joint hour-ahead energy and reserve scheduling framework is proposed. A finite-state Markov chain 10-minute-ahead wind power forecast model, based on spatio-temporal analysis, has been utilized to calculate the conditional probability distribution of the wind farm generation for each step. The presented framework is used to find the appropriate level for allocating wind based on the predicted output. Numerical studies, via the IEEE-96 test case, demonstrate the significant benefits obtained by incorporating the flexible wind reserve margin using a Markov-chain-based forecast. The actual and forecasted wind generation data are used to analyze the effectiveness of the presented model. The results communicate that scheduling the flexible wind reserve margin will allow the operator to increase the reliability margin of the system while reducing the total cost. Discounting the scheduled generation from wind would improve the reliability through handling the uncertainty at an early stage. It also addresses the existing cost trade-off between scheduling generation from wind and the risk associated with wind farm uncertainty and improves the overall cost of supplying the demand. The proposed structure can be effectively used to deal with the forecast errors and achieve a more secure system operation.

4. Offline Optimization of Reserve Policy Factors for Scheduling Wind Energy and Reserve

The focus of the present chapter is on developing a structure that uses offline analysis to develop wind reserve margin policies, which can be employed in real-time operations to deal with uncertainty. An algorithm, based on the approach used in chapter 3, has been applied to create offline policies for discounting wind generation and scheduling energy and reserve in presence of wind.

4.1 Introduction

Wind generation uncertainty encourages system operators to apply stochastic approaches. Stochastic programming methods can be too time-consuming to obtain an efficient solution in real-time operations, which would make them impractical. For this reason, inefficient, but fast, deterministic approaches are preferred over efficient, but slow, stochastic ones. The challenge to implement stochastic programming is also due to the computational burden that virtual bidding is adding to market security constrained unit commitment (SCUC) and security constrained economic dispatch (SCED) models by increasing the amount of active transmission constraints. Market pricing is also another barrier against the adoption of stochastic programming.

In real-world operational practices, the operating reserve is usually determined based on an ad-hoc deterministic rule. In existing market models, deterministic reserve proxy constraints are applied in SCUC and SCED. One basic policy, which is a necessary condition for *N*-1, states that the scheduled reserve quantity should exceed the single largest contingency. Other deterministic rules describe the required reserve as a function of both load level and wind generation level. The 3+5 rule suggests that the reserve should not be less than 3% of predicted load plus 5% of predicted wind generation [54].

It is worth noting that these rules are operational state independent except for acquiring reserves based on some fixed percentage of wind, hydro, or load level. This motivates developing improved deterministic policies to better exploit the flexibility of power systems in presence of operating condition uncertainty. Offline stochastic simulations can be used to generate such deterministic policies. Offline approaches eliminate real-time computational issues of stochastic programming.

This report aims to assess the benefit of such hybrid methods in dealing with uncertain operating conditions. In the previous chapter a framework was presented that enhanced the flexibility of the system by allowing the wind generators to leave a flexible reserve margin. The proper level of wind reserve margin can be determined using an optimization framework that tries to strike a balance between the operating costs and the risk associated with the mismanagement of wind generation.

With the advent of computing and data storage capabilities, utilities are going to be capable of handling extremely large data sets. These data sets, often called big data, are used to improve decision-making. The development of data mining techniques provides a promising solution to handle the mentioned challenge regarding running real-time stochastic programs.

Data mining approaches have been applied in various domains of power system studies including dynamic security assessment [55]-[58], load forecasting [59]-[60] and wind generation prediction [61]-[64]. Learning schemes have been proposed to leverage the power of data mining tools. In such schemes a knowledge base is, first, prepared through comprehensive offline studies, in which a number of forecasted operating states are used to create a set of training cases. Then, the knowledge base is used to create classification models that characterize the decision rules to determine policies. The decision rules are, finally, used to map the real-time measurements to the classifications of the system conditions for making operation decisions.

In this chapter, an optimization model serves as a hypothetical, ideal reference case to determine the dispatch and reserve policies. Given the large number of possible operating conditions, in order to be able to use this approach, one needs to classify the operating conditions and find the optimal policy for each category. The wind flexible reserve margin is assumed to be a function of the generation and load conditions. The system operator can then use the near real-time measurements fro m the wind farm to choose a proper policy based on the classified operating conditions.

In this study, a training procedure has been proposed for using stochastic methods as well as the wind forecasting models to come up with proper policies for deploying wind generation in power system. The merits of the proposed method are twofold. First, the uncertainty is addressed by leveraging the scenario-based stochastic method in offline analysis. Second, the real-time procedure stays easy to implement by deploying deterministic policies resulted from offline studies.

Subsequently, a testing method is derived to assess the performance of the policies obtained through the proposed training procedure for scheduling wind reserve margin. The performance of the proposed policy training algorithm is compared with its counterparts without applying the trained policies. The results show that the training based on the risk-aware scheduling can reduce the overall cost. Therefore, it is shown that the proposed structure allows for capturing the benefits of a stochastic scheduling without having to deal with a large set of scenarios in real-time.

4.2 Training the Policy Factors (Offline Analysis)

As described in chapter 3, a flexible wind dispatch policy is used, where the amount of the wind generation that the operator can utilize is expressed as a fraction of the forecasted wind generation. This fraction is referred to as the wind reserve margin policy factor throughout this report.

The algorithm proposed in the previous chapter for developing such policy factors, solves a scenario-based stochastic dispatch and reserve scheduling problem based on the short-term wind farm generation forecast. The short-term 10-minute wind generation forecast based on the finite state Markov chain model is used to develop a scenario tree for the wind generation in the next hour, i.e., for the next 6 time intervals of 10 minutes.

The resulted policy should tell the operator the level of wind farm generation that can be scheduled for the next hour. One challenge in performing this look-ahead dispatch is that the number of scenarios increases with the increase in the length of interval. Furthermore, if the system includes multiple wind farms, the total number of scenarios will increase rapidly. Running a stochastic optimization program for such cases would take a significant time and cannot be performed in real-time.

As mentioned in Section 4.1, one way to overcome this challenge is to resort to offline simulations for training the dispatch model. The results can be classified based on the initial conditions. In real time, the operator can use the near real-time measurements to map the current conditions of the system to the classified set and select the proper policy based on the results of the offline procedures. Fig. 4.1 presents an overview of the offline and real-time procedures.

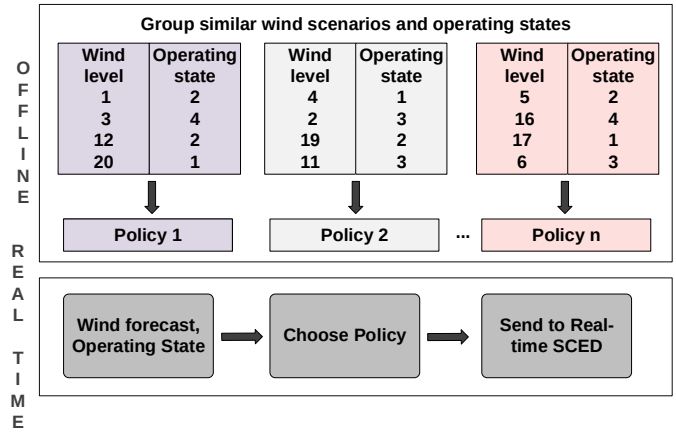

Fig. 4.1. The offline training and the real-time implementation procedures.

Note that the Markov chain wind forecast models that are used for this study are designed offline and their parameters, although different for different months and epochs, are assumed to be constant. This allows us to train the flexible wind dispatch policies for various initial conditions in an offline manner, based on the constant parameters of the forecast model.

The forecast model outlines the spatial and temporal dynamics of the wind farm aggregate power output using data-driven analysis. Due to the non-stationary distributions of wind farm generation, the models (Markov chains) used to derive

distributional forecasts, can have quite different parameters for different months and different epochs.

Therefore, forecast models are generated separately for each month and each epoch. Furthermore, when estimating the parameters of Markov chains, relevant historical data, i.e., the historical data from the same month and the same epoch, can be used. It is worth noting that the forecast Markov models can be updated, periodically, based on the new data.

Please note that the scenario sets used for the policy training procedure are chosen based on the assumptions regarding the wind forecast model that is used. The policy training procedure would be designed differently if a different wind forecast model is used. It is worth noting that the assumptions made when choosing a forecast model would impact the performance of the policy training algorithm. In other words, the training procedure must be designed in accordance with the observations from the wind farm data.

Another operating condition that affects the dispatch policy is the load condition. To take into account the diversity of load profiles and weather conditions, the calculations must be repeated for as many days as required to represent the modeled month/epoch. In the present study, the analysis has been performed for two load types (weekday and weekend).

Fig. 4.2 shows the training procedure for various time epochs and months; for each Markov model, 20 initial wind states have been trained and 2 different load levels have been considered. For each condition set, {month, epoch, load, wind state}, the policy factor is obtained using the two-phase method proposed in chapter 3. The outline of this two-phase method is briefly reviewed in the following section.

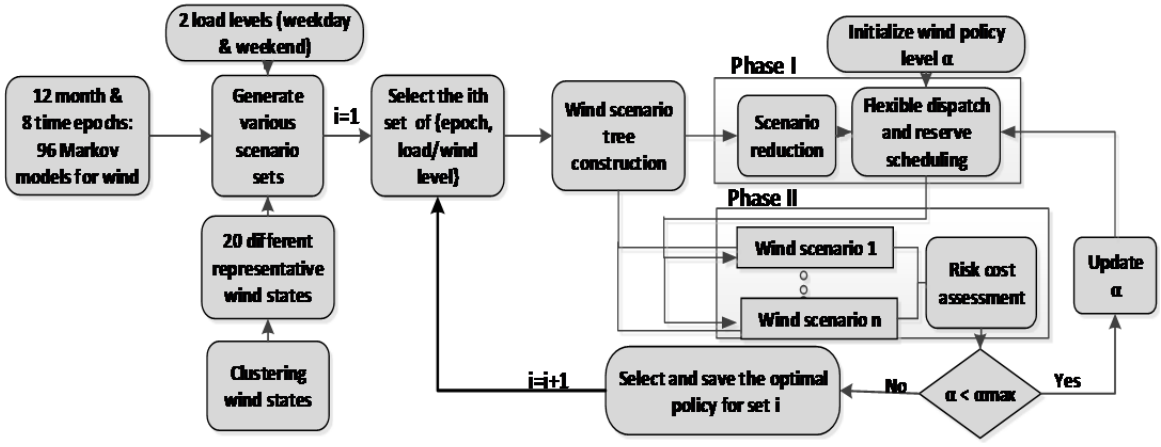

Fig. 4.2. Offline prediction-based policy training procedure.

In real-time, the actual wind power realization is compared to the trained initial wind levels and the nearest initial level is determined. Similarly, the nearest trained load level is deter-mined. The policy obtained for that nearest wind level and the nearest load level is then implemented in the real-time model.

4.3 Outline of Joint Energy and Reserve Scheduling

As described earlier in chapter 3, the approach for finding the best policy has been formulated in two phases. In the first phase a scenario-based stochastic dispatch and reserve scheduling problem is solved based on the short-term wind farm generation forecast. This problem uses a reduced set of scenarios and its goal is to find the appropriate energy and reserve that can be scheduled from the wind farm to minimize the total cost. The total cost consists of the operational cost associated with procuring energy and reserve as well as the expected costs associated with inadequate reserve allocation.

The solution of this first phase determines the dispatch and reserve decisions, i.e., p_{gt}, r_{gt}, p_{wt}, r_{wt}. The optimal values of these variables are then fed as inputs to the risk analysis problem in the second-phase. In this phase, a deterministic model is used to test the first phase decision against every possible scenario. This phase aims to model the uncertainty that has not been modeled in the first phase in the reduced set of scenarios.

Please note that the result of the first phase is not the true optimal value (extensive scenario-based stochastic model). This requires ensuring the stability of the scenario-based stochastic program, which is solved using the reduced set of scenarios. The stability of a stochastic program can be stated in form of in-sample and out-of-sample requirements [24]. Here, the results of the stochastic programming on the reduced set of scenarios is tested against all the scenarios to ensure out-of-sample stability. Given the first phase decisions for energy and reserve schedule, the second phase minimizes the realized costs associated with each possible scenario.

To find the best policy, the two-phase procedure is performed repetitively for various factors. Initially, a certain fraction of the predicted wind generation is assumed to be utilizable. Beginning with this small value for α, a stochastic program is solved using the reduced set of scenarios in the first phase. The obtained solution gives the optimum schedule as well as the operational cost for that specific value of α. In the second phase, a risk analysis model is run to come up with the average risk cost associated with that scheduling policy.

The overall problem can be described in the following simplified form:

$$\text{Min}_{\alpha}\, scheduling\ cost(\alpha) + \sum_s risk\ cost_s(p^*_{gt}, r^*_{gt}, p^*_{wt}, r^*_{wt}) \quad (4.1)$$

Subject to:

$$(p^*_{gt}, r^*_{gt}, p^*_{wt}, r^*_{wt}) \in argmin_{(p_{gt}, r_{gt}, p_{wt}, r_{wt})}\, scheduling\ cost(\alpha) \quad (4.2)$$

$$0 \leq \alpha \leq 1. \quad (4.3)$$

In order to obtain an approximate solution to this problem, the value of α is varied. The described procedure is repeated for various α values and the optimum operational and risk cost associated to each policy is recorded. The policy that has the minimum sum of the scheduling cost and the risk cost is expected to be the least-cost policy for scheduling energy and reserve from wind.

4.4 Real-time Implementation of Policies

This section describes the real-time implementation of proposed policy, i.e. the prediction-based policy, as well as three benchmark methods which are used for comparison. The real-time structure of the proposed prediction-based policy is explained in Section 4.4.1. The next policy, which will be described in Section 4.4.2, makes use of the forecasted distribution to schedule a certain percentile of the forecasted generation. The third policy, which is described in Section 4.4.3, is a fixed policy that utilizes a fixed fraction of the forecasted mean. Section 4.4.4 introduces the base case where no policy is used. Section 4.4.5 develops a structure for analyzing the performance of the described policies. Specifically, a risk analysis structure is proposed to test the real-time implementations.

4.4.1 Prediction-based Policy

In order to evaluate the results of the proposed training method, one should examine the policy derived by the offline procedure against a large set of scenarios. The testing procedure should be compatible with the way the policy has been determined. Note that the online implementation tool does not perform the risk analysis phase, i.e., it deploys the generated policy into the first phase problem to determine the energy and reserve schedule (p_{gt}, r_{gt}, p_{wt}, r_{wt}). The real-time procedure implemented in the current study is, thus, as follows:

Assume that the policies have been obtained for a number of condition sets, {month, epoch, load profile, wind state}, using the stochastic optimization model. For different initial wind states in any epoch, choose the policy $\bar{\alpha}$ based on the one developed for the nearest load and wind state. Put the policy in the optimization described below and solve

the stochastic process for the reduced set of scenarios. Fig. 4.3 shows the flowchart for this procedure. Note that the constraints in the following formulation are the same constraints as presented in chapter 3 and are not explicitly presented again for the sake of brevity.

$$\text{Min} \quad \sum_{g,t}\left(C_g^e p_{gt} + C_g^{rc} r_{gt}\right) + \sum_{w,t}(C_w^e p_{wt} + C_w^{rc} r_{wt}) + \sum_{s,t}\pi_s\{\sum_n C_c^n(ls_{nst}^{+} + ls_{nst}^{-}) + \sum_w\left(C_p + C_w^{re}\right)p_{wst}^{penalty} + \sum_g\left(C_g^{re} r_{gst}\right) + \sum_w(C_w^{re} r_{wst}) + \sum_w(C_w^{rc}\Delta_{wst})\} \quad (4.4)$$

Subject to:

constraints (3.4)-(3.10),

$$p_{wt} + r_{wt} \le \bar{\alpha} P_{wt}^{f}, \forall w, t \quad (4.5)$$

constraints (3.12)-(3.28).

In order to evaluate the performance of this policy, the results of this problem (p, r_{gt}, p_{wt}, r_{wt}) can be sent to a risk analysis program. This risk analysis is described in Section 4.4.4.

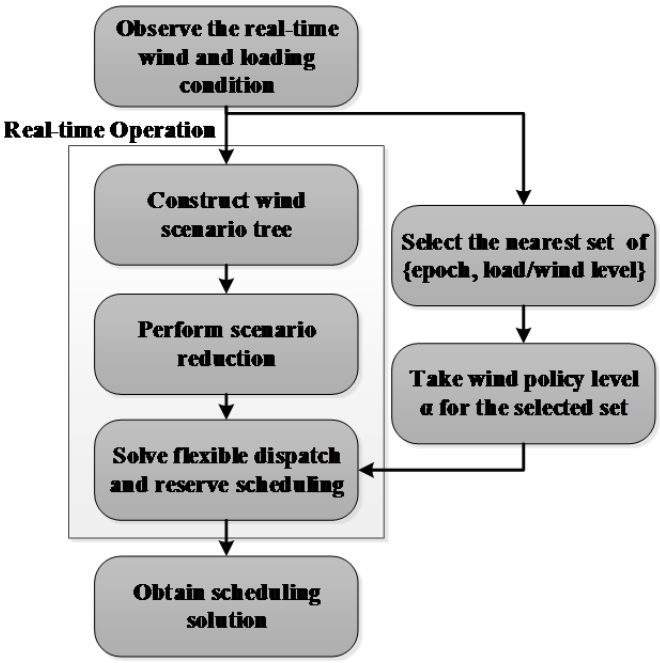

Fig. 4.3. Real-time implementation procedure of the proposed policy.

4.4.2 Probability Distribution Percentile-based Policy

In this approach a probabilistic metric (90% percentile of the cumulative distribution of predicted wind) has been used. Fig. 4.4 displays the procedure. This percentile is applied instead of the policy factor in the original 2-stage stochastic process for a reduced set of scenarios to allow for comparison with the proposed approach:

$$\text{Min} \quad \sum_{g,t}\left(C_g^e p_{gt} + C_g^{rc} r_{gt}\right) + \sum_{w,t}(C_w^e p_{wt} + C_w^{rc} r_{wt}) + \sum_{s,t} \pi_s \{ \sum_n C_c^n (ls_{nst}^{+} + ls_{nst}^{-}) + \sum_w \left(C_p + C_w^{re}\right) p_{wst}^{penalty} + \sum_g \left(C_g^{re} r_{gst}\right) + \sum_w (C_w^{re} r_{wst}) + \sum_w (C_w^{rc} \Delta_{wst}) \} \quad (4.4)$$

Subject to:

constraints (3.4)-(3.10),

$$p_{wt} + r_{wt} \leq per_{wt}^{f}, \forall w, t \quad (4.6)$$

constraints (3.12)-(3.28).

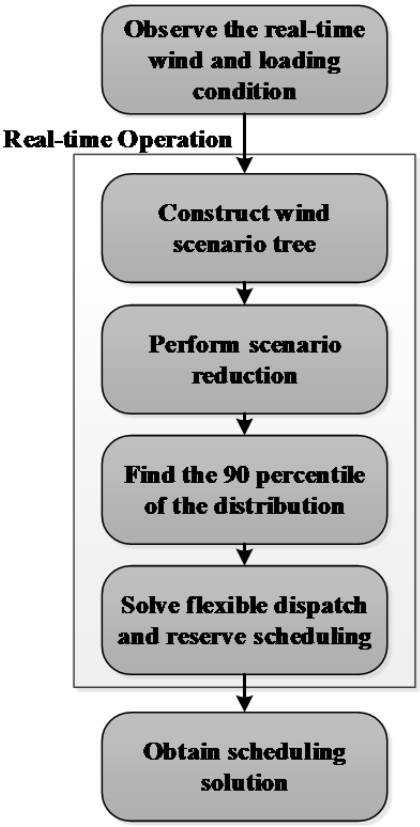

Fig. 4.4. Real-time implementation procedure of the probability distribution-based policy.

4.4.3 Fixed Policy

The fixed policy assumes a fixed value for policy factor α, regardless of the value of input for wind generation. This fixed policy is put in the original 2-stage problem formulation as shown below:

$$\text{Min} \quad \sum_{g,t}\left(C_g^e p_{gt} + C_g^{rc} r_{gt}\right) + \sum_{w,t}(C_w^e p_{wt} + C_w^{rc} r_{wt}) + \sum_{s,t} \pi_s \{ \sum_n C_c^n (ls_{nst}^+ + ls_{nst}^-) + \sum_w \left(C_p + C_w^{re}\right) p_{wst}^{penalty} + \sum_g \left(C_g^{re} r_{gst}\right) + \sum_w (C_w^{re} r_{wst}) + \sum_w (C_w^{rc} \Delta_{wst}) \} \quad (4.4)$$

Subject to:

constraints (3.4)-(3.10),

$$p_{wt} + r_{wt} \leq \bar{\alpha} P_{wt}^f, \forall w, t \quad (4.7)$$

constraints (3.12)-(3.28).

In this study, $\bar{\alpha}$ for the deterministic approach is assumed to be equal to 90%.

4.4.4 Base case

The base case is when no policy is employed, meaning that the operator doesn't discount the wind, or $\bar{\alpha}$ =1.

4.4.5 Performance Analysis Structure

A risk analysis program, similar to the one described in (3.29), can be used to evaluate the performance of the different policies. Fig. 4.5 shows the risk evaluation procedure used for testing the results of the described policies.

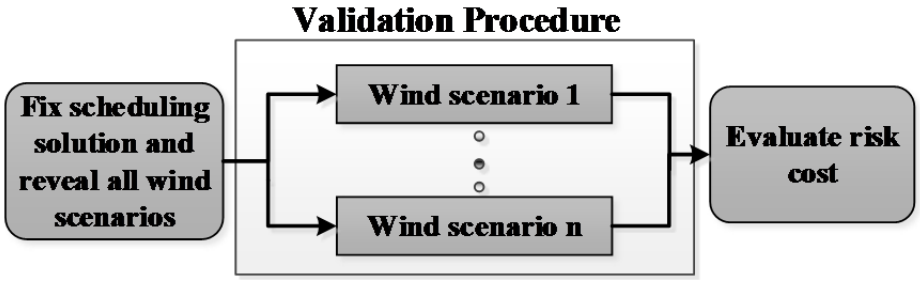

Fig. 4.5.Testing procedure based on risk evaluation.

The next section presents the numerical test results, performed on a test system, for the three policies described in Sections 4.4.1, 4.4.2 and 4.4.3.

4.5 Numerical Results

4.5.1 The Single Wind Farm Case

As mentioned before, the major limitation in a stochastic model is that modeling all the scenarios is not time efficient. If the number of scenarios is large, modeling all scenarios can make the problem intractable, especially, in a large system. Usually, a reduced set of scenarios is used instead. In this section the 3 different policies, which were proposed in Section 4.4, are tested. Note that all the three approaches described have a similar structure. First, a stochastic problem is solved for a reduced set of scenarios. To evaluate the performance, the energy and reserve schedule is then sent to a risk analysis stage that runs for all possible scenarios. To create a comparison benchmark, two more test structures are developed. The studies have been performed in a deterministic structure and for a large set of scenarios, as well. The three proposed algorithms have been performed for the deterministic case (1 scenario), the reduced set (5 scenarios) and a large set of scenarios (100 scenarios). These 6 algorithms are summarized in Table 4.1, where their name, their decision making technique and their scenario modeling approaches are shown.

The proposed structure has been applied to the IEEE-96 test case [65]. The test system is modified by integrating a 1500 MW wind farm, at bus 40, which accounts for roughly 30% of the total system-wide generation capacity. The wind generation data of a wind farm for the year 2010 [20] is used after proper scaling to suit the chosen wind farm capacity. For the current simulation, the finite state Markov model of the spatio-temporal analysis for the 9 AM-12 AM epoch is used.

Table 4.1: Policy generation algorithms classification

PB_D	Prediction-based policy	Deterministic
PB_RS	Prediction-based policy	Reduced set of scenarios
PB_LS	Prediction-based policy	Large set of scenarios
DPB-D	Distribution percentile-based policy	Deterministic
DPB-RS	Distribution percentile-based policy	Reduced set of scenarios
DPB-LS	Distribution percentile-based policy	Large set of scenarios
F-D	Fixed policy	Deterministic
F-RS	Fixed policy	Reduced set of scenarios
F-LS	Fixed policy	Large set of scenarios

The load classification used in this study is based on data from IEEE-96 system [65]. In the dataset, the daily load profiles are given for specific seasons and day types. In real-world case, having the real load data, the daily profiles could be clustered into classes to form different day types and seasons that may not actually correspond to a real season or day type.

In the current study, the attention has been focused on one month to be able to model more initial states. All simulation results presented are for month April, henceforth. All scenario reductions are performed using the procedure introduced in [44], which reduces the scenarios to their best approximation based on the Kantorovich distance of probability distributions. The algorithm eliminates one scenario at a time until the desired number of scenarios is achieved. For each initial wind level, the risk analysis phase has been run for all the possible scenarios created by the Markov chain forecast model. The results are expressed in terms of average scheduling and risk cost.

In order to analyze the performance of the above methods, a set of base case studies with no policies have been run where the operator counts on the wind predicted mean (in other words, $\bar{\alpha} = 1$) for 3 different problem structures. The first one, which is referred to as the benchmark case, is a deterministic version of the scheduling problem, the second one models a reduced set of scenarios, and the third one models a large set of scenarios.

Note that all tested methods have the same foresight regarding wind forecast and none of them is shortsighted. This ensures that the difference in the presented results reflect the difference in the applied policy.

Table 4.2 presents the average scheduling and total cost for each initial wind condition for the case with reduced set of scenarios. The results are for multiple initial levels which accounts for various penetration levels up to 30% penetration level. The number of scenarios that encountered load shedding in the testing stage is also listed for each test level. The sixth column shows the cost improvement beyond the benchmark case. The results show that the prediction-based policy has a lower total cost in almost all the studied wind penetration levels. It also has a significantly less number of the scenarios where load shedding occurs.

Table 4.2. Comparison between the Fixed, Distribution percentile-based and Prediction-based approaches (reduced set of scenarios)

Policy	Wind level (%)	Scheduling cost ($)	Total cost ($)	Number of scenarios with load shedding	Improvement in total cost (%)	EENS (MWh)	LOLP
F -RS	3	270325.9	273860.1	0	8.7	0	0
F –RS	6	261300.6	263067.6	0	6.26	0	0
F –RS	9	253163.1	258297.0	0	13.46	0	0
F –RS	12	247146.7	253124.4	0	11.04	0	0
F -RS	15	229262.3	235805.9	2	13.98	0.0001	0.0006
F –RS	18	222984.5	226252.8	2	18.04	0.0001	0.0006
F –RS	21	212396.8	220599.6	0	17.07	0	0
F –RS	24	204860.3	214388.1	5	24.06	0.0005	0.0025
F –RS	27	196204.7	220114.5	190	32.20	0.0202	0.0154
DPB -RS	3	270664.7	273851.1	0	8.7	0	0
DPB –RS	6	261438.8	265869.5	0	5.3	0	0
DPB –RS	9	253146.6	258553.7	0	13.4	0	0
DPB –RS	12	248045.4	255352.4	0	10.3	0	0
DPB –RS	15	228880.6	237527.1	10	13.4	0.0003	0.0027
DPB –RS	18	221784.0	227265.4	2	17.7	0.0001	0.0006
DPB –RS	21	211848.1	223870.1	0	15.8	0	0
DPB –RS	24	204950.6	216958.1	42	23.1	0.0023	0.0163
DPB –RS	27	194758.9	232768.2	355	28.3	0.307	0.258
PB-RS	3	270416.4	273866.0	0	8.70	0	0
PB-RS	6	262086.1	262691.4	0	6.39	0	0
PB-RS	9	254357.7	257999.9	0	13.56	0	0
PB-RS	12	247146.7	253124.4	0	11.04	0	0
PB-RS	15	229262.3	235805.9	2	13.98	0.0001	0.0006
PB-RS	18	222984.5	226252.8	2	18.04	0.0001	0.0006
PB-RS	21	212396.8	220599.6	0	17.07	0	0
PB-RS	24	207533.9	211699.2	0	25.01	0	0
PB-RS	27	200085.1	212229.5	129	34.63	0.111	0.1120

Table 4.3 shows the results when the same procedure is deployed, with the exception that the first phase stochastic optimization is performed for a large number of scenarios. The results show that the proposed stochastic approach performs better when more scenarios are modeled.

Table 4.3. Comparison between the Fixed, Distribution percentile-based and Prediction-based approaches (large set of scenarios)

Policy	Wind level (%)	Scheduling cost ($)	Average risk cost ($)	Total cost ($)	Number of scenarios with load shedding	Improvement in total cost (%)
F -LS	3	268259.6	5794.6	274054.3	0	8.64
F –LS	6	263562.4	45.3	263607.7	0	6.07
F –LS	9	259114.8	52.1	259166.9	0	13.17
F –LS	12	255547.2	36.3	255583.6	0	10.17
F -LS	15	240800.2	89.6	240889.9	0	12.13
F –LS	18	231853.5	36.5	231890.1	0	16.00
F –LS	21	216857.9	2672.65	219530.6	0	17.48
F –LS	24	217293.2	63.3	217356.5	0	23.01
F –LS	27	203945.1	908.9	204854.1	0	36.90
DPB -LS	3	268991.1	5671.7	274662.8	0	8.43
DPB –LS	6	268469.2	5779.6	274248.8	0	2.27
DPB –LS	9	263146.6	5407.1	268553.7	0	10.03
DPB –LS	12	256810.8	8.7	256819.5	0	9.74
DPB –LS	15	241307.2	32.5	241339.7	0	11.96
DPB –LS	18	232724.2	14.1	232738.3	0	15.69
DPB –LS	21	217301.1	2667.5	219968.6	0	17.31
DPB –LS	24	218826	4.0	218830.0	0	22.48
DPB –LS	27	205511.8	720.6	206232.4	0	36.48
PB-LS	3	268130.7	5954.8	274085.5	0	8.63
PB-LS	6	263527.1	57.4	263584.5	0	6.07
PB-LS	9	259114.8	52.1	259166.9	0	13.17
PB-LS	12	255547.2	36.4	255583.6	0	10.17
PB-LS	15	240273.1	170.1	240443.2	0	12.29
PB-LS	18	231813.6	41.4	231855	0	16.01
PB-LS	21	216070.5	2905.9	218976.4	0	17.68
PB-LS	24	217293.2	63.3	217356.5	0	23.01
PB-LS	27	203099.9	980.2	204080.1	0	37.14

As expected, the number of scenarios that lead to load shedding is decreased when a larger number of scenarios are modeled since modeling a larger number of scenarios in the first phase will leave less space for uncertainties to perturb the results. The simple fixed policy also performs well in comparison to the distribution percentile based policy. This serve as a reference that some very simple reserve rules can perform adequately if chosen based on the historical trends.

Please note that this deterministic policy (here, 0.9) has not been chosen based on extensive analysis. In other words, having chosen another deterministic policy could lead to better or worse results. This may be an indication that solving the problem for a simple uncertainty set for wind generation may ease the computation burden of stochastic analysis, especially, when drastic wind ramps are not modeled. The investigation of the performance of such uncertainty sets is left for future work.

All simulations are performed using the Gurobi solver in AMPL environment on an Intel (R) Core (TM)2 Duo CPU @3.16 GHz computer with 4 GB of memory. The average solution time of the offline model including the scheduling phase and the risk analysis phase for each specific alpha was about 124 seconds. The average solution times of the online hour-ahead model for the proposed algorithms are reported in Table 4.4.

The SCED problem has 4404 variables and has 6378 constraints for the deterministic model. These numbers are increased to 15732 variables and 20562 constraints in a two-stage stochastic program with a small set of scenarios. The two-stage stochastic program with a large set of scenarios had 285996 variables and 363464 constraints.

Table 4.4. Average solution times for the tested policies

Policy	Avg. solution time (S)	Policy	Avg. solution time (S)
F –RS	1.39	F –LS	82.30
DPB –RS	1.46	DPB –LS	80.21
PB-RS	1.36	PB-LS	75.31

In order to show the performance of the proposed method in alleviating the need for modeling all scenarios, the cost savings of the PB-RS approach, with respect to the benchmark are presented in Table 4.5. The second column shows the maximum potential cost savings by switching from a determinist structure (benchmark case) to a stochastic structure with a large set of scenarios. The last column shows what portion of the potential cost savings is captured by the proposed policy in a reduced scenario case. The results corroborate that the prediction-based method is capable of capturing the same cost savings while modeling fewer scenarios.

Table 4.5. Cost savings captured in the Prediction-based method

Wind level (%)	Cost savings in PB-RS	Potential Cost savings	Ratio
3	26098.7	25910.6	1.01
6	17941.5	17048.3	1.05
9	40482.6	39313.8	1.03
12	31409.8	28950.7	1.08
15	38331.8	33641.6	1.14
18	49807.0	44204.8	1.13
21	45418.7	47046.9	0.97
24	70601.6	64944.3	1.09
27	112433.8	120455.2	0.93

Fig. 4.6 shows the total cost for different wind levels, in comparison to the benchmark and the base case with a large set of scenarios, for two different cases. The first case is where the obtained policy, from the prediction-based method, is used in a deterministic structure. The second one is where the obtained policy is used in a stochastic structure with a reduced number of scenarios. As can be seen, the policy obtained from the prediction-based method performs closely to the base case modeling a large set of scenarios, both in a deterministic and a reduced stochastic structure.

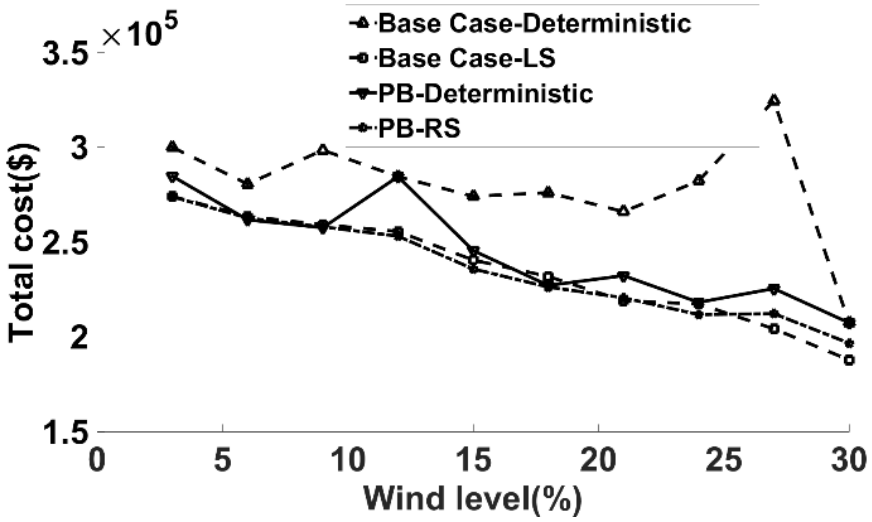

Fig. 4.6. Total cost for the proposed prediction-based method compared to the base case. PB: prediction-based policy, RS: reduced set of scenarios, LS: large set of scenarios.

4.5.2 Multiple Wind Farms

An extension for the problem is when there are multiple wind farms in the system. Discounting the generation from multiple wind farms would be more challenging in such situations. One important aspect when considering multiple wind farms is the fact that a large set of scenarios should be modeled. The need for modeling larger number of scenarios in a multi-wind farm system can be alleviated by taking advantage of offline analysis.

In this section, the proposed policy has been performed for two more test cases, one with two wind farm and one with three wind farms. For the two wind farm case, the same test system is modified by integrating two 750 MW wind farms, at buses 22 and 40, accounting for roughly 30% of the total system-wide generation capacity. For the three wind farm case, the system is modified by integrating three 500 MW wind farms, at buses 22 and 40 and 68. The results are shown in Table 4.6 and Table 4.7, respectively. The results confirm that the proposed reserve policy outperforms traditional techniques by capturing the majority of the potential savings.

Table 4.6. Comparison between the Fixed and Prediction-based approaches for two wind farms

Policy	Wind level (%)	Average risk cost($)	Total cost($)	Captured portion of potential cost savings
F –RS	6	511.2	275233.0	0.51
F –RS	12	361.1	269859.6	0.43
F –RS	15	639.6	267479.0	0.57
F –RS	18	436.8	264240.9	0.69
F –RS	21	0.8	259756.1	0.58
F –RS	24	0.1	259170.2	0.50
F –RS	27	0.0	254279.0	0.57
F –RS	30	0.0	249858.6	0
PB-RS	6	551.5	275082.6	0.82
PB-RS	12	401.1	269653.4	0.67
PB-RS	15	666.7	267249.7	0.81
PB-RS	18	585.5	264195.3	0.74
PB-RS	21	1.2	259550.9	0.76
PB-RS	24	0.0	258448.1	0.85
PB-RS	27	0.0	254083.3	0.7
PB-RS	30	0.0	249858.6	0

Table 4.7. Comparison between the Fixed and Prediction-based approaches for three wind farms

Policy	Wind level (%)	Average risk cost($)	Total cost($)	Captured portion of potential cost savings
F –RS	6	72	257.3	0.4
F –RS	12	234	248.4	0.2
F –RS	15	142	240.37	0.8
F –RS	18	144	225.3	0.1
F –RS	21	182	215.7	0.1
F –RS	24	175	205.7	0.1
F –RS	27	214	194.4	0.1
F –RS	30	142	256.5	0.7
PB-RS	6	234	248.4	0.2
PB-RS	12	775	237.2	0.9
PB-RS	15	651	223.3	0.7
PB-RS	18	412	213.6	0.6
PB-RS	21	1170	201.4	0.5
PB-RS	24	214	194.4	0.1
PB-RS	27	72	257.3	0.4
PB-RS	30	234	248.4	0.2

4.6 Conclusions

In this chapter the benefits of the prediction-based policy training method have been investigated. A flexible reserve margin based algorithm has been applied to train offline policies for discounting wind generation and scheduling energy and reserve in presence of wind. A scenario-based stochastic programming approach is leveraged to capture the effect of various possible wind scenarios based on short-term wind forecast.

A testing method is derived to assess the performance of the policies obtained through the proposed training procedure for scheduling wind reserve margin. The performance of the proposed policy training algorithm is compared with its counterparts without applying the trained policies. The results corroborate that the training based on the risk-aware scheduling can reduce the overall cost, while not imposing the burden of stochastic programming in real-time operation.

Numerical studies, via the IEEE-96 test case, demonstrate the benefits of the proposed structure.

5. Market Implications of Wind Reserve Margin

This chapter examines the market implications of wind reserve margin policies used to mitigate uncertainty from wind resources. The market implications of optimized reserve margin policy factors is studied.

5.1 Introduction

In the previous chapter, we developed a training structure to use stochastic analysis to come up with deterministic rules for scheduling reserve margins. This chapter investigates the market implications of deploying the deterministic reserve policy based on offline stochastic analysis. Analyzing the impacts of implementing new policies on the outputs of the electricity markets is an established way of determining the benefits of such new market policies. In this report, we compare the proposed approach with a typical deterministic approach that uses no policy. The generators' energy and ancillary service bids are modeled. In addition, a market settlement scheme is proposed that can be used for the policy proposed. In the proposed structure the generators are compensated for the energy and reserve that they provide. The reserve providers are compensated both for the reserve capacity and the reserve activation. The reserve activation payments are dependent upon the performance of the reserve resource for various realization scenarios. The following sections will discuss the formulation of these models and the results.

5.2 Reserve Policy factor Determination

The off-line training methodology is used for determining the policy factor for scheduling energy and reserve from wind generation. The policy factor is described as the fraction of the predicted available wind power to be scheduled for providing either energy or reserves. The offline analysis determines the policy factor for a verity of operating conditions, which are described in terms of the initial wind levels and the initial load levels.

In real-time, the actual wind power realization is compared to the trained initial wind levels and the nearest initial level is determined. Similarly, the nearest trained load level is determined. The policy obtained for that nearest wind level and the nearest load level is then implemented in the real-time model.

5.3 Implementation of the SCED using reserve policy factors

The model has been modified to enable calculating payments to different parties. In this model the energy schedule remains fixed and reserve schedule is discounted by α. To ensure consistency with the existing market structures, the SCED implementation has been kept simple by solving a deterministic problem.

The offline stochastic structure has been exploited to select a policy factor that can be passed into a deterministic scheduling framework. Energy schedule is fixed and the production part which was spared for reserve, is discounted.

The SCED implementation is formulated as given below:

$$\text{Min} \sum_{g,t}\left(C_g^e p_{gt} + C_g^{rc} r_{gt}\right) + \sum_{w,t}(C_w^e p_{wt} + \alpha C_w^{rc} r_{wt}) \quad (5.1)$$

s.t.:

$$P_g^{min}\overline{U}_{gt} \le p_{gt}, \forall g, t \quad (5.2)$$

$$p_{gt} + r_{gt} \le P_g^{max}\overline{U}_{gt}, \forall g, t \quad (5.3)$$

$$0 \le r_{gt} \le R_g^{10}\overline{U}_{gt}, \forall g, t \quad (5.4)$$

$$\sum_{q\in G} r_{qt} + \alpha \sum_{w\in W} r_{wt} \ge p_{gt} + r_{gt} + \sum_w \xi_{wt}, \forall g, t \quad [\gamma_{gt}] \quad (5.5)$$

$$\xi_{wt} \ge p_{wt} - \left(p_{wt}^f - \beta\sigma_{wt}\right), \forall w, t \quad (5.6)$$

$$p_{gt} - p_{g,t-1} \le R_g^{10}, \forall g, t, \overline{U}_{gt} = 1, \overline{U}_{g,t-1} = 1 \quad (5.7)$$

$$p_{g,t-1} - p_{gt} \le R_g^{10}, \forall g, t, \overline{U}_{g,t-1} = 1, \overline{U}_{gt} = 1 \quad (5.8)$$

$$p_{wt} + r_{wt} \le p_{wt}^f, \forall w, t \quad (5.9)$$

$$p_{kt} - B_k(\theta_{nt} - \theta_{mt}) = 0, \forall k, t \quad (5.10)$$

$$-P_k^{max} \le p_{kt} \le P_k^{max}, \forall k, t \quad (5.11)$$

$$\sum_{g\in g(n)} p_{gt} + \sum_{k\in\delta^+(n)} p_{kt} - \sum_{k\in\delta^-(n)} p_{kt} + \sum_{w\in w(n)} p_{wt} = d_{nt}, \forall n, t [\delta_{nt}] \quad (5.12)$$

$$p_{wt}, r_{wt} \ge 0, \forall w, t. \quad (5.13)$$

In the above formulation, αr_{wt} is the scheduled reserve from wind. Equation (5.9) states that the scheduled energy plus an up-scaled version of the reserve should not exceed the forecast. The descriptions of the other constraints are similar to what we described in chapter 4.

5.4 Contingency Analysis

To evaluate the efficiency of the proposed training-based policies in the market structure, a contingency analysis procedure has been performed. After the energy and reserve capacity are cleared in the SCED, the output schedule of the SCED structure is tested against a combination of different scenarios of wind and the single generator contingency events. The expected reserve activation payments for each resource is calculated based on the results of this contingency analysis stage.

The following formulation describes the re-dispatch following a combined contingency event.

$$\text{Min}\sum_t\Big(\sum_g\big(C_g^{re}r_{gct}\big)+\sum_w(C_w^{re}r_{wct})+\sum_w\big(C_p+C_w^{re}\big)p_{wct}^{penalty} + \sum_n C_c^n(ls_{nct}^+ + ls_{nct}^-)\Big) \quad (5.14)$$

s.t.:

$$p_{kct} - B_k(\theta_{nct} - \theta_{mct}) = 0, \forall k, t \quad (5.15)$$

$$-P_k^{max} \le p_{kct} \le P_k^{max}, \forall k, t \quad (5.16)$$

$$\sum_{g\in g(n)}\big(p_{gt}+r_{gct}\big)+\sum_{k\in\delta^+(n)}p_{kct}-\sum_{k\in\delta^-(n)}p_{kct}+\sum_{w\in w(n)}(p_{wt}+r_{wct})+ls_{nct}^+ - ls_{nct}^- = d_{nt}, \forall n, t \quad [\lambda_{n,t}^c] \quad (5.17)$$

$$r_{gct} \le r_{gt}, \forall g, c, t \quad (5.18)$$

$$-r_{gct} \le r_{gt}, \forall g, c, t \quad (5.19)$$

$$P_g^{min}\overline{U}_{gt}N_c^g \le p_{gt} + r_{gct} \le P_g^{max}\overline{U}_{gt}N_c^g, \forall g, c, t \quad (5.20)$$

$$-r_{wct} \le \alpha r_{wt} + p_{wct}^{penalty}, \forall g, c, t \quad (5.21)$$

$$0 \le p_{wt} + r_{wct}, \forall w, c, t \quad (5.22)$$

$$P_{wt} + r_{wct} + rr_{wct} \le W_{wct}, \forall w, c, t \quad (5.23)$$

$$rr_{wst}, ls_{nct}^+, ls_{nct}^-, P_{wct}^{penalty} \ge 0, \forall w, c, t. \quad (5.24)$$

Parameter W_{wct} in Equation (5.23) represents the realized power output of the wind farm and parameter N_c^g in Equation (5.20) is 0 if generator g is experiencing a contingency and 1 otherwise.

5.5 Market Settlement

In most electricity markets energy and ancillary services are cleared together using an optimization model that includes both energy and reserve bids in the objective function. The optimization procedure choses the lowest submitted bids to satisfy all physical and operational constraints.

Prices are calculated based on dual variables from the market model and generators are compensated based on these dual variables. Specifically, locational marginal prices

(LMPs) are used to settle energy compensations and reserve marginal prices (RMPs) are used to settle reserves compensations. The LMP for each node is the shadow price of the power balance equation (5.12) at that node. Load payments are calculated based on LMPs:

$$LP = \sum_{n,t} d_{nt}\delta_{nt} \quad (5.25)$$

The generators are entitled to payments for scheduled energy as well as the reserve capacity and reserve activation. Energy and reserve capacity payments are computed based on LMPs and RMPs. In the presented formulation, the RMP is the nonzero shadow price (shadow price for the binding constraint) for (5.5).

The reserve activation payments are only made if the generator responds in a contingency event. The expected activation payment in such a payment scheme can be formulated as:

$$RAP_{g,t} = \sum_{c\in S} \pi_c\{r_{gct}\lambda^c_{n(g),t}\} \quad (5.26)$$

where, $\lambda^c_{n(g),t}$ is the dual variable for (5.17). Here, $\lambda^c_{n(g),t}$ is a shadow price that reflects the marginal value of reserve for contingency c. The probability of each contingency is defined as the product of the probability of the related wind scenario and the probability of the respected generator contingency event. The probabilities of generator contingencies are calculated based on the Forced Outage Rate (FOR) values of generators. The payments in (5.26) is the expected compensation of reserve providers based on their activated service, which is exercised for individual contingencies.

5.6 Quality of Service

When a resource is scheduled to provide reserve capacity for contingency, it is supposed to be able to dispatch that amount. If this amount of reserve cannot be activated during a re-dispatch, then the resource provides a lower quality of service than anticipated. Based on scheduled capacity reserve from renewables, Equation (5.21) describes how the renewable resource is performing in exercising reserve. Variable r_{wct} measures how much reserve is dispatched from the resource *w*, where $p^{penalty}_{wct}$ represents the shortfall below the scheduled downward reserve.

The objective function (5.14) motivates a small shortfall. The large penalty included in the objective function prevents renewable resource from going below the scheduled downward reserve.

In this section the notion of quality of reserve (QOS) is defined to reflect the efficiency of the training algorithm in deriving reserve policies for renewables. QOS can be an indicator for efficiency of a model, too. The quality of service for reserve (QOS_r) can be characterized by the proportion of reserve capacity which is deliverable for each contingency in real time. An efficient model is expected to have a quality of reserve closer to one, indicating that a large portion of reserve capacity procured based on reserve policy is deliverable in real time:

Quality of service for energy (QOS_E) provided by wind resource for each contingency scenario is measured by the behavior of the wind resource in the re-dispatch

corresponding to that scenario. Note that in this report, the re-dispatch is performed to minimize the total cost as described in (5.14).

Since in the market model, a single variable has been used for both upward and downward reserve, we have classified the different probable situations to quantify the quality of service for each probable situation.

If the implemented reserve (r_{wct}) is positive, the wind generator has satisfied the energy promised, so: $QOS_E = 1$. As for reserve, if the available wind power is more than the total scheduled energy and reserve, $QOS_r = 1$. Otherwise,

$$QOS_r = \max(1, \frac{r_{wct}}{\alpha r_{wt}}). \quad (5.27)$$

If the implemented reserve (r_{wct}) is negative, two situations are possible:

1) The actual realized wind power is greater than the total energy and reserve implemented from wind: In this case, the quality of energy service and the quality of reserve service are both equal to 1.

2) The realized wind is equal to the total energy and reserve implemented: in this case, the quality of service for energy product is calculated based on the proportion of the scheduled energy that has been provided. This proportion can be described as:

$$QOS_E = 1 + \frac{r_{wct}}{p_{wt}} \quad (5.28)$$

The quality of service for energy product in this situation is calculated based on the proportion of the scheduled reserve that has been provided:

$$QOS_r = \max(0, 1 - \frac{p_{wct}^{penalty}}{\alpha r_{wt}}) \quad (5.29)$$

The above notions are used to measure the efficiency of the proposed policy method. The following section provides the numerical results.

5.7 Numerical Results and Analysis

The analysis in this section evaluates the prediction based policy and its counterpart where no policy is applied. The prediction based policies are selected based on the procedure described in chapter 4.

The policy (generated offline) is implemented in a deterministic real-time framework, i.e., a deterministic dispatch procedure described in Section 5.4. The hour-ahead SCED is solved based on the policy derived for the closest trained operating solution.

5.7.1 Data and Simulation Setup

The proposed structure has been applied to the RTS96 test case [65]. The test system is modified by integrating a 1500 MW wind farm, at bus 40, which accounts for roughly 30% of the total system-wide generation capacity. The wind generation data of a wind farm for the year 2010 [20] is used after proper scaling to suit the chosen wind farm capacity.

The hour-ahead model includes 10-minute intervals across a 1-hour horizon. For the current simulation, the Markov forecast for the 9 AM-12 AM epoch is used [20]. The load classification used in this study is based on data from RTS96 system [65]. All simulation results presented are for month April, henceforth.

The probabilities of generator contingencies are calculated based on the Forced Outage Rate (FOR) values provided in the IEEE RTS96 data [65].

5.7.2 Prediction-based Policy Method and No-policy Method Comparison

The solution of this look ahead SCED is analyzed across probable instances including various possible wind outcomes and possible contingencies. Each solution is tested against the combination of 100 wind scenarios generated based on the initial wind level and all the N-1 generation contingencies. The model contains 99 generators and, therefore, 99 generation contingency instances. Adding the wind scenarios, a total of 9900 instances are modeled for each solution.

In order to analyze the performance of this method, a set of base-case studies with no policies have been run where the operator counts on the wind predicted mean ($\bar{\alpha} = 1$).

Table 5.1 through Table 5.4 present the average market results over all the modeled instances. Table 5.1 summarizes load payments and energy revenues and Table 5.2 presents the quality of service for each tested wind level. The prediction based policy achieves a higher average quality of service. Table 5.3 and Table 5.4 presents the revenues from reserve markets for conventional and renewable producers. The capacity payments and the activation payments are reported in Table 5.3 and Table 5.4 respectively. The proposed policy has a higher payment for reserves to renewable resources. Table 5.5 compares the utilization of wind in the two methods. Overall, the policy method schedules more reserve from wind and incurs less penalty for not being able to provide the scheduled power. The average wind curtailment shows a slight increase in the policy method. Fig. 5.1 and Fig. 5.2 represent the quality of energy and quality of service across contingency scenarios. These results demonstrate that prediction based policy can significantly improve the reliability of the service provided by wind generators.

Table 5.1. Market measures: average system results

Wind level (%)	Load payment ($)		Energy revenue ($)	
	Base case	prediction based	Base case	prediction based
3	543273.5	523411.2	493606.9	495792.4
6	533273.5	513548.9	483308.9	487881.7
9	521838.5	517317.1	470107.7	474790.4
12	515750.4	515750.4	450450.5	450450.5
15	621048.2	514863.4	417451.2	433600.8
18	609915.7	514863.4	380112.5	430750.6
21	525703.1	525888.1	296385.9	300700.4
24	526082.2	528234.8	281678.7	274561.6
27	526799.7	528234.8	266709.2	268368.4

Table 5.2. Quality of service: average system results

Wind level (%)	Reserve QOS		Energy QOS	
	Base case	prediction based	Base case	prediction based
3	0.7693	0.9879	0.800	0.8815
6	0.5435	0.9497	0.810	0.9111
9	0.1404	0.9557	0.738	0.9068
12	0.0359	0.0359	0.619	0.6197
15	0.3991	0.6604	0.854	0.8759
18	0.3907	0.9443	0.809	0.9291
21	0.3507	0.8685	0.878	0.9491
24	0.3567	0.9449	0.752	0.9124
27	0.3572	1	0.872	0.9915

Table 5.3. Reserve capacity payments: average system results

Wind level (%)	Reserve capacity revenue (conventional generators) ($)		Reserve capacity revenue (wind generator) ($)	
	Base case	prediction based	Base case	prediction based
3	16434.76	6960.85	1062.90	716.49
6	16434.76	5692.86	984.262	971.3499
9	16306.72	3600.86	1388.25	1602.689
12	15974.01	15974.0	1582.65	1582.653
15	13022.48	5557.59	1979.55	1174.964
18	12364.79	2379.1	1637.68	2239.988
21	7669.869	3978.60	0	1345.384
24	6746.796	174.49	0	1030.558
27	6356.556	0	0	215.5465

Table 5.4. Reserve activation payments: average system results

Wind level (%)	Reserve activation revenue (conventional generators) ($)		Reserve activation revenue (wind generator) ($)	
	Base case	prediction based	Base case	prediction based
3	15585.05	14125.87	66.69	166.25
6	5444.044	5232.83	7.362	266.50
9	5087.439	3657.905	1.2246	202.54
12	5859.289	5859.289	0	0
15	3528.479	3252.916	1566.281	1431.56
18	8352.536	5262.85	0.0696	214.99
21	5458.106	5162.909	0.8255	350.77
24	13210.2	4258.596	0.1707	399.33
27	6024.633	0	0.1512	2818.54

Table 5.5. Wind utilization measures: average system results

Wind level (%)	Scheduled reserve from wind (MW)		Curtailed wind power (MW)		Wind penalty ($)	
	Base case	prediction based	Base case	prediction based	Base case	prediction based
3	25.22	36.81	3.322	4.300	133.4814	37.5581
6	23.35	53.84	0.355	0.791	155.6067	42.2518
9	33.18	97.65	0.084	0.544	255.4437	25.6938
12	38.63	38.64	0	0	415.446	415.446
15	50.94	68.99	0.024	0.109	84.7621	59.0765
18	49.92	144.21	0.017	0.503	380.9586	25.5383
21	0	92.57	0.102	1.051	512.1057	62.8103
24	0	194.42	0.011	0.615	934.6266	40.1877
27	0	179.62	0.047	4.577	767.2197	0.6998

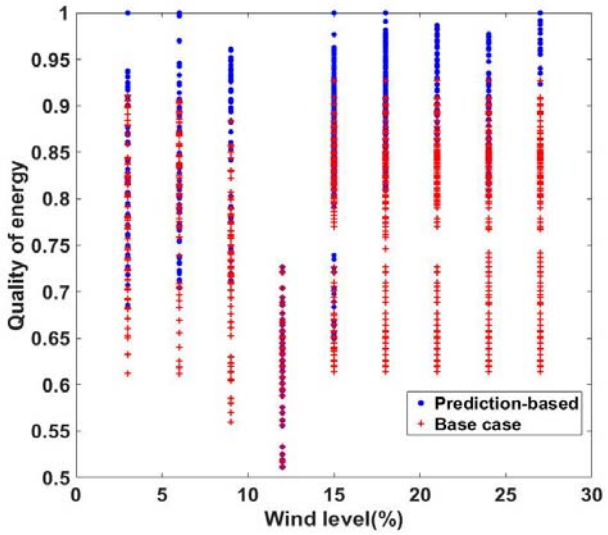

Fig. 5.1. Quality of energy service from wind farm for different wind scenarios

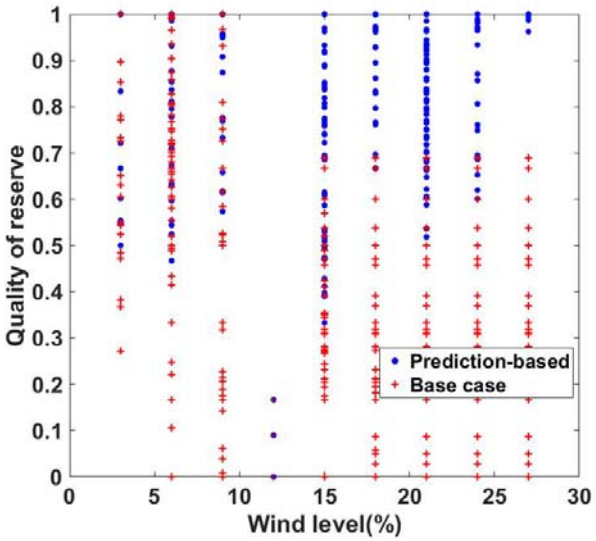

Fig. 5.2. Quality of reserve service from wind farm for different wind scenarios

5.8 Conclusions

Integration of renewable generation increases the uncertainty and variability that the operator must handle. Utilizing the concept of wind flexible reserve margin allows the operator to allocate a discounted amount of wind for energy, leaving a reserve margin to hedge against uncertainty. This study analyzes the utilization of such reserve margins in the ancillary service procurement.

This report compares the impacts of two different scheduling models, a base case model and a prediction based model. The prediction-based model uses a flexible reserve margin based algorithm which has been applied to train offline policies for discounting wind generation and scheduling energy and reserve in the presence of wind.

The market implications of transitioning to the prediction based approach are demonstrated. The results suggest that the prediction based model obtains higher quality of service from renewables. The prediction based approach was found to have lower load payments.

Future work can extend the proposed method to account for other types of uncertainty and locational aspects of the reserves. The approach discussed in this report can improve the reliability of reserve products provided by renewables.

6. Conclusions

This report discussed the ways employing emerging computational advances in system operation policies can improve the flexibility of the electricity industry in presence of high penetration of wind generation.

An offline policy generation technique is proposed based on stochastic reserve margin scheduling to hedge against the real-time uncertainty of wind farm generation. A flexible reserve margin based algorithm has been applied to train offline policies for discounting wind generation and scheduling energy and reserves in presence of wind. A scenario-based stochastic programming approach is leveraged to capture the effect of various possible wind scenarios based on short-term wind forecast and the loading conditions of the system. A testing method is derived to assess the performance of the policies obtained through the pro-posed training procedure for scheduling wind reserve margin.

Utilizing the concept of flexible wind reserve margin allows the operator to allocate a discounted amount of wind for energy, leaving a reliability margin to hedge against uncertainty. The extra production of the wind farm can then be used for balancing purposes. A finite-state Markov chain 10-minute-ahead wind power forecast model, based on spatio-temporal analysis, was utilized to calculate the conditional probability distribution of the wind farm generation. The presented framework is used to find the appropriate level for allocating wind based on the predicted output. Numerical studies, demonstrated the significant benefits obtained by incorporating the flexible wind reserve margin using a Markov-chain-based forecast. The results communicate that scheduling the flexible wind reserve margin will allow the operator to increase the reliability margin of the system while reducing the total cost. Discounting the scheduled generation from wind would improve the reliability by handling the uncertainty at an early stage. It also addresses the existing cost trade-off between scheduling generation from wind and the risk associated with wind farm uncertainty and improves the overall cost of supplying the demand.

The results show that the training based on the risk-aware scheduling can reduce the overall cost, while not imposing the burden of stochastic programming in real-time operation.

The analysis performed for determining the market implications of transitioning to the prediction based approach also suggest that the prediction based model obtains higher quality of service from renewables.

Future work can extend the proposed method to account for other types of uncertainty and locational aspects of the reserves. The approach discussed in this report can improve the reliability of reserve products from renewables.

References

[1] K. S. Cory and B. G. Swezey, "Renewable portfolio standards in the states: balancing goals and implementation strategies," National Renewable Energy Laboratory, 2007. [Online]. Available: http://www.imap.statesadvancingwind.org/assets/Uploads/Resources-pre-8-16/NREL-RPS-goals-implementation-Dec07.pdf.

[2] Global Wind Energy Council, "Global wind report: annual market update 2012," GWEC, Brussels, Belgium, Apr. 2013, [Online]. Available: http://www.gwec.net/wp-content/uploads/2012/06/Annual_report_2012_LowRes.pdf.

[3] M. Lucky, "Global solar, wind energy growth continues to impress," [Online]. Available: http://www.earthtechling.com/2013/07/global-solar-wind-energy-growth-continues-to-impress/.

[4] Federal Energy Regulatory Commission. Order No. 827. Reactive Power Requirements for Non-Synchronous Generation, June 16, 2016. [Online]. Available: http://www.ferc.gov/whats-new/comm-meet/2016/061616/E-1.pdf.

[5] A. Ellis, R. Nelson, E. Von Engeln, R. Walling, J. MacDowell, L. Casey, E. Seymour, W. Peter, C. Barker, B. Kirby, and J. R. Williams, "Reactive power performance requirements for wind and solar plants," in *Proc. IEEE PES General Meeting*, 2012, pp. 1 –8.

[6] X. Wang, P. Guo, and X. Huang, "A review of wind power forecasting models," *Energy Procedia*, vol. 12, pp. 770–778, September 2011.

[7] G. J. Osório, J. C. O. Matias, and J. P. S. Catalão, "A review of short-term wind power forecasting approaches," Proceedings of IET Renewable Power Generation Conference, pp. 1-4, September 2013.

[8] S.C. Pryor and R.J. Barthelmie, "Climate change on wind energy: A review," Renewable and Sustainable Energy Reviews, vol. 14, no. 1, pp. 430–437, January 2010.

[9] D.J. Sailor, M. Smith, and M. Hart, "Climate change implications for wind power resources in the Northwest United States," Renewable Energy, vol. 33, no. 11, pp. 2393–2406, November 2008.

[10] U. Firat, S. N. Engin, M. Saraclar, and A. B. Ertuzun, "Wind speed forecasting based on second order blind identification and autoregressive model," Proceedings of 9th International Conference on Machine Learning and Applications, pp. 618-621, Washington, December 2010.

[11] E. Edram and J. Shi, "ARMA based approaches for forecasting the tuple of wind speed and direction," Applied Energy, vol. 88, pp. 1405-1414, 2011.

[12] J.C. Palomares-Salas, J.J. G. de la Rosa, J.G. Ramiro, J.Melgar, A. Agüera and A. Moreno, "ARIMA vs. neural networks for wind speed forecasting," in Proceedings of IEEE Computational Intelligence for Measurement Systems and Applications, pp. 129-13, Hong Kong, May 2009.

[13] A. More and M. C. Deo, "Forecasting wind with neural networks," Marine Structures, vol. 16, pp. 35-49, 2003.

[14] W.Y. Chang, “Wind energy conversion system power forecasting using radial basis function neural network,” Applied Mechanics and Materials, vol. 284-287, pp. 1067-1071, 2013.
[15] J. Zeng and W. Qiao, "Support vector machine-based short-term wind power forecasting," Proceedings of IEEE Power Systems Conference and Exposition (PSCE), pp. 1-8, Phoenix, AZ, March 2011.
[16] J. Zhou, J. Shi, and G. Li, “Fine tuning support vector machines for short-term wind speed forecasting,” Energy Conversion and Management, vol. 52, no. 4, pp. 1990–1998, 2011.
[17] R. Jursa and K. Rohrig, “Short-term wind power forecasting using evolutionary algorithms for the automated specification of artificial intelligence models,” International Journal of Forecasting, vol. 24, no. 4, pp. 694–709, December 2008.
[18] J. P. S. Catalão, G. J. Osório, and H. M. I. Pousinho, “Short-term wind power forecasting using hybrid evolutionary intelligent approach”, Proceedings of 16th conference on Intelligent System Application to Power Systems., pp. 1-5, September 2011.
[19] J. Shi, J. Guo, and S.Zheng, “Evaluation of hybrid forecasting approaches for wind speed and power generation time series,” Renewable and Sustainable Energy Reviews, vol. 16, no. 5, pp. 3471–3480, June 2012.
[20] M. He, L. Yang, J. Zhang, and V. Vittal, “A spatio-temporal analysis approach for short-term forecast of wind farm generation,” IEEE Transactions on Power Systems, vol. 29, no. 4, January 2014.
[21] S. Murugesan, J. Zhang, and V. Vittal, “Finite state Markov chain model for wind generation forecast: a data-driven spatio-temporal approach,” IEEE PES Innovative Smart Grid Technologies, pp. 1–8, January 2012.
[22] M. He, L. Yang, J. Zhang, and V. Vittal, “Spatio-temporal analysis for smart grids with wind generation integration,” Proceedings of 2013 International Conference on Computing, Networking and Communications (ICNC), pp. 1107–1111, San Diego, CA, January 2013.
[23] Q. Zhang and S. A. Kassam, “Finite-state Markov model for Rayleigh fading channels,” IEEE Transactions on Communications, vol. 47, pp. 1688–1692, Nov. 1999.
[24] G. Papaefthymiou and B. Klockl, “MCMC for wind power simulation,” IEEE Transactions on Energy Conversion, vol. 23, no. 1, pp. 234–240, Mar. 2008.
[25] R. Doherty and M. O’Malley, “A new approach to quantify reserve demand in systems with significant installed wind capacity,” IEEE Transactions on Power Systems, vol. 20, no. 2, pp. 587–595, May 2005.
[26] J. Morales, A. Conejo, and J. Perez-Ruiz, “Economic valuation of reserves in power systems with high penetration of wind power,” IEEE Transactions on Power Systems, vol. 24, no. 2, pp. 900–910, May 2009.
[27] F. Bouffard and F. Galiana, “Security for operations planning with significant wind power generation,” IEEE Transactions on Power Systems, vol. 23, no .2, pp. 306–316, May 2008.
[28] H. Holttinen, M. Milligan, B. Kirby, T. Acker, V. Neimane, and T. Molinski, “Using standard deviation as a measure of increased operational reserve

requirement for wind power," Wind Engineering, vol. 32, no. 4, pp. 355–378, 2008.

[29] R. J. Bessa, M. A. Matos, I. C. Costa, L. Bremermann, I. G. Franchin, R. Pestana, N. Machado, H. P. Waldl, and C. Wichmann, "Reserve setting and steady-state security assessment using wind power uncertainty forecast: a case study," IEEE Transactions on Sustainable Energy, vol. 3, no. 4, pp. 827–835, October 2012.

[30] E. Ela, B. Kirby, E. Lannoye, M. Milligan, D. Flynn , B. Zavadil, and M. O'Malley, "Evolution of operating reserve determination in wind power integration studies," Proceedings of IEEE Power and Energy Society General Meeting, pp. 1-8, Minneapolis, MN, USA, July 2010.

[31] T. Yong, R. Entriken, and P. Zhang., "Reserve determination for system with large wind generation," Proceedings of IEEE Power and Energy Society General Meeting, pp. 1-7, Calgary, Alberta, Canada, July 2009.

[32] M. A. Ortega-Vazquez and D. S. Kirschen, "Estimating the spinning reserve requirements in systems with significant wind power generation penetration," IEEE Transactions on Power Systems, vol. 24, no. 1, pp. 114–124, February 2009.

[33] M. Matos and R. Bessa, "Setting the operating reserve using probabilistic wind power forecasts," IEEE Transactions on Power Systems, vol. 26, no. 2, pp. 594–603, May 2011.

[34] H. Holttinen, M. Milligan, E. Ela, N. Menemenlis, J. Dobschinski, B. Rawn, R. J. Bessa, D. Flynn, E. Gomez Lazaro, and N. Detlefsen, "Methodologies to determine operating reserves due to increased wind power," IEEE Transactions on Sustainable Energy, vol. 3, no. 4, pp. 713-723, October 2012.

[35] J. Liang, S. Grijalva, and R. G. Harley, "Increased wind revenue and system security by trading wind power in energy and regulation reserve markets," IEEE Transactions on Sustainable Energy, vol. 2, no. 3, pp.340-347, July 2011.

[36] D. He, J. Guo, and W. Lin, "The impact of trading wind power in both energy and regulation reserve market on system operation," in North American Power Symposium (NAPS), pp. 1-6, Urbana-Champaign, IL, USA, September 2012.

[37] A. N. Andersen, S. Strøm, J. Tang, T. Davidsen, and N. Dupont, "Proactive participation of wind turbines in the balancing markets," European Wind Energy Association Annual Conference, Copenhagen, Denmark, 2012.

[38] H. L. Durrwachter and S. K. Looney, "Integration of wind generation into the ERCOT market," IEEE Transactions on Sustainable Energy, vol. 3, no. 4, pp. 862 – 867, October 2012.

[39] J. Cardell and C. L. Anderson, "A flexible dispatch margin for wind integration," IEEE Transactions on Power Systems, vol. pp, no. 99, pp. 1–10, August 2014.

[40] A. Ross, D. H. Rhodes, and D. E. Hastings, "Defining changeability: reconciling flexibility, adaptability, scalability, modifiability, and robustness for maintaining system lifecycle value," Systems Engineering, vol. 11, no. 4, pp. 246-262, 2008.

[41] N. Menemenlis, M. Huneault, and A. Robitaille, "Thoughts on power system flexibility quantification for the short-term horizon," Proceedings of IEEE Power and Energy Society General Meeting, pp. 1-8, Detroit, MI, USA, July 2011.

[42] E. Lannoye, D. Flynn, and M. O'Malley, "The role of power system flexibility in generation planning," Proceedings of IEEE Power and Energy Society General Meeting, pp. 1-6, Detroit, MI, USA, July 2011.

[43] F. Bouffard and M. Ortega-Vazques, "The value of operational flexibility in power systems with significant wind power generation," Proceedings of IEEE Power and Energy Society General Meeting, pp. 1-5, Detroit, MI, USA, July 2011.

[44] N. Gröwe-Kuska, H. Heitsch, and W. Römisch, "Scenario reduction and scenario tree construction for power management problems," Proceedings of IEEE Bologna Power Tech Conference, pp. 1-7, Bologna, Italy, June 2003.

[45] F. D. Galiana, F. Bouffard, J. M. Arroyo, and J. F. Restrepo, "Scheduling and pricing of coupled energy and primary, secondary and tertiary reserves," Proceedings of IEEE, vol. 93, no. 11, pp. 1970–1983, November 2005.

[46] C. Grigg, P. Wong, P. Albrecht, R. Allan, M. Bhavaraju, R. Billinton, et al., "The IEEE Reliability Test System-1996. A report prepared by the Reliability Test System Task Force of the Application of Probability Methods Subcommittee," IEEE Transactions on Power Systems, vol. 14, no. 3, pp. 1010-1020, August 1999.

[47] B. Heath, C. Tyson and J. Lawhorn, "Determining capacity credit for wind used in MISO resource adequacy," Reliability and Risk Evaluation of Wind Integrated Power Systems, 1st ed., vol. 1, R. Billinton, R. Karki, A. K. Verma, Springer India, 2013, pp.1-11.

[48] Y. V. Makarov, C. Loutan, J. Ma, and P. de Mello, "Operational impacts of wind generation on California power systems, IEEE Transactions on Power Systems, vol. 24, no. 2, pp. 1039–1050, May 2009.

[49] M. A. Ortega-Vazquez and D. S. Kirschen, "Assessing the impact of wind power generation on operating costs," IEEE Transactions on Smart Grid, vol. 1, no. 3, pp. 295–301, 2010.

[50] M. S. Nazir and F. Bouffard, "Intra-hour wind power characteristics for flexible operations," Proceedings of IEEE Power and Energy Society General Meeting, pp. 1-8, San Diego, CA, July 2012.

[51] D. Chattapadhyay and R. Baldick, "Unit commitment with probabilistic reserve," Proceedings of IEEE Power and Engineering Society Winter Meeting, pp. 280–285, New York, 2002.

[52] Y. Dvorkin, D. S. Kirschen, and M. A. Ortega-Vazquez, "Assessing flexibility requirements in power systems," IET Generation, Transmission & Distribution, vol. 8, no. 11, pp. 1820-1830, 2014.

[53] A. Papavasiliou, S. Oren, and R. O'Neill, "Reserve requirements for wind power integration: A scenario-based stochastic programming framework," IEEE Transactions on Power Systems, vol. 26, no. 4, pp. 2197 – 2206, Nov. 2011.

[54] E. Ela, M. Milligan, and B. Kirby, National Renewable Energy Laboratory, "Operating reserves and variable generation," National Renewable Energy Laboratory, Technical Report, NREL/TP-5500-51978, August 2011. [Online]. Available: http://www.nrel.gov/docs/fy11osti/51978.pdf.

[55] Diao, K. Sun, V. Vittal, R. O'Keefe, M. Richardson, N. Bhatt, D. Stradford, and S. Sarawgi, "Decision tree-based online voltage security assessment using PMU measurements," IEEE Transactions on Power Systems, vol. 24, no. 2, pp. 832–839, May 2009.

[56] C. Jensen, M. El-Sharkawi, and R. Marks, "Power system security assessment using neural networks: Feature election using Fisher discrimination," IEEE Transactions on Power Systems, vol. 16, no. 4, pp. 757–763, November 2001.

[57] L. Moulin, A. daSilva, M. El-Sharkawi, I. Marks, and R. Marks, "Support vector machines for transient stability analysis of large-scale power systems," IEEE Transactions on Power Systems, vol. 19, no. 2, pp. 818–825, May 2004.

[58] F. Gomez, A. Rajapakse, U. Annakkage, and I. Fernando, "Support vector machine-based algorithm for post-fault transient stability status prediction using synchronized measurements," IEEE Transactions on Power Systems, vol. 26, no. 3, pp. 1474–1483, August 2011.

[59] S. Fan, L. Chen, and W. J. Lee, "Machine learning based switching model for electricity load forecasting," Energy Conversion and Management, vol. 49, no. 2, pp. 1331−1344, June 2008.

[60] H. Hahn, S. Meyer-Nieberg, and S. Pickl, "Electric load forecasting methods: Tools for decision making," European Journal of Operational Research, vol. 199, pp. 902–907, 2009.

[61] A. M. Foley, P. G. Leahy, A. Marvuglia, and E. J. McKeogh, "Current methods and advances in forecasting of wind power generation," Renewable Energy, vol.37, no.1, pp.1–8, January 2012.

[62] M. Lei, L. Shiyan, J. Chuanwen, Liu Hongling, and Z. Yan, "A review on the forecasting of wind speed and generated power," Renewable and Sustainable Energy Reviews, vol. 13, no. 4, pp. 915-920, May 2009.

[63] C. Wan, Z. Xu, P. Pinson, Z. Y. Dong, and K. P. Wong, "Probabilistic forecasting of wind power generation using extreme learning machine," IEEE Transactions on Power Systems, vol. 29, no. 3, pp. 1033–1044, May 2014.

[64] S. Salcedo-Sanz, E. G. Ortiz-García, Á. M. Pérez-Bellido, A. Portilla-Figueras, and L. Prieto, "Short term wind speed prediction based on evolutionary support vector regression algorithms," Expert Systems with Applications, vol. 38, no. 4, pp. 4052–4057, 2011.

[65] University of Washington, "Power system test case archive," Department of Electrical Engineering, 2007. [Online]. Available: http://www.ee.washington.edu/research/pstca/.

[66] F. D. Galiana, F. Bouffard, J. M. Arroyo, and J. F. Restrepo, "Scheduling and pricing of coupled energy and primary, secondary, and tertiary reserves," in Proc. IEEE, vol. 93, no. 11, pp. 1970–1983, Nov. 2005.

[67] University of Washington, "Power system test case archive," Dept. of Elect. Eng., 2007. [Online]. Available: http://www.ee.washington.edu/research/pstca/.

Part II

The Value of Flexible Wind Dispatch in Stochastic Unit Commitment

Georgios Patsakis
Shmuel S. Oren

University of California, Berkeley

For information about this project, contact:

Shmuel S. Oren
Department of Industrial Engineering and Operations Research
4141 Etcheverry Hall
University of California at Berkeley
Berkeley, CA 94720
tel: (510) 642-1836
fax: (510) 642-1403
email: oren@ieor.berkeley.edu

Power Systems Engineering Research Center

The Power Systems Engineering Research Center (PSERC) is a multi-university Center conducting research on challenges facing the electric power industry and educating the next generation of power engineers. More information about PSERC can be found at the Center's website: http://www.pserc.org.

For additional information, contact:

Power Systems Engineering Research Center
Arizona State University
527 Engineering Research Center
Tempe, Arizona 85287-5706
Phone: 480-965-1643
Fax: 480-727-2052

Notice Concerning Copyright Material

Table of Contents

List of Figures

List of Tables

Stochastic Unit Commitment Nomenclature

SETS

N	Set of buses.
E	Set of branches.
G	Set of generators.
G_F, G_S, G_W	Sets of fast/slow/wind generators.
G_i	Set of generators connected to node $i \in N$.
T	Set of consecutive integer time instances $\{1, \ldots, T_H\}$
S, S_t	Set of all scenarios/set of scenarios at time t in the scenario reduction algorithm.

VARIABLES

u_{gts}	Binary variable indicating commitment of generator $g \in G \setminus G_W$ at time $t \in T$ for scenario $s \in S$
v_{gts}	Binary variable indicating startup of generator $g \in G \setminus G_W$ at time $t \in T$ for scenario $s \in S$
w_{gt}	Binary variable indicating commitment of slow generator $g \in G_S$ at time $t \in T$
z_{gt}	Binary variable indicating startup of slow generator $g \in G_S$ at time $t \in T$
δ_{its}	Phase angle at node $i \in N$, time $t \in T$ and scenario $s \in S$
p_{gts}	Active power of generator $g \in G$ at time $t \in T$ for scenario $s \in S$
$p_{SH_{its}}$	Load shed at node $i \in N$, time $t \in T$ and scenario $s \in S$
$p_{WS_{gts}}$	Wind curtailment for wind site $g \in G_W$ at time $t \in T$ and scenario $s \in S$
x, y_s	Vector of all first/ second stage variables for scenario $s \in S$.

PARAMETERS

π_s	Probability of scenario $s \in S$
B_F^s	$\|E\|$ by $\|N\|$ matrix of susceptances (in the dc power flow equations) for scenario $s \in S$
B^s	$\|N\|$ by $\|N\|$ matrix of susceptances (in the dc power flow equations) for scenario $s \in S$
C_g	Marginal cost of generator $g \in G \setminus G_W$.
DT_g	Minimum down time of generator $g \in G \setminus G_W$
$F_l^{\max}$	Capacity of branch $l \in E$
i_{allin}	Binary parameter; if its value is 1, wind is treated as a must-take resource
K_g	Minimum load cost of generator $g \in G \setminus G_W$.
K_{SH}	Cost of load shed
$P_{gs}^{\min}$	Minimum capacity of generator $g \in G \setminus G_W$ for scenario $s \in S$ (set to zero if unavailable at this scenario).
$P_{gs}^{\max}$	Maximum capacity of generator $g \in G \setminus G_W$ for scenario $s \in S$ (set to zero if unavailable at this scenario).
P_{it}	Load at node $i \in N$ and time $t \in T$
P_{Wgts}	Available output for wind site $g \in G_W$ at time $t \in T$ in scenario $s \in S$
R_g^+	Minimum ramping of generator $g \in G$

R_g^-	Maximum ramping of generator $g \in G$
S_g	Start up cost of generator $g \in G \setminus G_W$.
T_H	Time horizon length of the SUC problem
UT_g	Minimum up time of generator $g \in G \setminus G_W$

1. Introduction

1.1. Background

The worldwide drive towards a cleaner and sustainable electricity generation mix has lead to increased renewable integration goals for the coming years. California, for example, is on track for achieving its 2020 goal of 33% of energy needs satisfied by renewable resources and now aims for 50% by 2030 [1]. Renewable resources have been traditionally treated - and are still treated by many system operators - as must-take resources (negative load), i.e. they are fully integrated in the electricity network regardless of their level or variability. Renewable curtailments only occur in cases where operational feasibility is at risk. The increased renewable integration, however, gradually brings about new operating conditions, such as steeper power ramps, overgeneration and decreased frequency response capabilities. Conventional generation by itself is unable or extremely costly to deal with these new conditions and a paradigm shift is necessary, in which renewable generation is called upon to contribute to ancillary services and grid flexibility by systematically dispatching at levels defined by operational and cost considerations. The need for such policies is already becoming apparent in regions with increased renewable integration; the California Independent System Operator (CAISO) curtailed about 1% of the total potential renewable generation during the first quarter of 2017, with solar curtailment reaching up to 30% at specific times, while it has already adopted market based curtailment mechanisms [2]. In Europe, on the other hand, directive 2009/28/EC is currently in force and stipulates that "Member States shall ensure that when dispatching electricity generating installations, transmission system operators shall give priority to generating installations using renewable energy sources in so far as the secure operation of the national electricity system permits and based on transparent and non-discriminatory criteria" [3]. As of November 2016, however, there is an initiative to review the directive and an active debate of whether to include renewable curtailments; in fact, the latest version of the proposal (February 2017) to revise the legislation does not include prioritizing renewable generation.

1.2. Overview of the Problem

In this work we focus on mobilizing the flexibility of wind dispatch. Current wind generators and power plants have advanced controls that allow them to operate practically at any point below their (maximum) available output [4], [5]. However, their available output itself depends on the weather conditions, i.e. the availability of wind. Consequently, they are considered semi-dispatchable (in contrast to conventional resources for which complete control over the output point is possible). These technical capabilities also enable us to consider the optimization of the wind generation setpoint, instead of integrating all of the available wind generation into the system. The benefits from curtailing wind production have been examined from various perspectives. In [6] and [7], NREL provides a series of cases of wind curtailment in systems in the US or abroad. In [8] and [9] CAISO uses the software PLEXOS to simulate a rolling unit commitment problem in the presence of wind curtailment for high wind penetration. In [10] it is shown that allowing for renewable curtailment enables significant reduction of the required system storage size, in [11] the benefits are motivated mainly through solving a Security Constrained Optimal Power Flow (SCOPF) problem and in [12] a dynamic interaction of wind curtailment with storage is examined when the ramping rates of power plants are considered. An overview of the motivation behind wind curtailment is given in [13], whereas in [14] wind curtailment is employed for active network management. A flexible wind dispatch margin for

the joint energy and reserves market and offline policies to obtain it are examined in [15] and [16].

The Unit Commitment (UC) problem is a widely studied mixed integer program [17]–[19] that determines the set of generators, among all the available ones, that will be committed to satisfy the load during the following day. The two stage Stochastic Unit Commitment problem (SUC) formulates the same decision in the presence of uncertainty (renewable generation, faults, load), captured by a finite set of possible realizations (scenarios) [20]–[22]. The size of the optimization problem scales linearly with the number of scenarios and for that purpose a large amount of research has been devoted to decomposition techniques to iteratively approximate the solution of the problem. Among these, in [23], the Progressive Hedging (PH) algorithm is adapted to successfully solve the SUC problem. In [24] a cutting plane algorithmic approach is used. In [25] a parallel implementation of Lagrangian relaxation in a high performance computing environment is employed. In [26] an asynchronous parallelized algorithm based on stochastic subgradient is utilized to efficiently solve the problem.

1.3. Main Issues

We aim to provide a complete framework to understand and evaluate the expected benefit from flexible wind dispatch in a SUC setting, while also introducing innovations in the implementation of the various components of the model. To begin with, since wind generation is not associated with any fuel costs in the objective, it is not self evident why we could be better off curtailing it and using costly conventional generation in its place. For this reason, we present small motivating examples to offer intuition regarding the most common setups where such benefit may occur: operation during oversupply, ramping requirements, technical minima of generators and congestion. We then proceed to describe the complete evaluation framework, by introducing its basic components: the Uncertainty and Optimization Modules.

The Uncertainty Module is based on existing wind speed modeling techniques, which we enhanced with a non parametric modeling methodology for the aggregate power curve, i.e. the mapping of wind speed to wind generation. When only aggregate wind generation data is available for every site, estimating the power curve based on individual wind generator curves could be problematic since not all aggregated generators have similar characteristics. If we instead use averages of historical power data for given wind speed intervals, we may incur losses in the modeling of the variability of output power generation or sensitivity to outliers in the data. In an effort to accommodate for that, we use a methodology based on robust local polynomial regression [27] and Maximum Likelihood Estimation (MLE) [28].

The Optimization module, on the other hand, is responsible for solving the SUC problem given a set of scenarios and it has two modes. In the first mode, it utilizes an algorithm provided in [29] and [30] for general two stage stochastic programs with binary first stage variables. The intuition behind the algorithm is that, if the different scenarios of a stochastic program impose similar requirements to the system, then it is possible that a good solution to the full problem will come from solving the significantly smaller subproblems that only look at a scenario in isolation. If the solutions we get by looking at specific scenarios do not perform well in the full problem (where all scenarios are considered), we can eliminate these solutions from consideration in the next iterations and resolve the subproblems. Even though SUC satisfies the requirements of the algorithm, direct application of the algorithm as used in the experimental results of [29], [30] does not yield a satisfactory convergence rate, since the scenarios of the SUC problem impose differnt requirements and therefore yield wildly different solutions when considered in isolation. However, if we use Lagrangian penalties in the the objective of the scenario subproblem to

convey information from other scenarios, we get scenario specific solutions that perform well for the full problem. The penalties we use are derived from the PH Lower Bounds [31] and updates.

Even though the first mode of the Optimization Module can provide high quality solutions, we may be interested in a fast heuristic approximation of the SUC solution instead. The second mode of the Module implements a combined scenario reduction and decomposition algorithm to provide a quicker answer by eliminating similar scenarios throughout the iterations of the decomposition algorithm. The main idea behind this elimination is evaluating the similarity of two scenarios based on them having comparable impacts when applied to the specific problem. For that purpose we use the suboptimal, scenario specific solutions that the decomposition algorithm calculates during its execution, as "features" of that scenario to evaluate distances between different scenarios and gradually reduce their number by keeping the most representative ones for our system.

We test our framework on a reduced model of the Western Electricity Coordinating Council (WECC) system [32], consisting of 130 thermal generators, 225 nodes and 371 lines for three wind penetration scenarios (low, medium and high). After the SUC problem is solved, we utilize its optimal solutions to compare the cost of policies that treat wind as a must-take resource versus ones that allow flexible wind dispatch. We also test our heuristic algorithm from mode 2 of the Optimization Module against the high quality solutions of mode 1. Regarding the value of wind flexibility, our results indicate negligible cost benefit in the low integration case, but an even above 20% cost improvement in the high integration case, supporting the argument (at least for our test case example) that flexible wind dispatch should be directly integrated in the operation of the power market.

1.4. Report Organization

This work is structured as follows: In section II, the motivational small examples are provided. In section III, the modeling and evaluation approach is described. In section IV, the decomposition algorithm and the heuristic decomposition and reduction algorithm are presented. In section V, simulation results for the WECC system are shown. Finally, in section VI we conclude and provide future research directions.

2. Motivating Examples

In order to motivate the discussion and provide some intuition on the cost benefits from allowing wind generation to deviate from the available wind power output, three stilized examples are examined. These examples try to illustrate that, even though wind generation is not associated with any cost in the objective of the unit dispatch problems, it can still be beneficial to spill wind resources for a cost efficient allocation of conventional generation. Fig. 2.1 outlines the parameters for these examples.

2.1. Technical Minima

In example 1, if the 40MW of wind power are treated as a must-take resource, the total residual load that needs to be satisfied by conventional generation would be 20MW. Due to the technical minimum 40MW of generator G_2, we need to use the more expensive G_1, resulting in a 1100 \$/h cost of operation. If instead the output of the wind generator is adjusted at 20MW, G_1 can be used and the cost drops to 1000 \$/h.

2.2. Startup Costs

In example 2, if wind power is a must-take resource, it can fully satisfy demand for time period 2. A residual load of 20MW should be satisfied by conventional generation in periods 1 and 3. That, however, means that generator G_1 must restart at period 3 and the startup costs are incurred twice, leading to a total cost of 1100\$ for the three periods. If, instead, 20MW of wind are spilled during the second time period, G_1 can stay on and the total cost is now 8500\$. Note that this intuition could be extended for more time periods or for instances with more conventional generators.

2.3. Ramping Constraints

In example 3, the goal is to satisfy $N-1$ security. More specifically, if any of the generators fail, we should be able to recover the lost generation within the next time unit (an hour is used here, but a smaller time resolution could be considered). Generators G_1 and G_2 are identical and have a lower startup cost than generator G_3, however their ramping rates are limited to 60MW/h, whereas G_3 has a ramping rate of 100MW/h. In the case where no wind spill is allowed, utilizing only the cheap generators does not yield a feasible solution, since assuming they share the residual load of 130MW by generating 65MW each, the ramping capabilities of G_1 are not sufficient in case G_2 fails (in case they share the load unevenly, the same problem arises if the highest generating unit fails). So the costly generator G_3 needs to be utilized, leading to a total cost of \$12900. Now, if instead we dispatch the wind unit at 40MW, by spilling 10MW of wind power, we can satisfy the residual load of 140MW by evenly sharing between G_1 and G_2, i.e. 70MW each. In case G_2 suffers a fault, we can cover 60MW of its generation by G_1 and the remaining 10MW we can obtain by ramping up the wind generation to its available output. For that, we exploit the fact that wind turbine controls allow for very fast ramping. The second dispatch amounts to a lower cost of \$11200.

2.4. Congestion

Finally, in example 4, a DC optimal power flow problem is solved to illustrate how allowing for flexible wind dispatch may lead to a more economical allocation by alleviating congestion. In the case where the 10pu of wind power are treated as a must-take resource, it turns out that in the optimum they all pass through branch $2-3$ to satisfy the load of bus 3, binding the phase angle difference between buses 2 and 3 as well. That means the flow of branch $2-3$ is at its capacity, so the flow on the line $1-2$ must be zero. Because of that, the phase of bus 1 has to equal that of bus 2 and that constrains the flow on line $1-3$ to 25pu. We observe that both line $1-2$ and line $1-3$ are not utilized close to their full capacity, whereas line $2-3$ is congested. Also, 5pu of the load is satisfied by the expensive generator G_2, leading to a total cost of \$130000/h. If we instead dispatch wind at 8pu, we can satisfy the load without using the expensive generator, by generating 32pu with G_1 and the remaining 8pu through wind, leading to a lower total cost of \$128000/h. The flows are in this case $P_{12} = 2$pu, $P_{23} = 10$pu and $P_{13} = 30$pu, which also corresponds to a better utilization of the line capacities.

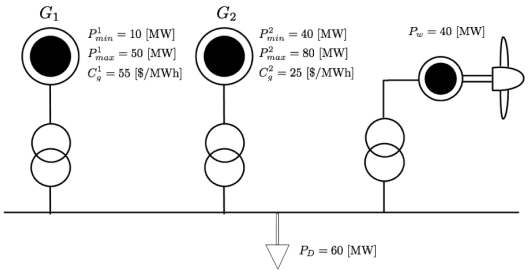

(a) Example 1. The generator specifications in this case are minimum and maximum generation limits (P_{min}, P_{max}) and marginal costs C_g. The available (maximum) wind power generation is P_w and the load is P_D.

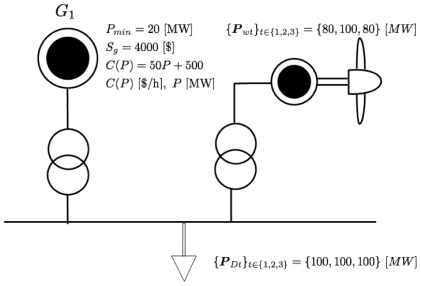

(b) Example 2. The generator specifications are the minimum generation limit (P_{min}), the startup cost S_g and the operating cost $C(P)$ as a function of the generation level P . The available (maximum) wind power generation P_{wt} and load P_{Dt} are given for three consecutive time periods, $t = 1,2,3$. G_1 is assumed turned off at the beginning.

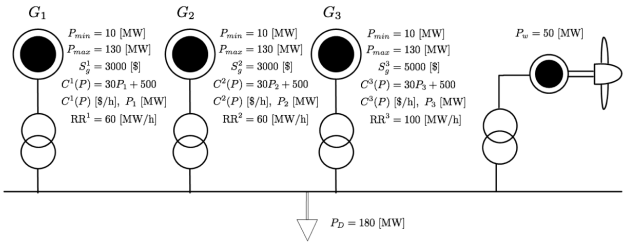

(c) Example 3. The generator specifications are minimum and maximum generation limits (P_{min}, P_{max}), the startup cost S_g, the operating cost $C(P)$ as a function of the generation level P and the ramping rate RR. The available (maximum) wind power generation is P_w and the load is P_D. The generators are initially assumed turned off and we are only interested in the first time period.

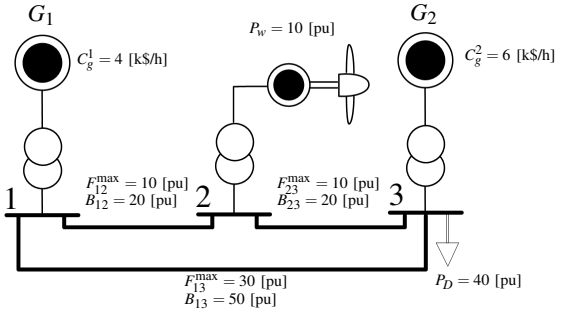

(d) Example 4. The system consists of three buses and three branches with susceptances B and capacities $F^{\max}$ as provided in the figure. The generator specifications are the marginal costs C_g, the maximum available wind production is P_w and the load is P_D.

Figure 2.1: Small examples to illustrate potential benefits of wind power spilling.

3. Model Outline

The examples of the previous section constitute favorable scenarios in which introducing flexible wind dispatch allows for a lower cost of operation, due to technical minima of conventional generation, efficient scheduling, ramping requirements or congestion. In order to make an argument for the general case, however, we need to consider a large set of scenarios, generated based on a model of the underlying uncertainty of an actual system. For that purpose,

the procedure depicted in Fig. 3.1 is adopted. The developed model comprises of two basic components, the Uncertainty Module and the the Optimization Module. The Uncertainty Module tries to capture the underlying uncertainty of the system, which in our case is assumed to come from wind generation and line or generator faults. The module is trained based on a data set and then used to generate scenarios whenever these are necessary. The Optimization Module, on the other hand, takes as input a set of scenarios and solves or heuristically approximates the solution of a stochastic unit commitment problem, providing in its output a commitment schedule of the slow generators for the next day. The Optimization Module can be treated as a black box that a system operator uses to make the day ahead scheduling based on a set of available scenarios. Furthermore, it has two settings; in the first setting the optimization treats wind generation as a must-take resource, whereas in the second setting wind generation is allowed to dispatch at lower levels.

Based on these modules, the testing process is the following: Initially, the Uncertainty Module generates a set of scenarios. These scenarios are treated as the uncertainty information the system operator utilizes to make the scheduling decision. Based on this information, the Optimization Module makes one scheduling decision for each of two cases: the one in which wind is a must-take resource, and the one that it is not. In the final step, we wish to evaluate the difference between the costs associated with each case. To that end, we generate a new set of scenarios from the Uncertainty Module, representing possible actual realizations of the uncertainty the next day, and compare the expected costs of each of the two cases (Test Optimal Commitment Block).

3.1. Uncertainty Module

The underlying uncertainty of the problem considered consists of three main components: the wind model, the power curve model and the reliability model. The purpose of the wind model is to generate synthetic wind speed time series with hourly resolution, representative of the wind sites under consideration. Subsequently, the power curve model takes as input the wind speed time series and outputs a wind power generation series for every wind site. Finally, the reliability model is a discrete distribution from where faults of lines and generators are drawn. Note the

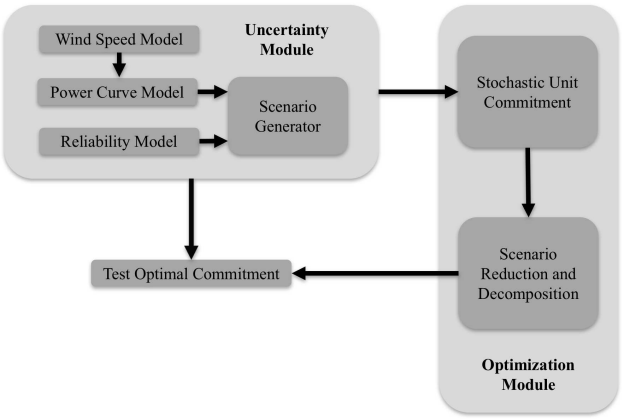

Figure 3.1: General model outline. The Uncertainty Module generates scenarios to be used as input for the Optimization Module, which defines an optimal commitment. It also generates a new set of scenarios to test this optimal commitment.

uncertainty model could be extended in a straightforward way to include load uncertainty as well, but in this work we do not consider it. This simplification is not unreasonable since the variability of load around its forecasted value is not as high as the variability of wind generation.

3.1.1 Wind Speed Model

This section describes the creation of a model that captures the characteristics of wind speed from multiple wind sites. The approach follows the basic steps from [33], [34] and [35]. The input data used to train the model are wind speed measurements ξ_{gk}^{train}, where $g \in G_W$ indicates the different wind sites and $k \in \{1,2,...\ T_{\text{train}}\}$ indicates the T_{train} hourly measurements that are available at every wind location. The goal is to train a model based on these measurements and then use it to generate artificial wind series. The steps employed are divided in two phases; in the first one (Learning Phase) the model is trained using the time series data, whereas in the second one (Time Series Generation Phase) randomly generated wind time series to be used in a Monte Carlo simulation are created based on the model.

a) Learning Phase

The learning phase aims to (approximately) transform the measurement data from the various locations to a set of independent Gaussian time series, whose characteristics will be captured using basic Auto-Regressive Moving Average (ARMA) models [36]. The following steps are employed.

Step 1: Since the data wind time series is not necessarily stationary, we initially remove diurnal and seasonal effects to get a new (approximately) stationary time series $\tilde{\xi}_{gk}^{\text{train}}$.

$$\tilde{\xi}_{gk}^{\text{train}} = \frac{\xi_{gk}^{\text{train}} - \mu_{gmd}}{\sigma_{gmd}} \ , \tag{1}$$

where μ_{gmd} and σ_{gmd} are the mean and standard deviation respectively of the time series created by the samples ξ_{gk}^{train} that correspond to epoch m and hour of day $d \in \{1,2,...\ 24\}$ for wind site $g \in G_W$.

Step 2: The stationary time series samples of the previous step do not necessarily follow a Gaussian distribution. Through a bijective mapping that employs the estimated non parametric Cumulative Distribution Function (CDF) $\hat{F}_g$ of the time series from Step 1 in site $g \in G_W$ and the inverse standard normal CDF Φ, the random samples $\tilde{\xi}_{gk}^{\text{train}}$ are mapped to samples $\hat{\xi}_{gk}^{\text{train}}$ drawn from the standard normal distribution, according to:

$$\hat{\xi}_{gk}^{\text{train}} = \Phi^{-1}(\hat{F}_g(\tilde{\xi}_{gk}^{\text{train}})) \tag{2}$$

Step 3: The data $\hat{\xi}_{gk}^{\text{train}}$ are now assumed Gaussian stationary time series, but the time series between the different locations can still be correlated. For that reason, based on the ideas discussed in [33], the diagonalization of the symmetric $|G_W| \times |G_W|$ matrix Σ, where $\Sigma_{ij} = \sigma_{ij}^2$ are the sample covariances between the time series in two different locations i and j

$$\sigma_{ij}^2 = \frac{1}{T_{\text{train}}} \sum_{k=1}^{T_{\text{train}}} \hat{\xi}_{ik}^{\text{train}} \hat{\xi}_{jk}^{\text{train}} \ , \tag{3}$$

is employed $\Sigma = UDU^T$, where D diagonal and U orthogonal. The linear transformation induced by the matrix U^T will map the $|G_W|$ correlated Gaussian time series for every location to Γ uncorrelated ones (in our case $|G_W| = \Gamma$, however in the case of a large number of wind sites we may choose to only keep the $\Gamma < |G_W|$ most important eigenvalues and corresponding

eigenvectors). Let $\{\hat{\Xi}\}_{gk} = \hat{\xi}_{gk}^{\text{train}}$ be the matrix whose rows correspond to the correlated time series, then the rows of $\{\Omega\}_{\gamma k} = \omega_{\gamma k}^{\text{train}}$, for $\gamma \in \{1,\ldots,\Gamma\}$ and $k \in \{1,\ldots,T_{\text{train}}\}$.

$$\Omega = U^T \hat{\Xi} \tag{4}$$

will comprise of Γ time series that will be assumed independent.

Step 4: For any fixed γ, the time series $\omega_{\gamma k}^{\text{train}}$ is modeled using a univariate ARMA(p,q) model, utilizing the Box–Jenkins method [36].

b) Time Series Generation Phase

At this point the model for wind speed time series has been trained. The goal of the Time Series Generation Phase is to generate scenarios of synthetic wind time series $\xi_{gts}^{\text{sample}}$ based on this model. Each scenario $s \in S$ consists of T_H time samples $t \in T$ for every wind site $g \in G_W$. The following procedure is employed:

Step 1: The first step of the process is to generate Γ time series $\omega_{\gamma ts}^{\text{sample}}$ for every scenario $s \in S$, based on the ARMA model of Step 4 of the Learning Phase.

Step 2: The inverse transformation of (4), for every scenario $s \in S$, yields a time series $\hat{\xi}_{gts}^{\text{sample}}$ with $t \in T$, corresponding to each wind location $g \in G_W$.

Step 3: The inverse transformation of (2) then yields a time series $\tilde{\xi}_{gts}^{\text{sample}}$ for every scenario and every wind site.

Step 4: Finally based on the epoch and the time of day we want to simulate, the diurnal and seasonal effects are added back in, using the inverse of (1), to yield the final wind speed time series $\xi_{gts}^{\text{sample}}$ with $t \in T$, $s \in S$ and $g \in G_W$.

3.1.2 Power Curve Model

For every site of wind generation an aggregate power curve that will provide an estimate of the wind power generation given the wind speed needs to be constructed. For that purpose, wind data and the corresponding wind power generations are used to train a power curve model. The power generation data points come from an aggregation of multiple wind turbines in each site, with potentially different individual power curves and characteristics. Therefore, the use of the standard parametric power curve model of a single wind turbine to describe the wind speed and power relationship [37] would not be a satisfactory approximation and a data driven non-parametric fit is more suitable. The model should also be able to capture the nonlinear behavior of the power curves, that is dependent on the wind speed operating point. For the aforementioned reasons, the local polynomial regression scheme described below was employed.

A further observation on modeling aggregate wind power generation by fitting a curve to the aggregate generation data is the fact that the fitting tends to smoothen out the power generation, i.e. high and low wind power generation measurements for the same wind speed will be mapped to a fixed intermediate value through the fitted curve. These high and low values of aggregate generation do not necessarily correspond to measurement errors, but they may instead represent the fact that wind speed is not the same as the measured one for all individual wind turbines that are aggregated, or that aggregate wind power depends on more than one factors than wind speed alone. Neglecting these values due to the aggregation may be acceptable if the focus is mean power generation, but since we plan to use the model for time series sampling in an environment with increased wind penetration, we would be smoothing out $\delta P/\delta t$ effects that are becoming increasingly important in power systems (and therefore imposing looser ramping requirements). For that reason, and due to lack of more detailed generation data, the aggregate generation at every wind speed is instead modeled as a random variable whose mean is given by the aforementioned local polynomial regression method.

More specifically, for every fixed $g \in G_W$ the measurement data $\left(\xi_{gk}^{\text{train}}, P_{gk}^{\text{train}}\right)$, $k \in \{1,\ldots,T_{\text{train}}\}$ are sorted (based on the lexicographical ordering) in L wind speed intervals (a_i, b_i), where $i \in \{1,2,...L\}$, with approximately equal number of measurements, represented by a central wind speed point c_i. Denote the length of each interval by $h_i = b_i - a_i$.

For every wind site $g \in G_W$, we want to train a distribution for the wind power $P_{Wg}(v_g)$, given the wind speed v_g. For simplicity in the notation, the subscript g indicating the wind site is dropped, but we imply that the fitting process is repeated for every site g. We assume the distribution for $P_W(v)$ is normal with mean $m_i(v)$ and the variance for every interval $i \in \{1,\ldots,L\}$ is assumed constant σ_i. We approximate the mean around every center c_i locally by a p degree polynomial $m_i(x) \approx \beta_{i0} + \beta_{i1}(x-c_i) + \beta_{i2}(x-c_i)^2 + ... + \beta_{ip}(x-c_i)^p$.

The following process is adopted to fit a local polynomial for a fixed interval $i \in \{1,2,...L\}$. The data measurements are not considered equally trustworthy, but instead every measurement $\left(\xi_k^{\text{train}}, P_k^{\text{train}}\right)$, $k \in \{1,\ldots,T_{\text{train}}\}$ is weighted according to a reliability constant r_k, which has two multiplicative components: $r_{ki} = \eta_{ki} q_{ki}$:

η_{ki} represents a reduction of our trust in the local approximation due to the horizontal distance (distance in the axis of wind speeds) from the interval center. According to a standard local polynomial regression assumption, the Epanechnikov Kernel function is used to define a weight $\eta_{ki} = \frac{3}{4h_i}(1 - \frac{(\xi_k^{\text{train}} - c_i)^2}{h_i^2})\,\mathbf{1}_{\{|\xi_k^{\text{train}} - c_i| \le h_i\}}$.

q_{ki} represents a reduction of our trust in the measurement due to the vertical distance (distance in the axis of wind power) of the measurement point from the mean of the fit at that point. Of course, the fit is not known from the beginning, so an iterative procedure is used, following [27], where an initial fit $m_i^{(0)}$ of the local polynomials is calculated with all $q_k^{(0)}$ initialized at 1, then at step τ the errors $e_k^{(\tau)} = P_k^{\text{train}} - m_{i_k}^{(\tau-1)}(\xi_k^{\text{train}})$ are calculated (where i_k is the interval that measurement k belongs). Following that, the weights of the new fit are defined as $q_k^{(\tau)} = B(e_k^{(\tau)}/(6s))$, where s is the median of $|e_k^{(\tau)}|$ and $B(\cdot)$ a kernel function on $[-1,1]$. This penalty guaranties a robust fit to outliers, since measurements that are far from the fitted curve will receive low weights and therefore their impact on the objective of the optimization problem formulated below will be small.

The fit is achieved by solving the following maximum likelihood problem with respect to $\sigma_i^2, \beta_{ij}, j \in \{1,\ldots,p\}$, for every i:

$$\text{maximize} \quad \prod_{k=1}^{T_{\text{train}}} \left(\frac{1}{\sqrt{2\pi\sigma_i^2}} \exp\left(-\frac{(P_k^{\text{train}} - m_i(\xi_k^{\text{train}}))^2}{2\sigma_i^2} \right) \right)^{r_{ki}}, \tag{5}$$

which yields:

$$\sigma_i^2 = \frac{\sum_{k=1}^{T_{\text{train}}} r_{ki}(P_k^{\text{train}} - m_i(\xi_k^{\text{train}}))^2}{\sum_{k=1}^{T_{\text{train}}} r_{ki}} \tag{6}$$

and the β_{ij} are given by a standard weighted least squares fitting.

3.2. Stochastic Unit Commitment

The generating units available to the system operator are divided into slow and fast, based on how long prior to operation a commitment decision for that unit has to be made. The output of the SUC problem is the commitment of slow generating units into the grid. The challenge

is that the commitment decision for slow units has to be made a day before operation, when the underlying uncertainty is still unknown, i.e. the commitment decisions (binary variables) for these units have to be the same across all scenarios (first stage variables). On the other hand, the other variables of the problem, such as the commitment of fast generating units and the generation levels, are allowed to vary depending on which scenario of nature was realized (the decision for them is made with knowledge of the uncertainty), hence the value that they are assigned can be different for every scenario (second stage variables).

Our formulation closely follows that of [20], adapted to explicitly model the flexibility of wind resources. The same methodology could be applied to determine the value of other types of renewable resources, like solar, but the focus here is wind generation, so the model is built around that. Note that the UC modeling standard in industry has slightly evolved from the model used in this work, so as to be able to cope with large scale systems. More specifically, tighter formulations of some constraints (such as ramping constraints) are utilized, a modified set of varibles has been offering improved computational performance by handling efficiently generator technical minima, whereas the shift factor formulation enhanced with lazy constraint evaluation has been noted to offer greater computational benefits (since the operators know which constraints are usually tight and need to be introduced) [38]. However, the qualitative and computational ideas conveyed in this work do not depend on the exact formulation, so we prefered using the model from [20] to allow comparison.

The objective of the SUC problem (7) is minimizing the expected, over the different scenarios, operational costs (startup, minimum load and fuel costs), as well as the highly penalized load shed variables. Note that wind generation is not penalized in the objective. Constraint (7b) imposes the load flow balance at every node. The matrix $B^s$is adjusted depending on the network configuration for every scenario (unavailability of lines). Constraint (7c) imposes limits for the load shed variables on every node and (7d) imposes the minimum and maximum operational limits of the generating units. Note that in case the unit is unavailable in scenario s, then both $P_{gs}^{\max}$ and $P_{gs}^{\min}$ are set to zero in the data, forcing the generation of the unit to zero. Possible unavailability of the wind resources is neglected in the current study. Furthermore, if the unit is not committed at this time point, then the variable u_{gts} is zero with the same effect. Constraint (7e) restrains wind generation below the maximum available capacity for that scenario. Constraint (7f) imposes that wind is a must-take resource (i.e. the wind spill is zero) in case the parameter i_{allin} is set to one. Note, however, that the policy adopted here is that wind is not spilled unless the operation of the system becomes technically infeasible. In that second case, the constraint is instead put in the objective with a big-M penalty, and then the impact of the penalty is subtracted from all the relevant quantities. This is actually close to what operators do in the must-take case, since they will only force curtailments of wind if the system feasibility is compromised. Constraint (7g) imposes that line flow limits (the matrix B_F^s is adjusted based on the line availability). Constraint (7h) imposes the ramping limitations. Constraints (7i) - (7k) impose the minimum up and down time requirements. Finally, (7l) and (7m) are the non-anticipativaty constraints for the commitment of the slow generators, i.e. it has to be the same for all the scenarios.

$$\text{minimize} \quad \sum_{s\in S}\pi_s \sum_{t\in T}\sum_{g\in G\setminus G_W}(S_g v_{gts} + K_g u_{gts} + C_g p_{gts} + K_{SH}\, p_{SH_{its}}) \tag{7a}$$

subject to

$$\sum_{g\in G_i} p_{gts} - \sum_{j\in N} B^s_{i,j}\delta_{jts} = P_{it} - p_{SH_{its}}, \quad \forall i \in N, \forall t \in T, \forall s \in S \tag{7b}$$

$$0 \le p_{SH_{its}} \le P_{it}, \quad \forall i \in N, \forall t \in T, \forall s \in S \tag{7c}$$

$$P^{\min}_{gs} u_{gts} \le p_{gts} \le P^{\max}_{gs} u_{gts}, \quad \forall g \in G\setminus G_w, \forall t \in T, \forall s \in S \tag{7d}$$

$$p_{gts} + p_{WS_{gts}} = P_{Wgts}, \quad \forall g \in G_w, \forall t \in T, \forall s \in S \tag{7e}$$

$$0 \le p_{WS_{gts}} \le (1 - i_{\text{allin}}) P_{Wgts}, \quad \forall g \in G_w, \forall t \in T, \forall s \in S \tag{7f}$$

$$-F^{\max}_l \le \sum_{i\in N} B^s_{F_{li}}\delta_{jts} \le F^{\max}_l\ , \quad \forall l \in E, \forall t \in T, \forall s \in S \tag{7g}$$

$$-R^-_g \le p_{gts} - p_{g(t-1)s} \le R^+_g\ , \quad \forall l \in E, \forall t \in T, \forall s \in S \tag{7h}$$

$$\sum_{\tau=t-UT_g+1}^{t} v_{g\tau s} \le u_{gts}\ , \quad \forall g \in G\setminus G_w, \forall t \in \{UT_g, \ldots, T_H\}, \forall s \in S \tag{7i}$$

$$\sum_{\tau=t+1}^{t+DT_g} v_{g\tau s} \le 1 - u_{gts} \quad \forall g \in G\setminus G_w, \forall t \in \{1, \ldots, T_H - DT_g\}, \forall s \in S \tag{7j}$$

$$v_{gts} \ge u_{gts} - u_{g(t-1)s}\ , \forall g \in G\setminus G_w, \quad \forall t \in T, \forall s \in S \tag{7k}$$

$$u_{gts} = w_{gt}\ , \forall g \in G_S, \quad \forall t \in T, \forall s \in S \tag{7l}$$

$$v_{gts} = z_{gt}\ , \forall g \in G_S, \quad \forall t \in T, \forall s \in S \tag{7m}$$

$$p_{gts} \ge 0, \quad \forall g \in G, \forall t \in T, \forall s \in S \tag{7n}$$

4. Solution Algorithm

4.1. A Scenario Decomposition Approach

The optimization problem formulated in the previous section has the form of a two-stage stochastic program. For concreteness, let x be the vector of first stage variables, i.e. the slow generator (binary) commitment, and y_s be the vector of the second stage variables for scenario $s \in S$. Let X be the feasibility set for x imposed by the constraints involving only first stage variables, i.e. constraint (7b), and $Y(x,s)$ be the set of y_s imposed by the rest of the constraints, for scenario $s \in S$, if the first stage variables are fixed at a value of x. Then, for a suitably defined function ϕ that captures the unweighted contribution of every scenario in the objective, the optimization problem takes the form:

$$\begin{aligned} \underset{x,\{y_s\}_{s\in S}}{\text{minimize}} \quad & \sum_{s\in S} \pi_s \phi_s(x,y_s) \\ \text{subject to} \quad & x \in X \\ & y_s \in Y(x,s)\ , \forall s \in S \end{aligned} \tag{8}$$

Let f_s, for $s \in S$, be the set of (well defined) functions:

$$f_s(x) = \underset{y_s \in Y(x,s)}{\text{minimize}} \quad \phi_s(x,y_s)\ , \tag{9}$$

i.e. each evaluation of the function $f_s(x)$ accounts in solving an optimization problem over the second stage variables, for fixed scenario $s \in S$ and first stage variable x. Now (8) is reformulated:

$$\underset{x\in X}{\text{minimize}} \quad \sum_{s\in S} \pi_s f_s(x) \tag{10}$$

The binary nature of the first stage decisions in (10) allows the decomposition scheme proposed in [29] and elaborated in [30] to be employed in order to decompose the problem and reduce the computational burden. The intuition behind the success of this algorithm so far is that, in case the different scenarios of stochasticity impose similar requirements to the optimization problem, it is possible that the global optimal solution will be among the scenario specific solutions. In our problem, however, the scenarios could impose different requirements to the system, but that can be accommodated for by the algorithm through the use of Lagrangian penalties that will eventually drive the scenario specific solutions together towards the same point. The form of decomposition utilized in this work is given in Fig. 4.1.

The main body of the algorithm is divided into two phases, the Lower Bounding and Lagrangian Update Phase and the Upper Bounding Phase and Cut Phase. In the Lower Bounding Phase, we fix every scenario $s \in S$ and solve for the optimal first stage decision given that scenario, over a space $X \setminus W$. This yields $|S|$ scenario specific solutions for the first stage variables x_s^t at iteration t. In the first iteration, the set W is empty and the penalty coefficients w_s^t are zero, so we are essentially solving $|S|$ scenario subproblems without any interaction, i.e. we are solving the initial problem after relaxing the non anticipativaty constraints. Since we are solving a relaxation, at least for the first iteration, we are guaranteed to get a lower bound on the optimal solution to (10). For the next iterations, it is still straightforward [31] to show we get lower bounds for (10) solved in the restrained space of first stage variables $X \setminus W$.

Following that, the objective value penalties w_s for every scenario $s \in S$ are updated. These penalties aim to drive the scenario solutions together. Intuitively this is achieved in the following

way: say that x is just an one dimensional x and for some iteration t we have that the mean of the scenario specific solutions is $\hat{x}^t$. If for some scenario $s \in S$, the scenario specific solution x_s^t is away from the mean of the scenarios (say $x_s^t = 0$ and $\hat{x}^t = 0.9$), we would like to penalize this deviation in the objective of the scenario subproblem the next time we iterate, at time $t+1$. So, at iteration $t+1$ a term $(x_s^t - \hat{x}^t)x$ will appear in the objective of scenario s, so that the new solution x of the scenario will be driven towards the scenario mean (in the arithmetic example, the penalty in the objective would be $(0-0.9)x = -0.9x$ which will drive x to be 1 in the minimization, i.e. closer to the previous iteration mean.)

In the Upper Bounding Phase of the algorithm, the $|S|$ scenario specific solutions for the first stage variables found during the previous phase are tested into the full problem. If feasible, each one of them yields an upper bound to (10). That way, we can possibly update the upper bound and the first stage solution that yields it.

We then add the points $\{x_s^t\}_{s \in S}$ in the set W. Our objective function value has already been calculated for all of these points, so we can exclude them from further consideration, except for the one that has yielded the best upper bound so far. That is, the execution of the Lower Bounding Phase for the next iteration should only consider points not in W. In practice, this is achieved by adding a global cut in the optimization problems solved in the first phase, for every point in W so as to cut off this particular point. More specifically, a "No-Good-Cut" is employed, i.e. a constraint of the form

$$x^T(1 - x_s^t) + (1 - x)^T x_s^t \geq 1 \,, \tag{11}$$

in order to cut off the point x_s^t.

The parameter ρ_t is initialized before the optimization and defines how aggressively the penalties are imposed in the objective. Very large values of ρ_t however could lead to oscillatory behavior, by driving the mean to be very high or very low during successive iterations. Very low values of ρ_t lead to slow convergence of the scenarios to the same point. If we want to ensure convergence for the dual problem of the Lower Bounding Phase, the sequence of ρ_t should satisfy some properties (i.e. its limit being zero, and the series diverging to infinity would be sufficient). For our purposes and the precision of the final solution we aim to achieve, even a costant ρ can work satisfactorily. Also, the objective penalties are more useful at the beginning of the algorithm, since they lead the possibly very different scenario specific solutions towards the same point x, while the global cuts are more useful after the first iterations, to reduce the optimality gap by cutting out points when the scenario solutions are similar to each other and the Lagrangian penalties do not offer significant improvements any more. The global cuts are not useful during the initial steps of the algorithm since the scenario objectives change significantly due to the penalties, so it is unlikely that we would end up to the same point x anyway (so there is no need to cut it off). The complementary behavior of these two characteristics can lead to a very good performance if exploited. The global convergence of the algorithm is guaranteed [29], but we can also terminate earlier, when we have sufficiently small duality gap for the application.

4.2. A Progressive Hedging Scenario Reduction and Decomposition Heuristic

The algorithm presented in the previous section will, by construction, lead to high quality solutions. Its convergence to the optimal solution is guaranteed [29], but we can also stop its execution once a guarantee of a small gap is available. However, at every iteration we still need to solve $|S|$ subproblems for a fixed scenario (in the Lower Bounding Phase) and $|S|^2$ subproblems for fixed scenario and fixed first stage variables (in the Upper Bounding Phase). Even though in

Initialization Phase

$t \leftarrow 0$, $UB \leftarrow \infty$, $LB \leftarrow -\infty$, $w_s^t \leftarrow 0$, $\forall s \in S$, $W \leftarrow \emptyset$

Main Body

repeat

$t \leftarrow t+1$,

Lower Bounding and Lagrangian Update Phase

Solve scenario subproblems:

for $s \in S$ **do**

$x_s^t \in \underset{x \in X \setminus W}{\operatorname{argmin}} \{f_s(x) + x^T w_s^{t-1}\}$

end for

Update Lower Bound:

$\mathrm{LB} \leftarrow \sum_{s \in S} \pi_s f_s(x_s^t)$

Update objective weights:

for $s \in S$ **do**

$\hat{x}^t \leftarrow \sum_{s \in S} \pi_s x_s^t$

$w_s^t \leftarrow w_s^{t-1} + \rho_t \ (x_s^t - \hat{x}^t)$

end for

Upper Bounding and Cut Phase

Evaluate scenario solutions for Upper Bounds:

for $s \in S$ **do**

$\mathrm{UB}_s \leftarrow \sum_{i \in S} \pi_j f_i(x_s^t)$

end for

Update Upper Bound:

$\mathrm{UB} \leftarrow \min\{\mathrm{UB}, \{\mathrm{UB}_s\}_{s \in S}\}$

Exclude points tested:

for $s \in S$ **do**

$W \leftarrow W \cup \{x_s^t\}$

end for

until $\mathrm{UB} \leq \mathrm{LB}$

Figure 4.1: Decomposition scheme proposed in [29], adapted to solve the SUC problem. The Lower Bounding Phase involves solving smaller optimization problems than the original, since the scenario is fixed, whereas the Upper Bounding Phase involves smaller problems since the first stage and the scenario are fixed. As discussed in section VI, not both phases are necessarily executed at every iteration.

practice, for the simulations we conducted, the algorithm terminated after a few iterations and we only actually apply the upper bounding phase $4-5$ times, the computational burden of the algorithm can still be high for an increased number of scenarios. For that reason, we motivate and propose a scheme that yields a fast heuristic approximation of the solution.

In our case, the scenarios involve continuous (wind power generation) and non continuous variables (discrete faults, represented by binary parameters). Defining distances between these scenario vectors could be problematic (susceptible to scaling issues between the continuous and the discrete part for example). Our goal is to define the scenario distances in a way that takes into advantage not the scenario vector itself, but the impact that that scenario inflicts upon the

Initialization Phase
$t \leftarrow 0$, $S_t \leftarrow S$, $w_s^t \leftarrow 0$, $\forall s \in S$ and $D_{ij}^t \leftarrow 0$, $\forall i, j \in S$
$(x_{S_t}^{t+1}, y_{S_t}^{t+1}, w_{S_t}^{t+1}) \leftarrow PH(S_t, 0, 0, w_{S_t}^t, 0)$
$t \leftarrow t+1$
Main Body
repeat
  if $t \leq M$ **then**
    Reduction Phase
    $(x_{S_t}^{t_0}, y_{S_t}^{t_0}, w_{S_t}^{t_0}) \leftarrow (x_{S_t}^t, y_{S_t}^t, w_{S_t}^t)$
    Run PH for M_t steps:
    for $i \in 0..(M_t - 1)$ **do**
      $(x_{S_t}^{t_{i+1}}, y_{S_t}^{t_{i+1}}, w_{S_t}^{t_{i+1}}) \leftarrow PH(S_t, x_{S_t}^{t_i}, y_{S_t}^{t_i}, w_{S_t}^{t_i}, \rho_t)$
    end for
    Calculate state of system for every scenario:
    $z_s^t \leftarrow z(x_s^{t_{M_t}}, y_s^{t_{M_t}})$, $\forall s \in S_t$
    Update scenario distances:
    $D_{sk}^t \leftarrow D_{sk}^{t-1} + ||z_s^t - z_k^t||$, $\forall s, k \in S_t$
    Initialize new scenario set:
    $S_{t+1} \leftarrow S_t$
    repeat
      Pick k^*: $(k^*, l^*) \in \underset{k,l \in S_t, k \neq l}{\operatorname{argmin}} \{D_{kl}^t\}$
      Perform scenario reduction:
      $S_{t+1} \leftarrow S_{t+1} \setminus \{k^*\}$, $\pi_{l^*} \leftarrow \pi_{k^*} + \pi_{l^*}$
    until reduction termination criterion
    Update reduced set of variables for the next iteration:
    $(x_{S_{t+1}}^{t+1}, y_{S_{t+1}}^{t+1}, w_{S_{t+1}}^{t+1}) \leftarrow (x_{S_{t+1}}^{t_{M_t}}, y_{S_{t+1}}^{t_{M_t}}, w_{S_{t+1}}^{t_{M_t}})$
  else
    Execution Phase
    $S_{t+1} \leftarrow S_t$
    $(x_{S_{t+1}}^{t+1}, y_{S_{t+1}}^{t+1}, w_{S_{t+1}}^{t+1}) \leftarrow PH(S_t, x_{S_t}^t, y_{S_t}^t, w_{S_t}^t, \rho_t)$
  end if
  $t \leftarrow t+1$
  Termination Criterion
  End iterations when the scenario solutions get close to each other:
  $\varepsilon^t \leftarrow \sum_{s \in S_t} \pi_s ||x_s^t - \sum_{s' \in S_t} \pi_{s'} x_{s'}^t||$
until $\varepsilon^t < eps$

function $PH(S, x_S^t, y_S^t, w_S^t, \rho_t)$
  $\hat{x}^t \leftarrow \sum_{s \in S} \pi_s x_s^t$
  $w_s^{t+1} \leftarrow w_s^t + \rho_t (x_s^t - \hat{x}^t)$, $\forall s \in S$
  $(x_s^{t+1}, y_s^{t+1}) \in \underset{(x,y) \in X(s)}{\operatorname{argmin}} \{f_s(x,y) + x^T w_s^{t+1} + \frac{\rho_t}{2} ||x - \hat{x}^t||_2^2\}$, $\forall s \in S$
  return $(x_S^{t+1}, y_S^{t+1}, w_S^{t+1})$
end function

Figure 4.2: Scenario Reduction Progressive Hedging.

power system state. More specifically, if the optimal solution of the SUC problem was available and the state of the power system for two scenarios in that solution was the same or similar, then perhaps only one of these scenarios is necessary to capture the requirements that this uncertainty realization entails for the power system. Of course, the solution to the SUC problem is not available in advance, but at every step of a scenario decomposition algorithm we get an approximation of it. So at every step we can use these suboptimal, scenario specific, system states (i.e. power flows in our case) as features to define distances, based on continuous variables, that represent the impact of a scenario on the power system. The proposed integration of the decomposition and scenario reduction steps can be combined with existing scenario reduction

and machine learning techniques to obtain more sophisticated clustering schemes, but in this study a simple reduction approach is adopted to illustrate the effectiveness of our approach. We also use PH as the decomposition algorithm, since its use is well established for the SUC problem [23].

The basic steps of the algorithm, as implemented in this work, are depicted in Fig. 4.2. The algorithm keeps a record of the remaining scenarios S_t at every iteration step t. For simplicity, the algorithm is described in two distinct phases; in the first M steps of the algorithm execution a reduction in the number of scenarios is allowed (Reduction Phase), while afterwards (Execution Phase) the set of scenarios is assumed fixed and PH is executed until it converges (or until the weighted distance between the scenario solutions is below some threshold eps). During each iteration t of the Reduction Phase, we perform M_t steps of PH. Following that, based on the scenario solutions available at that iteration, the state z_s^t of the system is calculated for every scenario. In our implementation, the state consists of the power flows of the network at every time instant, and a satisfactory performance is observed in this case, but of course we could instead include a richer set of variables. The scenario distances are then calculated and from a pair of scenarios with small distance to each other one is eliminated and its probability is added to the other. Note that if the scenarios were exactly the same, the new problem with the reduced number of scenarios would have the same solution set and objective evaluation as the old one.

Both the iterations of the Reduction Phase M and the steps per iteration M_t could be set as constants, or depend on convergence properties of the algorithm instead; for example we could interrupt the scenario reduction if the distances of the remaining scenarios are above a threshold instead of a fixed M or only calculate system states after the scenario solutions are sufficiently close to each other instead of after a fixed number of M_t PH iterations. However, setting a hard upper limit for M and M_t allows us to control the maximum number of MIPs solved by the algorithm and hence the computational burden.

Since the initial iterations of the algorithm are performed on a more detailed set of scenarios, we expect that when the reduction set is finalized, a good initialization point will be available for the remaining execution of the algorithm. In fact, the algorithm could consist entirely of the Reduction Phase or the requirement of convergence of all the scenarios to the same solution in the end could be relaxed. In that case, in practice, we test all the solutions we got up to that point for every scenario in the reduced set over the full set of scenarios and pick the one that yields the best upper bound to our problem.

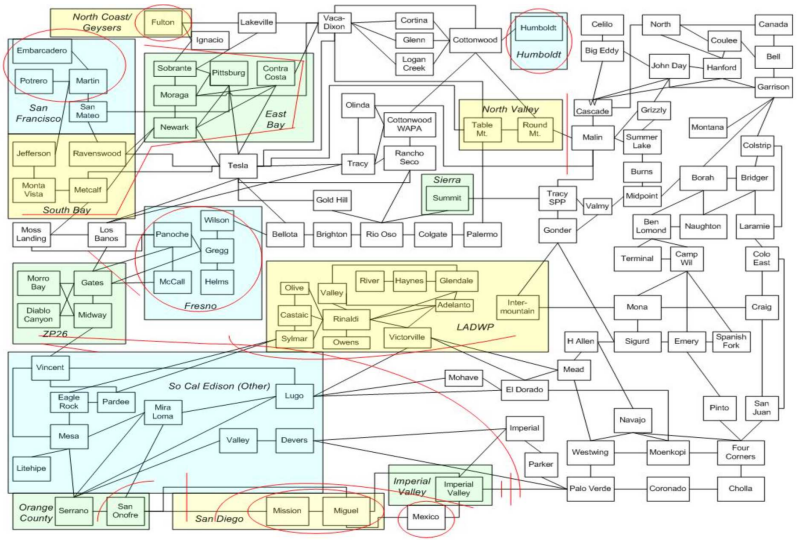

Figure 5.1: Map of the reduced 225 bus WECC system [32].

5. Simulation Results

For the SUC formulation, we consider a reduced model of the Western Electricity Coordinating Council (WECC) system [32] with 225 buses, 371 lines and 130 conventional generators, shown in Fig. 5.1. The same model is used in [34] and [25]. A typical winter weekday is simulated for three different integration cases: high, medium and low. High integration corresponds to 33% wind energy penetration, the medium integration corresponds to 19% penetration and the low integration to 13%. The average load is 28056MW, with a minimum of 21438MW and a maximum of 32300MW. The capacity of thermal generation is 31281MW and the total generating capacity, not including wind resources, is 51402MW. The cost of load shedding is assumed \$5000/MW-h. As mentioned, wind in the "must-take" case study, all the wind is integrated unless this leads to system infeasibility. For these cases, an underestimation of the cost is used that comes from imposing a big-M penalty on wind spill instead, where the M is chosen twice the cost of load shed (and this penalty is then subtracted from the objective for the results). The generation mix in terms of type, number of generators and total capacity is shown in Table 5.1.

The uncertainty model is trained based on data taken from [20]. These correspond to yearly time series of wind speeds and wind power generations with hourly resolution for five aggregate wind sites. The initial source was 2006 wind production data from the National Renewable Energy Laboratory database. A discrete distribution is assumed for the reliability model, as in [34]. More specifically, a probability of generator failure of 1% and a probability of transmission line failure of 0.1% is assumed, independently.

All the simulations are performed on the Cab cluster of the Lawrence Livermore National Laboratory. The Cab cluster consists of 1296 nodes with 20736 cores, equipped with an Intel Xeon E5-2670 processor at 2.6 GHz and 32 GB per node. For the simulations, Mosel 4.0.4 was used with Xpress [39]. More specifically, the simulations were parallelized in 10 nodes of the Cab cluster by utilizing the dedicated features of Mosel [40].

Type	Units	Capacity [MW]
Nuclear	2	4499
Gas	101	21781
Coal	3	199
Oil	1	121
Dual Fuel	23	4679
Import	5	9931
Hydro	6	8613
Biomass	3	502
Geothermal	2	1073
Hydro	6	8613
Wind Low	5	1414
Wind Medium	5	2121
Wind High	5	2828

Table 5.1: Generator mix for the test system.

5.1. The Value of Wind Reserve

A total of 160 scenarios was generated and used as an input to the SUC problem. We explore two alternative policies; one that allows for wind reserves and one that assumes wind is a must-take resource, for the three integration cases. A 2% optimality guarantee is set as a termination criterion to the algorithm of Fig. 4.1. The objective costs were chosen according to [34], normalized in \$M, and a small value for ρ_t was chosen ($\rho = 0.005$). Note that the value of ρ actually depends on the normalization used in the objective, so the actual value is not very informative and in our case it was found through trial and error. In order to objectively compare the two policies, a new set of 160 scenarios is generated, representing the actual realization of the uncertainty the day ahead, and the out-of-sample testing results are shown in Table 5.2. We observe that in most cases the solution of the optimization problem (training set) is close to the evaluations of that solution to a new set of scenarios (test set). The evaluations of the first stage solution against the test set correspond to possible realizations of the uncertainty of the next day, so they will provide the basis to illustrate the benefit of wind spilling to the actual operation.

Indeed, Tables 5.3 and 5.4 show the policy testing results. The fuel cost without load shedding is also provided in an effort to remove the actual value of the load shedding cost from the results. We observe that in the case of low and medium wind integration, wind spilling does not result in a significant benefit. However, for high wind integration, the cost of operation is significantly lower when wind spill is allowed and load shed does not happen, whereas demanding the wind energy to be fully integrated leads to both an inefficient dispatch (high fuel costs) and an increased load shedding.

5.2. The Scenario Reduction Scheme

The heuristic scenario reduction is evaluated and some of the results are presented in Tables 5.6, 5.6 and 5.7. The scenarios are reduced in a linear fashion from their initial number (160) to the number indicated in the tables, in M steps. The results of the optimization over the full set are repeated for comparison. We notice that the heuristic approximation is able to provide a good estimate of the final solution value; in fact the estimate is more accurate than the difference of the evaluations between the test set and the training set. The computational effort is largely controllable, since both the rate of reduction and the final number of scenarios are controllable parameters. To get a rough estimate, the algorithm was stopped after 11 iterations. If convergence

Wind Integration Level	Training Set Total Cost [$M]		Test Set Total Cost [$M]	
	Must Take	Wind Spill	Must Take	Wind Spill
Low	8.28	8.25	8.23	8.23
Medium	7.02	6.97	6.98	6.95
High	12.82	6.10	16.09	6.11

Table 5.2: Comparison of total cost evaluated on the training set (representing the samples the operator uses to make the dispatching decision) and on the test set (representing the expected cost of operation over a set of probable realizations). Note that in this case the cost of loadshed is an important part of the objective, and since this parameter was arbitrarily set we are also presenting the results without it.

Wind Integration Level	Cost without load shed [$M]		Wind Penetration [%]	
	Must Take	Wind Spill	Must Take	Wind Spill
Low	8.23	8.23	13.2	13.0
Medium	6.98	6.95	19.8	18.9
High	7.27	6.11	26.3	23.4

Table 5.3: SUC solution evaluated on the test set: Mean cost of operation (without accounting for load shed) and wind penetration (percentage of mean, over the scenarios, wind energy over mean total generated energy)

was not achieved yet, the scenario specific solutions (for each of the scenarios in the final, reduced set) were tested against the training set and the best one was chosen.

In Fig. 5.2 an interesting observation is made. The final set of reduced scenarios consists of a few scenarios with very high probabilities (these correspond to the base cases of the normal or close to normal operation for the system, which is the most common occurrence) and a few low probability events (these correspond to rare events which impose very different requirements on the system and seem like abnormal operation). In that way, the reduction heuristic allows rare events to influence the optimization problem with small probabilities, whereas the scenarios that mostly correspond to similar operating conditions are treated in a unified way instead of being treated in isolation.

Wind Integration Level	Wind Spill [%]		Load Shed [%]	
	Must Take	Wind Spill	Must Take	Wind Spill
Low	0	1.06	0	0
Medium	0	4.48	0	0
High	0.3	11.1	0.26	0

Table 5.4: SUC solution evaluated on the test set: Percentage of mean (over scenarios) wind spill over mean available generation and percentage of mean loadshed over the total load.

Objective Cost	Training Set	Test Set
Full Set (160 scenarios)	8.253	8.229
10 scenarios, 5 steps	8.266	8.235
30 scenarios, 5 steps	8.252	8.219
10 scenarios, 10 steps	8.259	8.235
30 scenarios, 10 steps	8.254	8.223

Table 5.5: Expected total cost for full problem versus various execution of the reduction algorithm, in the case of low integration where wind spill is allowed. The scenarios are linearly reduced from initial to final number in the number of steps (M) indicated. One iteration per reduction step is performed ($M_t = 1$). The total number of iterations was restricted to 11.

Time [s]	Reduction Phase	Total Time
10 scenarios, 5 steps	327	516
30 scenarios, 5 steps	394	582
10 scenarios, 10 steps	500	518
30 scenarios, 10 steps	569	597

Table 5.6: Comparison of the execution times of the heuristic for the low integration case with wind spill. The total number of iterations for the reduction was restricted to 11. The total time does not include the evaluations for the different possible scenario solutions of the reduced set in the case of non convergence (approx. 300s for all the cases, due to the parallel execution)

The reduction algorithm seems to perform very well in providing an approximation of the optimal cost. For that purpose, its use in studies regarding the cost impact of renewables in the power system, whereas also identifying a grouping of scenarios, is highly motivating. However, at this point there is no guarantee on how the objective will change by completely eliminating one of the scenarios. For that reason, the algorithm at this point cannot provide a guaranteed evaluation of the actual optimization problem solved. Pursuing such a guarantee will be a future goal of research.

Objective Cost	Training Set	Test Set
Full Set (160 scenarios)	6.965	6.947
10 scenarios, 5 steps	6.988	6.965
30 scenarios, 5 steps	6.970	6.955
10 scenarios, 10 steps	6.995	6.968
30 scenarios, 10 steps	6.964	6.950

Table 5.7: Expected total cost for full problem versus various execution of the reduction algorithm, in the case of medium integration where wind spill is allowed. The scenarios are linearly reduced from initial to final number in the number of steps (M) indicated. One iteration per reduction step is performed ($M_t = 1$). The total number of iterations was restricted to 11.

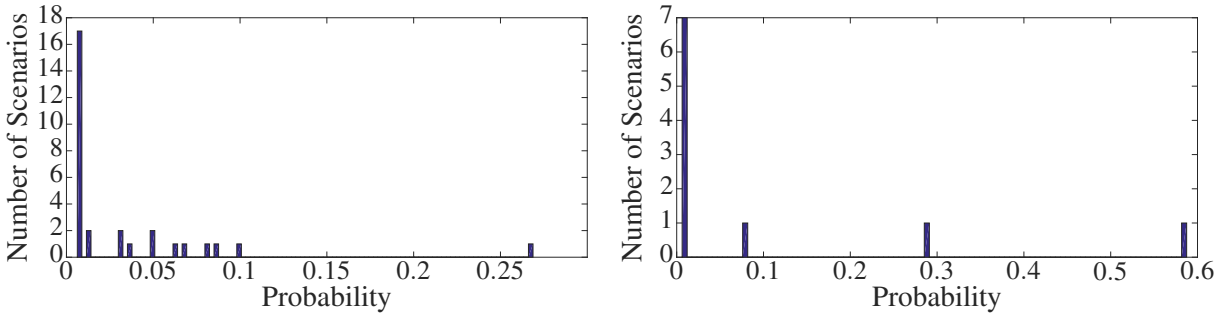

(a) Reduction to 30 scenarios in 10 steps.

(b) Reduction to 10 scenarios in 10 steps.

Figure 5.2: These plots indicate how many scenarios were assigned a probability within a certain interval after the reduction. We note that one or two scenarios have a relatively high probability, whereas the other ones have much smaller probabilities. The explanation of that graph is that the scenario with the high probability corresponds to a base case behavior, which incorporates most of the requirements for the system in normal or close to normal operation, whereas the remaining scenarios correspond to rare events that have very different impact on the system and are not similar to each other to be grouped together, so each one of them retains its initial, small probability.

6. Conclusions and Discussion

The main objective of this report is to convey that wind resources, and renewables in general, should be treated, to the extent possible, as any other resource for the unit commitment problem, if the goal is for their integration levels to increase in the future. Renewable integration is vital to achieve environmental goals, but it often competes with ensuring the secure and reliable operation of the grid due to the variability and stochasticity of the available wind power. However, current wind turbines are capable to control their output power setpoint within the limits allowed by wind availability. By exploiting this capability a safer and more economic grid operation can be ensured.

In order to explicitly exploit the extent of controllability of wind generation, a stochastic unit commitment approach is employed to determine the dispatch of wind generation for a number of possible scenarios. Two cases, one in which wind is treated as a must-take resource and one that the wind output setpoint is also optimized, are considered for three integration scenarios in a reduced California test case. A clear benefit for the second strategy is obtained only in the high integration case.

At this point it is important to repeat with a critical view some of the assumptions of the current study, to initiate discussion and motivate a set of questions for future research. Firstly, the unit commitment problem as we formulated it did not include an objective term for the reduction of emissions. Including such a term would of course reduce the wind spilling benefits. However, the weight of such a term is at this point not as objective and universal as the operational costs of conventional generators and its value is still a source of debate, so for that reason it was omitted. Various study cases could of course extend our current results for the existence of such a term. Secondly, the results are based on a reduced system developed based on an earlier version of the WECC system. For that reason, we cannot claim that the results could generalize in a similar

fashion for the full system as is, however the system used still provides a useful test case and most of the logic that was described could carry on. Thirdly, a major contributing factor in wind shedding is congestion. One could argue that if renewable generation integration increases, then the transmission system will also be enhanced to accommodate for it. However, changing the existing transmission system is accompanied by extra costs and the benefit from that could only be to accommodate some rare instances for which spilling some wind generation could also relieve the stress for the system. Since the focus at this point is not planning and investment on the transmission system, enhancements to it are not considered.

Finally, one could question the usefulness of solving the SUC problem at high precision. After all, the number of necessary scenarios to solve is not specified, and the error in capturing uncertainty could very well be higher than the precision level of the solution. However, at this point the plain UC problem is solved with very high precision every day since there are economic implications of these solutions. For example, NYISO eventually solves the UC problem at $200 precision, and even though the solution they get is not necessarily the optimal for the problem they are solving, the heuristics and refinements they use (such as gradually fixing binary variables) are standardized to provide a high precision approximation. This kind of precision is necessary since commitment of small gas units, for example, depends on it and perturbations could lead to very different commitments. So, if the way to generate scenarios is precisely modeled and standardized, these levels of precision are indeed necessary in solving the SUC problem as well.

Regarding policy implications of adopting the proposed strategy, active wind spilling based on market operations can allow for a more efficient allocation (increased total welfare for the society), which could translate to benefits for the customers (in the form of reduced bills). The conventional generators will also be benefited, since they will not be the ones to fully carry the burden from renewable integration. In the current form of the SUC objective, clean energy generation will be diminished. However, introducing a price for carbon in the objective that reflects economic welfare would resolve the problem; until such a price is set any economic comparison of the tradeoffs between clean energy and economic dispatch is by default hard anyway. Furthermore, since wind generation will be decreased, investments on wind resources may be discouraged. If this is found to be the case, an initial lump transfer investment incentive could be a preferred way to deal with it than actively introducing frequent economic inefficiencies in the day ahead markets or than compensating the wind generators for their spilled energy (unless this is committed as a reserve).

References

[1] "Flexible Resources Help Renewables ," California ISO, 2016. [Online]. Available: https://www.caiso.com/Documents FlexibleResourcesHelpRenewables_FastFacts.pdf

[2] "Curtailment Fast Facts," California ISO, 2017. [Online]. Available: https://www.caiso.com/Documents/CurtailmentFastFacts.pdf

[3] E. Union, "Directive 2009/28/EC of the European Parliament and of the Council of 23 April 2009 on the promotion of the use of energy from renewable sources and amending and subsequently repealing Directives 2001/77/EC and 2003/30/EC," *Official Journal of the European Union*, vol. 5, p. 2009, 2009.

[4] P. Moutis, S. A. Papathanassiou, and N. D. Hatziargyriou, "Improved load-frequency control contribution of variable speed variable pitch wind generators," *Renewable Energy*, vol. 48, pp. 514–523, 2012.

[5] S. I. Nanou, G. N. Patsakis, and S. A. Papathanassiou, "Assessment of communication-independent grid code compatibility solutions for VSC–HVDC connected offshore wind farms," *Electric Power Systems Research*, vol. 121, pp. 38–51, 2015.

[6] S. Fink, C. Mudd, K. Porter, and B. Morgenstern, "Wind energy curtailment case studies," *NREL subcontract report, NREL/SR-550*, vol. 46716, 2009.

[7] L. Bird, J. Cochran, and X. Wang, "Wind and solar energy curtailment: experience and practices in the United States," *US National Renewable Energy Laboratory, NREL/TP-6A20-60983*, p. 3, 2014.

[8] S. Liu, "Phase I.A. Stochastic Study Testimony of Dr. Shucheng Liu on behalf of the California Independent System Operator Corporation," 11 2014.

[9] K. Meeusen, "Phase I.A. Stochastic Study Testimony of Dr. Karl Meeusen on behalf of the California Independent System Operator Corporation," 11 2014.

[10] A. Solomon, D. M. Kammen, and D. Callaway, "The role of large-scale energy storage design and dispatch in the power grid: a study of very high grid penetration of variable renewable resources," *Applied Energy*, vol. 134, pp. 75–89, 2014.

[11] D. J. Burke and M. J. O'Malley, "Factors influencing wind energy curtailment," *IEEE Transactions on Sustainable Energy*, vol. 2, no. 2, pp. 185–193, 2011.

[12] L. S. Vargas, G. Bustos-Turu, and F. Larraín, "Wind power curtailment and energy storage in transmission congestion management considering power plants ramp rates," *IEEE Transactions on Power Systems*, vol. 30, no. 5, pp. 2498–2506, 2015.

[13] R. Golden and B. Paulos, "Curtailment of Renewable Energy in California and Beyond," *The Electricity Journal*, vol. 28, no. 6, pp. 36–50, 2015.

[14] L. Kane and G. W. Ault, "Evaluation of wind power curtailment in active network management schemes," *IEEE Transactions on Power Systems*, vol. 30, no. 2, pp. 672–679, 2015.

[15] M. Hedayati-Mehdiabadi, J. Zhang, and K. W. Hedman, "Wind power dispatch margin for flexible energy and reserve scheduling with increased wind generation," *IEEE Transactions on Sustainable Energy*, vol. 6, no. 4, pp. 1543–1552, 2015.

[16] M. Hedayati-Mehdiabadi, K. W. Hedman, and J. Zhang, "Reserve Policy Optimization for Scheduling Wind Energy and Reserve," *IEEE Transactions on Power Systems*, 2017.

[17] M. Carrión and J. M. Arroyo, "A computationally efficient mixed-integer linear formulation for the thermal unit commitment problem," *IEEE Transactions on power systems*, vol. 21, no. 3, pp. 1371–1378, 2006.

[18] P. Damcı-Kurt, S. Küçükyavuz, D. Rajan, and A. Atamtürk, "A polyhedral study of ramping in unit commitment," *Univ. California-Berkeley, Res. Rep. BCOL*, vol. 13, p. 1777, 2013.

[19] S. Fattahi, M. Ashraphijuo, J. Lavaei, and A. Atamtürk, "Conic relaxations of the unit commitment problem," in *Under review for Energy (conference version appeared in CDC 2016), available online at http://www. ieor. berkeley. edu/˜ lavaei/UC_Conic_*, 2016.

[20] A. Papavasiliou and S. S. Oren, "Multiarea stochastic unit commitment for high wind penetration in a transmission constrained network," *Operations Research*, vol. 61, no. 3, pp. 578–592, 2013.
[21] S. Takriti, J. R. Birge, and E. Long, "A stochastic model for the unit commitment problem," *IEEE Transactions on Power Systems*, vol. 11, no. 3, pp. 1497–1508, 1996.
[22] P. Carpentier, G. Gohen, J.-C. Culioli, and A. Renaud, "Stochastic optimization of unit commitment: a new decomposition framework," *IEEE Transactions on Power Systems*, vol. 11, no. 2, pp. 1067–1073, 1996.
[23] K. Cheung, D. Gade, C. Silva-Monroy, S. M. Ryan, J.-P. Watson, R. J.-B. Wets, and D. L. Woodruff, "Toward scalable stochastic unit commitment," *Energy Systems*, vol. 6, no. 3, pp. 417–438, 2015.
[24] K. Kim and V. M. Zavala, "Algorithmic innovations and software for the dual decomposition method applied to stochastic mixed-integer programs," *Optimization Online*, 2015.
[25] A. Papavasiliou, S. S. Oren, and B. Rountree, "Applying high performance computing to transmission-constrained stochastic unit commitment for renewable energy integration," *IEEE Transactions on Power Systems*, vol. 30, no. 3, pp. 1109–1120, 2015.
[26] I. Aravena, A. Papavasiliou *et al.*, "An Asynchronous Distributed Algorithm for solving Stochastic Unit Commitment," Université catholique de Louvain, Center for Operations Research and Econometrics (CORE), Tech. Rep., 2016.
[27] W. S. Cleveland, "Robust locally weighted regression and smoothing scatterplots," *Journal of the American statistical association*, vol. 74, no. 368, pp. 829–836, 1979.
[28] M. J. Wainwright, M. I. Jordan *et al.*, "Graphical models, exponential families, and variational inference," *Foundations and Trends® in Machine Learning*, vol. 1, no. 1–2, pp. 1–305, 2008.
[29] S. Ahmed, "A scenario decomposition algorithm for 0–1 stochastic programs," *Operations Research Letters*, vol. 41, no. 6, pp. 565–569, 2013.
[30] K. Ryan, D. Rajan, and S. Ahmed, "Scenario decomposition for 0-1 stochastic programs: Improvements and asynchronous implementation," in *Parallel and Distributed Processing Symposium Workshops, 2016 IEEE International*. IEEE, 2016, pp. 722–729.
[31] D. Gade, G. Hackebeil, S. M. Ryan, J.-P. Watson, R. J.-B. Wets, and D. L. Woodruff, "Obtaining lower bounds from the progressive hedging algorithm for stochastic mixed-integer programs," *Mathematical Programming*, vol. 157, no. 1, pp. 47–67, 2016.
[32] N.-P. Yu, C.-C. Liu, and J. Price, "Evaluation of market rules using a multi-agent system method," *IEEE Transactions on Power Systems*, vol. 25, no. 1, pp. 470–479, 2010.
[33] D. D. Le, G. Gross, and A. Berizzi, "Probabilistic Modeling of Multisite Wind Farm Production for Scenario-Based Applications," *Sustainable Energy, IEEE Transactions on*, vol. 6, no. 3, pp. 748–758, 2015.
[34] A. Papavasiliou and S. S. Oren, "Stochastic modeling of multi-area wind production," in *12th International Conference on Probabilistic Methods Applied to Power Systems*, 2012.
[35] J. M. Morales, R. Minguez, and A. J. Conejo, "A methodology to generate statistically dependent wind speed scenarios," *Applied Energy*, vol. 87, no. 3, pp. 843–855, 2010.
[36] G. E. Box, G. M. Jenkins, G. C. Reinsel, and G. M. Ljung, *Time series analysis: forecasting and control*. John Wiley & Sons, 2015.
[37] M. Lydia, S. S. Kumar, A. I. Selvakumar, and G. E. P. Kumar, "A comprehensive review on wind turbine power curve modeling techniques," *Renewable and Sustainable Energy Reviews*, vol. 30, pp. 452–460, 2014.
[38] K. Van den Bergh, K. Bruninx, E. Delarue, and W. Dhaeseleer, "A mixed-integer linear formulation of the unit commitment problem," *KU Leuven Energy Institute Working Paper WP EN2013-11. Online: http://www. mech. kuleuven. be/en/tme/research/energy_environment/Pdf/wpen2013-11. pdf*, 2013.

[39] C. Guéret, C. Prins, and M. Sevaux, "Applications of optimization with Xpress-MP," *contract*, p. 00034, 1999.
[40] Y. Colombani and S. Heipcke, "Multiple models and parallel solving with Mosel, February 2014," *Avalaible at: http://community. fico. com/docs/DOC-1141*.

Part III

Risk-aware Optimal Bidding for Renewable Farms

Kwami Senam Sedzro
Alberto J. Lamadrid

Lehigh University

For information about this project, contact:

Alberto J. Lamadrid
Department of Economics
College of Business and Economics
Rauch Business Center 451
Lehigh University
Bethlehem, PA 18015
Office: RBC 451
Email: ajlamadrid@lehigh.edu
Phone: 610.758.0239

Power Systems Engineering Research Center

The Power Systems Engineering Research Center (PSERC) is a multi-university Center conducting research on challenges facing the electric power industry and educating the next generation of power engineers. More information about PSERC can be found at the Center's website: http://www.pserc.org.

For additional information, contact:

Power Systems Engineering Research Center
Arizona State University
527 Engineering Research Center
Tempe, Arizona 85287-5706
Phone: 480-965-1643
Fax: 480-727-2052

Notice Concerning Copyright Material

Table of Contents

List of Figures

1. Introduction

The urgent need for a more sustainable world is hastening the pace of renewable integration into the electric grid. Due to the inherent intermittency of renewable power output, the reliability a highly renewable-penetrated electric grid is at risk. To balance out hardly predictable supply-demand mismatches, large reserve capacities with flexible operating modes (on/off status, minimum/maximum operation time, ramping capability, etc.) are desired. As a result, grid O&M costs are likely to increase. In the attempt of making renewable farms responsible for any mismatch between their day-ahead unit commitment process (DACP) bid and their actual power output, some market policies impose supply shortfall penalties [1].

To help renewable farms be marketable while keeping the grid reliable, the focus of a significant amount of research in the literature is on devising better methods of integrating renewable energy converters (RECs) to the existing power grid. A first category of work seeks solution in more accurate short-term (24-36 hours) forecasting techniques [2, 3, 4]. Given that forecasting errors cannot be completely eliminated, others have investigated renewable integration strategies such as promoting fair market processes for renewables [2], implementing intra-day markets to leverage the relative accuracy of short-term forecasts [5], developing hybrid systems [6], etc.

In the specific scope of this work, Dukpa et al. proposed an optimal participation strategy for a renewable energy converter (REC) coupled with an energy storage device (ESD) that maximizes profit and mitigate the risk of supply shortfalls. The authors confirm that it is imperative to combine an ESD with a REC to achieve an increased reliability and profitability. Bathurst et al. [2], Matevosyan and Soder [7], and Morales et al. [8] studied the wind farm profit maximization problem in a stochastic programing approach. Botterud et al. [9] and Morales et al. [8] further added a risk sensitivity term, the conditional value at risk (CVaR) to the objective in order to control the variability of the expected profit. Pinson et al. [10] proved that the optimal day-ahead bid can be expressed as a probabilistic quantile on prices as in the newsvendor problem, a classic problem in inventory theory [11]. Moreover, Bitar et al. [12] derived an explicit formula for optimal contract offering and the corresponding optimal expected wind farm profit in a competitive two-settlement market settings.

We exploit the analytical results of [12] to derive a criterion for renewable farms' participation in the grid reliability efforts. The renewable energy farms' bidding strategy is formulated as a portfolio optimization problem assuming a storage system. The portfolio is made of the day-ahead, real-time and reserve offers. First, we formulate the renewable farm's day-ahead bidding problem as a newsvendor one. Next we evaluate renewable farm's reliability performance assuming the derived news' vendor based optimal policy. We provide further market opportunity to the renewable farm by assuming it can participate in the reserve market as well. We assume the farm dispose of energy storage. The approach developed in this work has two original defining concepts. First, its principal aim is not to arbitrage the day-ahead versus the real-time markets. Rather, it purposes to provide a reliable and yet economically sound day-ahead energy offer. Second, it provides risk-sensitive real-time and reserve offers that account for all possible imbalance penalties and real-time prices along with reasonable storage size and cost function. In what follows, Section 2 describes the market model under consideration in this work, introduces the analysis of the day-ahead energy bidding as a newsvendor problem. Section 3 describes the resulting risk-aware real-

time and reserve bidding problem in the presence of an ESD. In Section 5, we present some preliminary insights and future directions.

2. Day-ahead bidding as a Newsvendor Problem

Inspired by the work in [12], we pose the day-ahead optimal bidding problem as a Newsvendor Problem.

The market considered is of the traditional two-settlement structure. Under this model, the farm places its bid made of the amount of energy B^t he plans to output and the price p^t he will sell it for any time slot t the next day. The system operator (SO) clears the market at a price p^t and any suppliers i with offer price $p^{i,t}$ less than or equal to p^t are selected and get p^t for each unit of energy output the next day at time t. At the time of realization, depending on the grid balancing needs (with the use of emergency generators) in any time slot t, the SO charges for any unit of negative deviation the penalty charge q^t. For any extra unit of energy above $B^{i,t}$, the supplier i is charged λ^t. According to the formulae established by Bitar et al. (in Bringing wind to market), the optimal day-ahead bid at time t B^{t*} is the inverse of the CDF (cumulative density function) of the price quantile γ^t given by:

$$\gamma^t = \frac{p^t + \mu_{\lambda^t}}{\mu_{q^t} + \mu_{\lambda^t}} \tag{1}$$

where μ_{q^t} and μ_{λ^t} are the expected negative and positive imbalance prices at time t. The true q^t and λ^t are known ex-post.

Knowing the farm's energy output distribution for every time slot and the expected imbalance penalties and day-ahead market clearing prices, one can derive the optimal day-ahead bid. Given that the distribution is involved in the determination of the DA bidding solution, the bid B^{t*} obtained is the best across the entire spectrum of all possible realizations.

However, in each instance only one element in the spectrum can be realized at the time. This leaves room for improvement. To enable the renewable farm to actively participate in the real-time market, assume that the REC is coupled with an energy storage device and the farm can participate in the reserve market as well. The next section presents the strategy for an active spot and reserve market participation.

Since the optimal DA bid is expressed as the inverse of the CDF, it can be rightly said that for the same price quantile γ^t the wave farm will always bid higher than the wind farm in the DA market. This implies that the DA bidding strategy is risk-sensitive. In fact, with a broader PDF, the wind farm's risk error in selecting a single realization is higher than that of the wave farm.

3. Risk-aware real-time and reserve strategy

We assume that the farm submits optimal day-ahead bid B^{t*} obtained in the first stage de- scribed in Section 2. Due to intermittent output, one should expect a discrepancy between B^{t*} and the actual realization g^t. Instead of "polluting the grid" with or spilling the difference $(g^t - B^{t*})$, it can be traded in the real-time market, in the reserve market or stored in the ESD. At this stage, the objective is to determine the real-time and reserve offers while managing the charge/discharge of the ESD and keeping an eye on the risk of profit loss. We use the conditional value at risk (CVaR) as a risk measure.

The farm's profit can be expressed as the difference between its total revenue (from the actual realizations of day-ahead, real-time and reserve markets) and all charges incurred (storage operation/depreciation cost and realization mismatches in day-ahead and real-time markets). This profit uses expected real-time price and imbalance penalties. However, these prices are random processes. To evaluate and account for the uncertainties associated to these chosen parameters, we define the CVaR using the achievable profit for each possible combination of real-time price ρ^t and imbalance penalties q^t and λ^t. The second stage objective function is to maximize the weighted sum of the expected profit and the CVaR while satisfying equilibrium constraints.

Preliminary results suggest that, narrow profit distributions are less risky and thus tolerate expected profit functions. Widespread profit distributions may be, in turn, more risk-sensitive.

4. Sensitivity Analysis

In normal market operation, the real-time market clearing price can be very volatile. To evaluate the sensitivity of the profit and the major decision variables *RT* (real-time optimal realization), *DA* (day-ahead optimal realization), *RegA* (optimal reserve energy output) and *RV* (optimal reserve capacity) with regards to the real-time price,ρ, we perform a simulation study on a range of prices. We assume a real-time price value ρ from 0 to 4.95.

Fig.1 and Fig.2 plot input prices and energy offer and realization.

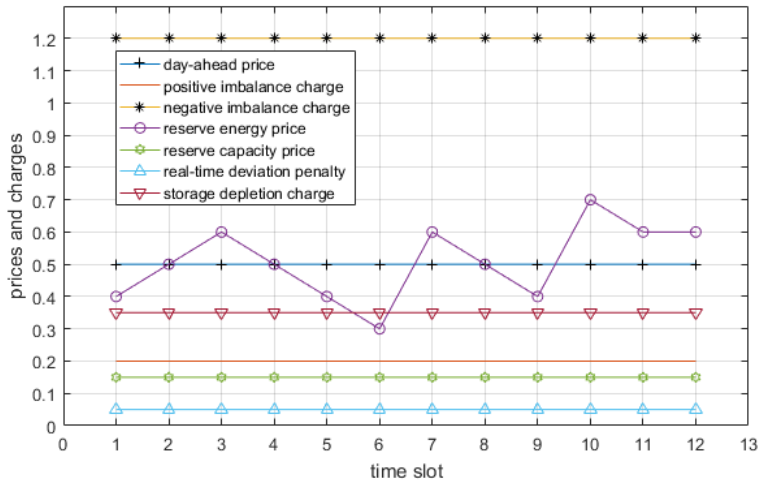

Figure 1: Input price signals

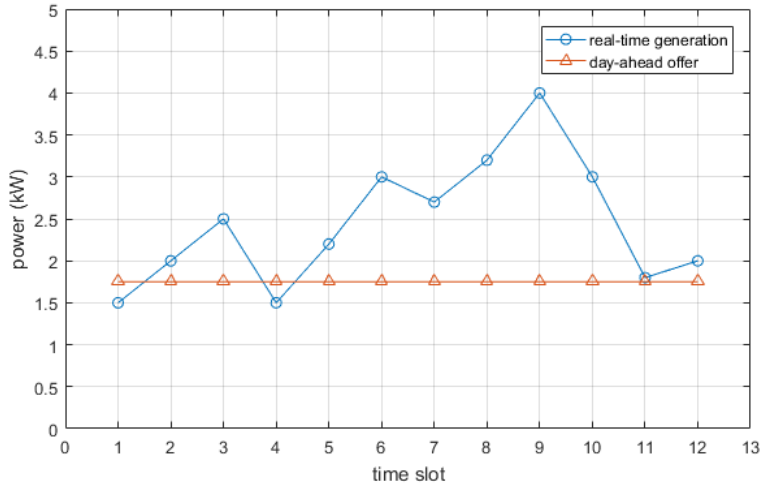

Figure 2: Day-ahead offer vs realization

The time horizon considered lasts 1 hour and comprises 12 equal time slots. Both the day-ahead B^{t*} and real-time RT^t realizations are allowed to deviate from their respective bids B^* and RT_o in any time slot. Fig.3 shows the sensitivity of different optimal realizations to the real-time price

variations. Realization values shown here are averages over the twelve time slots. The corresponding objective values are represented in Fig. 4.

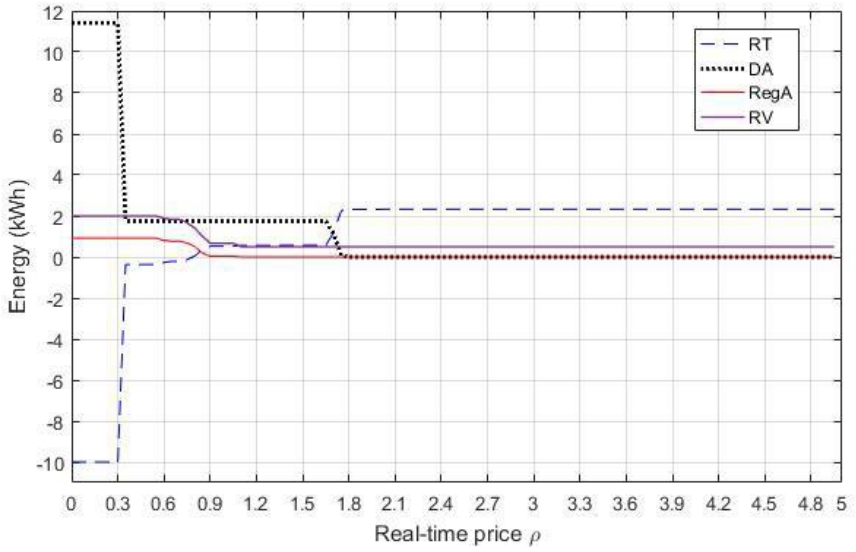

Figure 3: Sensitivity of decision variables to real-time price

The sensitivity analysis reveals three major regimes characterized by equations (2) through (4).

$$(R1):\ \rho^t \leq p^t - \mu_\lambda^t \tag{2}$$

$$(R2):\ p^t - \mu_\lambda^t \leq \rho^t \leq \mu_\mathrm{q}^t + \mu_\mathrm{v}^t \tag{3}$$

$$(R3):\ \rho^t \geq \mu_\mathrm{q}^t + \mu_\mathrm{v}^t \tag{4}$$

The upper bound of the domain ($R1$) is 0.3 in this case and the lower bound of ($R3$) is 1.7. In ($R1$), the low real-time price makes it profitable to buy energy from the real-time market in order to output more than the day-ahead bid B^*. In the regime ($R3$), the high real-time price discourages participation in any other market. The available output is traded in the real-time market. It is only in regime ($R2$) that it is profitable to stick to the bids.

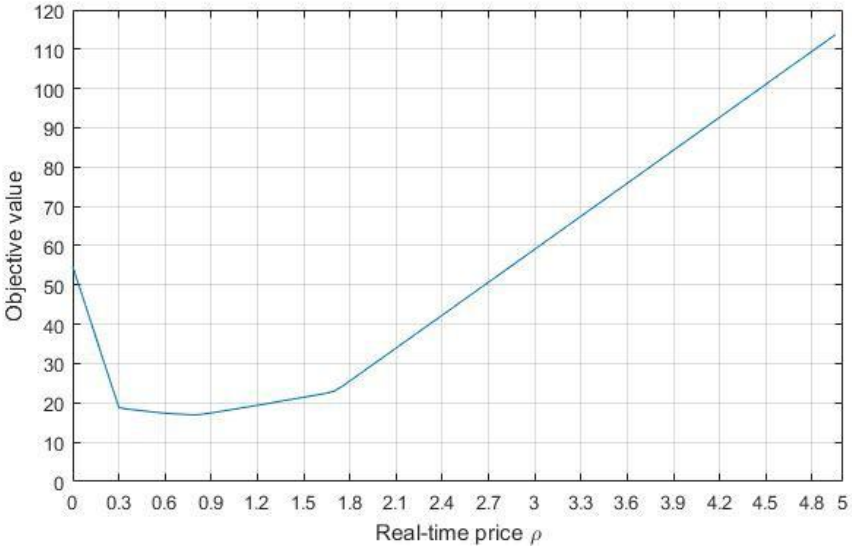

Figure 4: Sensitivity of the objective value to real-time price

5. Conclusions and future work

A major drive of the day-ahead bid is the type of renewable resource. The real-time and reserve decisions are mainly driven by the market signals through the profit distribution. In fact, it is generally conceived that wave farm output is more predictable than the output of a wind farm. This is due to the higher variability of wind speed. This volatility is translated by a broader probability density (PDF) function for the wind power output, while the PDF of the wave output is narrower. The day-ahead offer of a wave farm is susceptible to be higher than that of a comparable wind farm. The solution for a time slot with a wider profit distribution is likely more risk-sensitive than that of a time slot with narrower profit distribution. The sensitivity analysis with respect to real-time price reveals a threshold behavior. Three bidding strategy regions were found. Outside the thresholds, the decision is straightforward. Inside the thresholds, an optimization model is required in order to achieve the best profit.

Future work will consist of designing and conducting simulation case studies to validate the key insights across different renewable technologies (solar, wind and wave) and different profit distributions.

References

[1] H. Holttinen, "Optimal electricity market for wind power," Energy Policy, vol. 33, no. 16, pp. 2052–2063, 2005.

[2] G. N. Bathurst, J. Weatherill, and G. Strbac, "Trading wind generation in short term energy markets," IEEE Transactions on Power Systems, vol. 17, no. 3, pp. 782–789, 2002.

[3] J. Usaola and J. Angarita, "Bidding wind energy under uncertainty," in 2007 Inter- national Conference on Clean Electrical Power. IEEE, 2007, pp. 754–759.

[4] I. Marti, G. Kariniotakis, P. Pinson, I. Sanchez, T. Nielsen, H. Madsen, G. Giebel, J. Usaola, A. M. Palomares, R. Brownsword et al., "Evaluation of advanced wind power forecasting models–results of the anemos project," in European Wind Energy Conference, EWEC 2006, 2006, pp. 9–pages.

[5] Y. V. Makarov, C. Loutan, J. Ma, and P. De Mello, "Operational impacts of wind generation on california power systems," IEEE Transactions on Power Systems, vol. 24, no. 2, pp. 1039–1050, 2009.

[6] E. D. Castronuovo and J. P. Lopes, "On the optimization of the daily operation of a wind-hydro power plant," IEEE Transactions on Power Systems, vol. 19, no. 3, pp. 1599–1606, 2004.

[7] J. Matevosyan and L. Soder, "Minimization of imbalance cost trading wind power on the short-term power market," IEEE Transactions on Power Systems, vol. 21, no. 3, pp. 1396–1404, 2006.

[8] J. M. Morales, A. J. Conejo, and J. Pe´rez-Ruiz, "Short-term trading for a wind power producer," IEEE Transactions on Power Systems, vol. 25, no. 1, pp. 554–564, 2010.

[9] A. Botterud, J. Wang, R. Bessa, H. Keko, and V. Miranda, "Risk management and optimal bidding for a wind power producer," in IEEE PES General Meeting. IEEE, 2010, pp. 1–8.

[10] P. Pinson, C. Chevallier, and G. N. Kariniotakis, "Trading wind generation from short-term probabilistic forecasts of wind power," IEEE Transactions on Power Sys- tems, vol. 22, no. 3, pp. 1148–1156, 2007.

[11] N. C. Petruzzi and M. Dada, "Pricing and the newsvendor problem: A review with extensions," Operations Research, vol. 47, no. 2, pp. 183–194, 1999.

[12] E. Y. Bitar, R. Rajagopal, P. P. Khargonekar, K. Poolla, and P. Varaiya, "Bringing wind energy to market," IEEE Transactions on Power Systems, vol. 27, no. 3, pp. 1225–1235, 2012.